CLASSIFICATION AND QUANTIFICATION OF DAMAGE DUE TO ABRASION IN VARIOUS SELF-CONSOLIDATING CONCRETE MIXTURES USING ACOUSTIC EMISSION MONITORING

by

© Katherine E. Ridgley

A Thesis submitted to the

School of Graduate Studies

in partial fulfillment of the requirements for the degree of

Master of Engineering

Faculty of Engineering and Applied Science – Civil Engineering

Memorial University of Newfoundland

May 2018

St. John's, Newfoundland, Canada

Abstract

The purpose of this thesis was to evaluate and compare the abrasion resistance of various self-consolidating concrete types by means of acoustic emission (AE) analysis. The variables adjusted throughout the study were the type of concrete (normal concrete and self-consolidating concrete), the type of supplementary cementing materials (SCM), the crumb rubber (CR) content and the inclusion of synthetic fibers (SF) of varying lengths and types (flexible and semi-rigid). The abrasion test was performed on cubic concrete specimens in accordance with the rotating-cutter method. Results from the three abrasion tests showed that metakaolin (MK) had the highest abrasion resistance among the mixtures which incorporated SCMs, CR was found to negatively affect the abrasion resistance of the tested samples and flexible SFs exhibited better abrasion resistance compared to their semi-rigid fiber counterparts. Also, the shorter fibers had more resistance capacity against abrasion than the longer fibers of the same type. The effect of changing the aforementioned variables on the abrasion behaviour was evaluated based on the abrasion data and with the assistance of AE analysis. AE signal characteristics such as amplitude, number of hits, and cumulative signal strength were gathered during the test period for each sample. Three additional parameters were determined through b-value analysis and intensity analysis which produced severity (*Sr*), and historic index (*H (t)*). The results from the entire study showed a direct correlation between the previously mentioned AE parameters and the abrasion damage in all tested mixtures. The results also allowed for damage classification charts to be developed using the AE intensity parameters [*H(t)* and *Sr*] to determine the ranges that indicate the extent of damage due to the abrasion of the tested specimens.

Acknowledgements

This work would not have been made possible without the excellent guidance and assistance from my supervisors and co-researcher, Dr. Assem A. Hassan, Dr. Bruce Colbourne and Dr. Ahmed A. Abouhussien. Without your tireless effort and help throughout this process this project would not have been possible for me to complete so successfully. I am greatly indebted to each of you for all you have taught me during my Masters. Thank you for all of your help over the course of the last year. I am also very grateful to the wonderful Technical Services employees at Memorial University of Newfoundland who assisted in fabricating the testing set up and were on hand to offer assistance in the laboratory at all times. Without all of your hard work our research would not be carried out.

This research would also not be possible without the generous financial contributions through the NSERC-CRD. My team and I send the warmest thank you to you for your financial support and belief in our work.

Last but not least, I must thank my family for their endless support in my pursuit of education. My parents, Dianne and Edward Ridgley, have always encouraged and guided me through life with immense amounts of love and support for whatever path I decide to travel. Their appreciation in my passion for education and research has helped me get to where I am today. I also must thank my sister and her husband, Victoria and David Januszkiewicz, for letting me live with them while I pursued my graduate degree, having such a wonderful home in St. John's is something I will forever be grateful for.

To anyone considering the pursuit of a graduate degree it is a highly rewarding experience where I gained exceptional knowledge in my field as well as life. Education is invaluable, tangible and continual learning is something I will always pursue.

Disclaimer

It is to be noted that the published versions of each paper presented in Chapters 2, 3, and 4 have been slightly modified to satisfy the required thesis format.

Co-Authorship Statement

I, Katherine E. Ridgley, hold the principal author status for all the manuscript chapters (Chapter 2, 3 and 4) in this thesis. However, each manuscript is co-authored by my supervisors (Profs. Assem A. A. Hassan, and Bruce Colbourne) and co-researcher (Ahmed A. Abouhussien), whose contributions have significantly facilitated the development of this work. Dr. Assem A. A. Hassan and Dr. Bruce Colbourne presented the idea for this project to me and it was my task to carry out the work necessary to complete this manuscript and fulfill the masters requirements.

In the papers presented in Chapter 2, 3 and 4, I performed all experimental work including the preparation of the 15 mixtures, the test setup fabrication and the tests performed. I then collected the data from those tests, analysed the data and formulated the results and conclusions presented in this thesis.

My co-researcher Dr. Ahmed A. Abouhussien was present and offered assistance in the experimental phase and assisted me in finalizing the manuscripts for each paper presented. Described below is a detailed breakdown of the work facilitated by my team and I.

- Paper 1 in Chapter 2: Katherine E. Ridgley, Ahmed A. Abouhussien, Assem A. A. Hassan, and Bruce Colbourne (2018) "Characterization of Damage Due to Abrasion in SCC by Acoustic Emission Analysis" Magazine of Concrete Research, Published Online Ahead of Print (http://www.icevirtuallibrary.com/doi/abs/10.1680/jmacr.17.00445)

I was the primary author, with second, third and fourth authors contributing to the idea, its formulation, development, and refinement of the format in which it has been presented.

- Paper 2 in Chapter 3: Katherine E. Ridgley, Ahmed A. Abouhussien, Assem A. A. Hassan, and Bruce Colbourne (2018) "Evaluation of Abrasion Resistance of Self-Consolidating Rubberized Concrete by Acoustic Emission Analysis" Journal of Materials in Civil Engineering (ASCE), 30(8): 04018196 (https://ascelibrary.org/doi/abs/10.1061/%28ASCE%29MT.1943-5533.0002402)

I was the primary author, with second, third and fourth authors contributing to the idea, its formulation, development, and refinement of the format in which it has been presented.

- Paper 3 in Chapter 4: Katherine E. Ridgley, Ahmed A. Abouhussien, Assem A. A. Hassan, and Bruce Colbourne, "Evaluation of Abrasion Resistance of Self-Consolidating Rubberized Concrete by Acoustic Emission Analysis", Materials and Structures (Accepted for Publication: Manuscript # MAAS-D-18-00279R3)

I was the primary author, with second, third and fourth authors contributing to the idea, its formulation, development, and refinement of the format in which it has been presented.

November 26, 2018

Katherine E. Ridgley Date

Table of Contents

List of Tables

List of Figures

List of Symbols, Nomenclature or Abbreviations

AE is the acoustic emission

ASTM is the American Society for Testing and Materials

C.A. is the coarse aggregate

C/F is the coarse to fine aggregate ratio

CR is the crumb rubber

CSS is the cumulative signal strength

dB is the decibel unit

F.A. is the fine aggregate

FA is the fly ash

H (t) is the historic index

HRWRA is the high-range water-reducer admixture

MK is the metakaolin

N is the number of hits

NC is the normal concrete

NDT is the non-destructive testing

SCC is the self-consolidating concrete

SCM is the supplementary cementing material

SCRC is the self-consolidating rubberized concrete

SF is the silica fume

SFs is the synthetic fibers

SG is the slag

SHM is structural health monitoring

S_r is the severity

W/B is the water to binder ratio

1. Introduction and Overview

The civil engineering discipline relies heavily on three core construction materials – steel, timber and concrete. Concrete is the most widely used material worldwide with more than ten billion tons produced each year (Meyer, 2002). Concrete has proven to be a reliable and exceptional building material as it is continually changing and improving. Research develops new concrete materials as the industry pushes towards more sustainable methods. This study focused on filling a niche within concrete research and development that incorporated the use of a high performing concrete adequate for use in structures such as bridges, piers and offshore structures and incorporated some factors related to sustainability. Sustainable concrete structures are more desirable financially and environmentally.

1.1. Background

Abrasion is defined as "the removal of surface material from any solid through the frictional action of another solid, a liquid, or a gas or combination thereof," (McGraw Hill Education, 2002). Abrasion creates discontinuity on a surface from scratching and roughening (McGraw Hill Education, 2002). This problem is very common in areas where concrete interfaces with ice floes in water. It can also occur in concrete floors/roads which become worn down over time due to human or vehicular traffic. Gritty, abrasive substances in high-velocity flowing water can cause cavitation and wear a surface substantially (Scott and Safiuddin, 2015). Abrasion resistance of concrete can therefore be thought of as a materials ability and capacity to resist this form of attack (Scott and Safiuddin, 2015). This resistance

is heavily reliant on the microstructure of the concrete surface. The cement paste, fine and coarse aggregates and paste-aggregate bond are the three factors that carry the bulk of the materials capacity to resist abrasion in all concrete types (Papenfus, 2003).

Self-consolidating concrete (SCC) is widely used in industry and the largest draw to its usage is that it can be employed on projects where reinforcement is dense or where the concrete needs to be placed in areas which may be difficult to access with normal concrete (NC). It is produced in a variety of ways such as using decreased amounts of coarse aggregate, adding in chemical admixtures to reduce water content and incorporating supplementary cementing materials (SCMs) (Lachemi et al., 2007; Das and Chatterjee, 2012; Karahan et al., 2012;Mehta and Monterio, 2014).

Common SCMs used in SCC include fly ash (FA), silica fume (SF), natural pozzolans and/or metakaolin (MK). SCMs are useful in concrete mixtures as they enhance mechanical properties and can improve the fresh properties which is important for creating SCC. SCMs can enhance compressive strength, result in less permeable concretes and increase the overall durability by decreasing permeability and increasing corrosion resistance (Peurifoy, Schexnayder, et al., 2018). Utilizing SCMs is considered a sustainable and economical practice as a majority of the materials are by products of industry. SCMs can also increase abrasion resistance through changing the pore structure and enhancing the compressive strength. For example, SCMs were found to increase abrasion resistance capacity in concrete mixtures which incorporated 10% silica fume when compared to NC samples (Ghafoori and Diawara, 1999). Similarly, NC specimens which used class C and F fly ash

also enhanced the ability to resist abrasion (Liu, 1981). Less emphasis has been placed on researching the other common SCMs such as MK and slag (SG).

Another reusable material which may be used in concrete is waste rubber. Disposal of this material is an increasingly serious issue in the world as the number of vehicle tires scraped each year rises (Thomas, et al. 2014). If disposal is not done properly the consequences could be severe for the environment so researchers have found new ways to repurpose the otherwise discarded rubber and use it for concrete production. The use of crumb rubber (CR) as an ingredient in concrete has been found to have many advantages such as producing eco-friendly lightweight concrete. Experiments with CR have been carried out previously which involved the combination of SCC and CR – which is referred to as self-consolidating rubberized concrete (SCRC) which combines the beneficial factors of both materials (Ismail and Hassan 2016). Unfortunately, CR can have a negative impact on the mechanical properties of SCRC (Najim and Hall, 2012, Rahman et al., 2012). However, the use of CR in conjunction with SCMs can compensate for this loss (Ismail and Hassan, 2016).

Past studies suggest that using MK in the SCC mixture enhances the viscosity and assists the aggregates and CR to bind together (Ismail and Hassan, 2016). As for the effects CR can have on abrasion resistance, some studies illustrated that when it was used in normal concrete it increased the abrasion resistance but had a conversely negative effect on the compressive strength (Thomas et al. 2014, Thomas et al. 2016). Most studies regarding abrasion resistance of CR concretes focus solely on normal concrete and there is an evident lack of research done on SCRC.

Synthetic fibers (SFs) are commonly used in concrete mixtures to change its composition and properties. SFs are typically used to enhance flexural strength, tensile strength and overall toughness of a material (Ismail and Hassan, 2017). Bolat et al. (2014) found that using the optimal dosage of SFs increased the rupture modulus and impact resistance. SFs come in many forms such as polypropylene, nylon, polyethylene and polyester. Similar to CR, SFs will decrease the fresh properties of a mixture making the specified goals for SCC difficult to obtain. There is little to no research concerning the abrasion resistance of SCC with SFs reinforcement.

Abrasion resistance of concrete can be tested for in several ways which are detailed in many ASTM standards. Abrasion damage is typically quantified in two ways – percent of weight lost due to abrasion and depth of wear due to abrasion, this is stipulated in ASTM C944 (ASTM, 2012). For chapters 2, 3 and 4 this data was recorded during testing and used to quantify which samples performed better or worse in comparison to one another. This study attempts to to establish a new method for damage quantification for abrasion resistance.

Acoustic Emission (AE) monitoring is a method for non-destructive testing (NDT) of concrete structures and materials. AE happens when a tested material is damaged and as a result elastic waves are generated from the source of said damage. The waves that are emitted are then recorded by the AE sensors and that data is analyzed to determine the extent and variety of damage (Ziehl, Galati et al. 2008), (Zaki, Chai, et al. 2015). AE monitoring is a well-established form of structural health monitoring (SHM) and has been used previously to evaluate various topics such as: the fracture process in high strength concrete beams (Vidya, Sagar and Prasad, 2009), concrete slab systems (Ziehl, Galati et al.

2008) and for evaluating fatigue damage and acoustic absorption capacity of rubberized and normal concretes (Wang et al. 2013; Ismail and Hassan, 2016a). Although AE monitoring has been used widely in research, there has yet to be any available studies which used AE monitoring to detect and quantify abrasion damage.

1.2. Research Objectives

The target of this study was to establish how abrasion resistance could be affected, either negatively or positively. The previously mentioned three variables were examined to determine which materials would provide improved abrasion resistance. SCC was the concrete type selected for this investigation to evaluate its abrasion resistance compared with NC. Plain SCC is inherently more resistant to abrasion than NC as indicated in a previous study which evaluated 16 mixes with varying w/b ratio and binder content (12 SCC, 4 NC) and found that in every case the SCC samples had increased abrasion resistance 50-70% higher than the NC samples and SCC also exhibted approximately 15-30% higher compressive strength (Ghafoori, Najimi, 2013).

The main objectives of this study were as follows:

- Discover the best performing type of SCMs used in SCC development
- Study the effect of using crumb rubber (CR) in percentages as a fine aggregate replacement to find the optimum level for use in SCC and,
- Examine the influence of adding synthetic fibers (SFs) of differing types and sizes into the SCC mixtures on the abrasion resistance.

- The overarching objective in this study was to perform AE analysis to establish a correlation between the abrasion resistance of all tested mixtures and the sound waves emitted when the abrasion tests were performed.

The first three objectives are focused on in more detail in Chapters 2, 3 and 4 respectively, with the fourth being discussed at length in each chapter. Each sub-study used plain NC and plain SCC as a baseline for comparison of results. This project focused on evaluating the abrasion resistance of a broad variety of SCC mixtures, which had not been looked at extensively in previous studies.

1.3. Thesis Outline

As previously mentioned, the studies overall goal was to determine the abrasion resistance of SCC with SCMs, CR and SFs used in the mixtures to evaluate which materials would have negative and positive effects on the abrasion resistance. Chapter 2 *"Characterization of damage due to abrasion in SCC by acoustic emission analysis"* is a detailed discussion of the effect of SCMs on abrasion resistance and how the AE monitoring was correlated to the damage from the testing. Chapter 3 "*Evaluation of Abrasion Resistance of Self-Consolidating Rubberized Concrete by Acoustic Emission Analysis"* focuses on the abrasion resistance of SCRC and Chapter 4 "*Assessing abrasion performance of self-consolidating concrete containing synthetic fibers using acoustic emission analysis"* looks into the use of SFs at resisting abrasion. The study is concluded in an over-arching Summary in Chapter 5.

1.4. Chapter References

Bolat H, Şimşek O, Çullua M, Durmuş G, Can Ö. The effects of macro synthetic fiber reinforcement use on physical and mechanical properties of concrete. Composites Part B: Engineering 2014; 61: 191-198.

Das D and Chatterjee A (2012) A comparison of hardened properties of fly-ash-based self-compacting concrete and normally compacted concrete under different curing conditions. Magazine of Concrete Research 64(2): 129–141.

El-Chabib, H., and Syed, A. (2013). "Properties of self-consolidating concrete made with high volumes of supplementary cementitious materials." Journal of Materials in Civil Engineering, 25(11), 1579–1586.

Ghafoori N and Diawara H (1999) Abrasion resistance of fine aggregate replaced silica fume concrete. ACI Materials Journal, 96(5): 559–569.

Ghafoori, N., Najimi, M., & Aqel, M. A. (2013). Abrasion resistance of self-consolidating concrete. Journal of Materials in Civil Engineering 26(2): 296-303.

Ismail, M. K., and Hassan, A. A. A. (2016a). "Impact resistance and acoustic absorption capacity of self-consolidating rubberized concrete." ACI Materials Journal, 113(6), 725–736.

Ismail, M. K., and Hassan, A. A. A. (2016b). "Use of metakaolin on enhancing the mechanical properties of SCC containing high percentages of crumb rubber." Journal of Cleaner Production, 125, 282–295.

Ismail MK, Hassan AAA. Impact resistance and mechanical properties of self-consolidating rubberized concrete reinforced with steel fibers. Journal of Materials in Civil Engineering 2017; 29(1): 04016193

Karahan O, Hossain KMA, Ozbay E, Lachemi M and Sancak E (2012) Effect of metakaolin content on the properties self-consolidating lightweight concrete. Construction and Building Materials 31: 320–325.

Lachemi M, Hossain KMA, Patel R, Shehata M and Bouzoubaâ N (2007) Influence of paste/mortar rheology on the flow characteristics of high-volume fly ash self-consolidating concrete. Magazine of Concrete Research 59(7): 517–528.

Liu TC (1981) Abrasion resistance of concrete. ACI Journal 78(5): 341–350.

McGraw-Hill Dictionary of Scientific and Technical Terms, 6th ed., McGraw-Hill, New York, 2002

Mehta P, Monteiro P (2014) Concrete: Microstructure, Properties, and Materials. 4th Edition. 2014 McGraw-Hill Education.

Meyer C. Concrete Materials and Sustainable Development in the United States. Columbia University Special Publication ACI 206, 2002.

Najim, K. B., and Hall, M. (2012). "Mechanical and dynamic properties of self-compacting crumb rubber modified concrete." Construction and Building Materials, 27(1), 521–530.

Ozbay, E., Lachemi, M., and Sevim, U. K. (2011). "Compressive Strength, abrasion resistance and energy absorption capacity of rubberized concrete with and without slag." Materials and Structures, 44(7), 1297–1307.

Papenfus N (2003) Applying concrete technology to abrasion resistance. Proceedings of the 7th International Conference on Concrete Block Paving (PAVE AFRICA 2003), Sun City, South Africa, ISBN Number: 0-958-46091-4.

Peurifoy R, Schexnayder C, Schmitt R, Shapira A. Construction Planning, Equipment, and Methods, Ninth Edition 9th Edition 2018; McGraw Hill Education Publishing.

Sagar RV, Prasad BKR. Laboratory investigations on cracking in reinforced concrete beams using on-line acoustic emission monitoring technique. Journal of Civil Structural Health Monitoring 2013; 3: 169-186.

Scott BD and Safiuddin M (2015) Abrasion resistance of concrete – Design, construction and case study. Concrete Research Letters 6(3): 136–148.

Thomas, B. S., Gupta, R. C., Kalla, P., and Cseteneyi, L. (2014). "Strength, abrasion and permeation characteristics of cement concrete containing discarded rubber fine aggregates." Construction and Building Materials, 59, 204–212.

Thomas, B. S., Kumar, S., Mehra, P., Gupta, R. C., Joseph, M., and Csetenyi L. J. (2016). "Abrasion resistance of sustainable green concrete containing waste tire rubber particles." Construction and Building Materials, 124, 906–909.

Wang, C., Zhang, Y., and Ma, A. (2013). "Investigation into the fatigue damage process of rubberized concrete and plain concrete by AE analysis." Journal of Materials in Civil Engineering, 23(7), 886–892.

Ziehl, P. H., Galati, N., Nanni, A., and Tumialan, J. G. (2008). "In-situ evaluation of two concrete slab systems. II: evaluation criteria and outcomes." Journal of Performance of Constructed Facilities, 22, 217–227.

2. Characterization of Damage Due to Abrasion in SCC by Acoustic Emission Analysis

2.1. Abstract

This investigation evaluates and compares the abrasion resistance of various concrete types by means of acoustic emission (AE) analysis. Normal concrete (NC), self-consolidating concrete (SCC), and SCC with variable supplementary cementing materials (SCMs) were tested under the rotating cutter method for abrasion resistance. The effect of using different SCMs in SCC mixtures including fly ash, metakaolin (MK), silica fume, and slag on the abrasion resistance of SCC was examined. In conjunction with the abrasion testing, AE monitoring was simultaneously conducted on all mixtures using AE attached sensors. AE parameters such as signal amplitude, signal strength, number of hits, duration, and cumulative signal strength (CSS) were collected during the abrasion tests. Three additional parameters were determined through further analyses: b-value, severity (*Sr*), and historic index (*H (t)*). Results from the abrasion tests indicated that the SCC mixture containing MK had the highest abrasion resistance among all tested mixtures. The studied AE parameters including CSS, number of hits, b-value, *H (t)*, and *Sr* were well correlated to the extent of abrasion damage in all tested specimens. The progression of abrasion damage was associated with increased AE activities indicated by high fluctuations in the b-value and *H (t)* along with ever-increasing values of CSS, number of hits, and *Sr*. The AE intensity analysis quantified which ranges for *H (t)* and *Sr* would indicate the extent and severity of the damage due to abrasion by means of developed damage classification charts.

2.2. Introduction

Self-consolidating concrete (SCC) is a highly workable concrete intended for use in heavily reinforced or hard-to-reach areas (Rao et al., 2012; Safiuddin et al., 2012; Aslani, 2013). SCC can be produced through the use of chemical admixtures to reduce the water content, decreasing the proportions of coarse aggregate in the mixture and/or incorporating supplementary cementing materials (SCMs) such as fly ash, silica fume, metakaolin, and/or natural pozzolans (Lachemi et al., 2007; Das and Chatterjee, 2012; Karahan et al., 2012). Similar to any concrete, SCC can be subject to various types of deterioration, depending on the type of the structure and its exposure condition. One of the most important types of this deterioration is the abrasion of concrete surface.

Abrasion is a form of natural attack on concrete, which can be defined as the process of scraping or wearing away of a material. Concrete abrasion can occur in several ways, including wear on floors due to human traffic, wear due to vehicles, abrasive substances in flowing water, and/or high-velocity waters that create cavitation (Scott and Safiuddin, 2015). Abrasion can also occur in areas with heavy ice flow when concrete is used in Arctic environments (Scott and Safiuddin, 2015). Resistance to abrasion depends on the hardness of the concrete system as a whole (aggregate and paste hardness combined) and the aggregate/paste bond (Papenfus, 2003). Aggregate hardness is a very important aspect as it makes up the majority of the mix proportions (Papenfus, 2003) but in the case of SCC, less coarse aggregate is used to give it the flowability it requires thus putting more dependence for the abrasion resistance on the paste. The paste strength is enhanced with materials which

have higher surface area and can adhere to the aggregates to create fewer air voids in the system.

Abrasion resistance of concrete can be increased by increasing the binder content (at a given W/B ratio), using SCMs (which may depend on the age of testing), using superplasticizers to optimize the water content (reduce the W/B), applying sufficient consolidation, and/or using more durable aggregates (Papenfus, 2003; Turk and Karatas, 2011). Abrasion resistance of concrete can be tested in a variety of ways according to the available ASTM standards. For example, ASTM C 779 tests the abrasion resistance of horizontal concrete surfaces in three different test setups depending on the type and degree of abrasive force (ASTM, 2012). Also, the ASTM C 418 method evaluates the abrasion resistance of concrete via sandblasting (ASTM, 2012). This procedure simulates the action of waterborne abrasives and abrasives under traffic on concrete surfaces. On the other hand, ASTM C 1138 is an underwater concrete abrasion test intended to simulate the behaviour of swirling water containing transported solid objects that produce abrasion of concrete and cause potholes and related effects (ASTM, 2012). The simplest abrasion test setup used in the literature on various concrete types is the ASTM C 994 rotating cutter method (ASTM, 2012). This test method has proven successful in past studies of highway and bridge concrete surfaces subject to traffic (Dong et al., 2013). It was this particular method (ASTM C944, rotating cutter method) which was selected for this study due to its reliablity in practice for testing the abrasive wear process on concrete

The utilization of SCMs in the SCC mixtures is anticipated to improve their abrasion resistance. Previous studies on normal-vibrated concretes confirmed that fly ash class C

and F showed better abrasion resistance than Portland cement concrete (Liu, 1981). Similarly, silica fume concrete has shown to be more resistant to wear with increasing amounts of the material, up to 10% (Ghafoori and Diawara, 1999). Turk and Karatas (2011) evaluated the abrasion of SCC with varying dosages of fly ash and silica fume through the use of the ASTM C779 test. Their results showed that the SCC with silica fume had the least amount of wear (Turk and Karatas, 2011). Yet, the effect of including other types of SCMs (such as metakaolin and slag) on the abrasion resistance of SCC mixtures is lacking. Acoustic emission (AE) is a method of non-destructive testing (NDT) and structural health monitoring (SHM) of civil infrastructure. It can be useful when visual inspection cannot be carried out and/or when regular site visits for physical monitoring are not feasible. AE occurs when transient waves are generated from a localized area due to any damage within a solid material (Invernizzi et al., 2013). AE sensors gather these waves and the data can then be analyzed to quantify and characterize the types of damage that may have occurred and identify the source location of this damage (Bunnori et al., 2011). AE technique has a wide variety of uses in NDT and SHM for concrete materials/structures. For example, AE monitoring has been used to detect and quantify various damage mechanisms in concrete, including evaluating the fracture process of high-strength concrete beams (Vidya Sagar and Prasad, 2009), early crack detection in concrete structures (Bunnori et al., 2011), crack propagation in RC shear walls (Farhidzadeh et al., 2012), and many other structural applications. AE is sensitive to micro-cracking, making it successful in being able to monitor and detect deterioration and damage within a concrete test specimen (Invernizzi et al., 2013).

AE has yet to be used to monitor damage due to abrasion, thus warranting further investigation. AE technique can be used to remotely monitor concrete abrasion or surface wear in areas difficult to access or inspect. For instance, offshore structures, which may be exposed to ice abrasion, could be monitored using AE sensors. The main objective of this study is to utilize AE monitoring to detect the damage due to abrasion in variable SCC (with different SCMs) and normal-vibrated concrete mixtures. The study attempts, in particular, to relate the damage from the abrasion to the recorded AE activity during the abrasion test. This relation will then lead to being able to diagnose the damage from the abrasion by evaluating the signals given off by the AE phenomenon and gathered by the sensors.

2.3. Experimental Procedure

2.3.1. Materials Properties and Mixture Design

Six concrete mixtures were developed and tested in this study. Four of the six mixtures were SCC containing fly ash (FA), metakaolin (MK), silica fume (SF), and ground granulated blast furnace slag (SG). The other two tested mixtures were plain SCC and normal concrete (NC), chosen to act as control mixtures. The four mixtures with SCMs had replacement proportions of 30% FA, 20% MK, 8% SF, and 30% SG. These replacement levels were obtained from a previous study (Abouhussien and Hassan, 2015) conducted to evaluate the optimum percentage of each of these SCMs in concrete. All tested mixtures had a total cementitious content of 500 kg/m3. The water-to-binder (W/B) ratio was set at a constant value of 0.4 in this investigation. The coarse-to-fine aggregate (C/F) ratio was

0.7 for the SCC mixtures and 2.0 for the normal-concrete mixture. The normal-concrete mixture was designed with the same binder content and W/B ratio as the other tested SCC mixtures to highlight the influence of increasing the C/F ratio on the abrasion resistance. A high-range water-reducing admixture (HRWRA) was used in the SCC admixtures to maintain proper workability and to create adequate slump flow in the range of ~700 ± 50 mm, as per ASTM C1611 (ASTM, 2009). Each of the six tested mixtures used type GU Canadian Portland cement conformed to ASTM Type I with a specific gravity of 3.15 (ASTM, 2017). The two types of aggregate used were natural sand and 10-mm coarse aggregate. Both aggregates had a specific gravity of 2.6 and water absorption of 1%. The specific gravities of FA, MK, SF, and SG were 2.38, 2.5, 2.27, and 2.9, respectively. The HRWRA used was similar to that described in ASTM C 494 Type F (ASTM, 2013), with a specific gravity of 1.2 and pH of 9.5. **Table 2-1** shows the details of the six mixtures developed in this study.

Table 2-1 Mixture Proportions

Mixture Type	Cement	SCM (%)	SCM (kg/m^3)	C/F	W/B	C.A. (kg/m^3)	F.A. (kg/m^3)	Water (kg/m^3)	HRWRA (l/m^3)
NC	500	0	0	2.0	0.4	1111.53	555.77	200	0
SCC	500	0	0	0.7	0.4	686.54	980.77	200	2.37
FA	350	30% FA	150	0.7	0.4	670.04	957.20	200	2.08
MK	400	20% MK	100	0.7	0.4	677.70	968.14	200	5.42
SF	460	8% SF	40	0.7	0.4	681.27	973.24	200	4.17
SG	350	30% SG	150	0.7	0.4	682.14	974.49	200	2.25

2.3.2. Test Sample Details, Abrasion Test, and AE Monitoring Setup

For each mixture, three cylinders and three prisms were cast. All specimens were cured at 25°C in a moist-curing room for a period of 28 days before testing. The cylinder samples

were used to test the compressive strength (2:1 cylinder strength) according to ASTM C 39 (ASTM, 2011), while the prism samples were cut into three 100-mm cubes for the preparation of the ASTM C 944 abrasion test (ASTM, 2012). The prisms were cut into 100-mm cubes to maximize the area of abrasion on the samples as the ASTM C944 stipulates the rotating cutter must be 82.5-mm in diameter (ASTM, 2012). Three samples were used for each mixture as this is a common standard in concrete testing methods to allow for adequate average results.

The abrasion test consisted of a drill press with a chuck capable of holding and rotating the cutter and constantly applying a force of 98 N on the specimen being tested (**Figure 2-1**). The abrasion test was set to run for six rounds, one-minute intervals each, with a total abrasion time of six minutes. The weight loss of the specimens was taken after each of the one-minute intervals to calculate the percent mass loss due to abrasion. In addition to measuring the weight loss, the depth of wear resulting from abrasion was also estimated using electronic calipers. These two parameters were used to evaluate the abrasion rate as they are the recommended method for quantification of damage in the ASTM standard C944 Rotating Cutter Method.

Each mixture has three samples undergo the abrasion and compression testing to estimate the average result. The surface used to evaluate the abrasive wear on the specimens was the cast surface rather than the cut surface, this was done to ensure the test was performed on the strongest side of the sample from a pore-structure perspective. The cut surface would already be damaged and would not provide true results.

Figure 2-1 Abrasion Test Setup

Piezoelectric AE sensors with integral preamplifier (model R6I-AST) were attached to the cube samples and connected to a data acquisition system to record the signals being emitted during the test (Physical Acoustics, 2005; Mistras Group, 2007). The system has a set amplitude threshold of 40 dB and a full list of the other parameters as shown in **Table 2-2**. The amplitude, signal strength, duration, energy and absolute energy, counts, rise time, average frequency, and peak frequency were detected and recorded during the test. Full descriptions of these parameters and more information on AE terminology can be found elsewhere (ASTM, 2014).

Table 2-2 AE System Setup

AE hardware setup	
Threshold	40 dB_{AE}
Sample rate	1 MSPS
Pre-trigger	256 μs
Length	1k points
Preamp gain	40 dB
Preamp voltage	28
Analog filter	1-50 kHz
Digital filter	100-400 kHz
Peak definition time	200 μs
Hit definition time	800 μs
Hit lockout time	1000 μs
Maximum duration	1000 μs

2.3.3. Acoustic Emission Intensity Analysis

AE intensity analysis is a method of analysis which looks at the strength of the AE signals obtained during testing to be able to develop additional AE parameters and eventually relate them to types and extent of damage in concrete. Some parameters such as amplitude and signal strength are set within the AE data acquisition system, while others have to be calculated post-testing. These calculated AE intensity analysis parameters can be used to create damage intensity classification charts. This analysis was carried out in this study in order to determine and quantify the damage to the concrete due to abrasion during testing. The AE signal strength data, which was collected during the abrasion tests, was used to complete an intensity analysis to assess the effects of abrasion in all tested mixtures. This analysis involved calculating two additional AE parameters: severity (Sr) and historic index (*H (t)*). Historic index indicates sudden variations in the cumulative signal strength (CSS) versus time curve and was calculated using **Equation 1**.

1. $H(t) = \frac{N}{N-K} \frac{\sum_{i=K}^{N} S_{oi}}{\sum_{i=1}^{N} S_{oi}}$

In this equation, N is the cumulative number of hits until time (t), and Soi can be denoted as the signal strength of the ith event. Severity can then be calculated based on the average signal strength of the J hits by using **Equation 2.**

2. $S_r = \sum_{i=1}^{J} \frac{S_{oi}}{J}$

With regards to the values of the constants K and J in **Equations 1** and **2**, their values may depend on the damage mechanism and type of structure (Vélez et al., 2015). The values of K and J have been previously determined in other tests (ElBatanouny et al., 2014; Abdelrahman et al., 2015), which incorporated AE analysis in concrete structures and indicated their suitability for use in concrete materials/structures.

The value of K was determined depending on the cumulative number of hits (N) as follows: a) K = 0: if N ≤ 50, b) K = N – 30: if 51 ≤ N ≤ 200, c) K = 0.85N: if 201 ≤ N ≤ 500 and d) K = N – 75: if N ≥ 501.

Instead of being calculated, J was set to a constant value of 50 (ElBatanouny et al., 2014; Abdelrahman et al., 2015). The magnitudes of both *H (t)* and *Sr* were calculated using **Equations 1 and 2** for all tested samples.

2.3.4. Acoustic Emission B-Value Analysis

In addition to the AE intensity analysis, further b-value analysis on the AE data was completed for the aim of evaluating abrasion damage in all tested specimens. This b-value analysis utilizes the amplitude and number of hits to calculate an additional parameter

known as b-value. The b-value is originally based on seismic equations and has successfully been employed to indicate the distribution of the frequency-magnitude of AE events to assess different damage mechanisms in concrete (Colombo et al., 2003; Ohtsu and Tomoda, 2008; ElBatanouny et al., 2014). The b-value has been calculated throughout the test periods for all tested specimens by using **Equation 3**.

3. $\log(N) = a - b\log(A)$

Where N = the number of hits having amplitudes larger than A, A = the signal amplitude (dB), a = an empirically derived constant, and b = the b-value (Colombo et al., 2003; Ohtsu and Tomoda, 2008; ElBatanouny et al., 2014).

2.4. Results and Discussion

As previously stated, the percent weight loss for each sample was measured during the abrasion test at one-minute intervals for a total of six minutes. The wear depth was also measured to further show the physical effects of the abrasion on the concrete. The results from this data collection during testing can be seen in **Tables 2-3** and **2-4**. **Figure 2-2** presents the average weight loss plotted against time after each minute for all tested samples. The average percent weight loss was calculated by taking the average results of the three replicated samples of each mixture. It appears from **Figure 2-2** that the weight loss followed a linear relationship over time. The tested samples lost more weight as the time increased up to six minutes. This linear relationship could be related to that the increase in the depth of wear was more associated with a wear in the fine materials rather than the coarse aggregate particles.

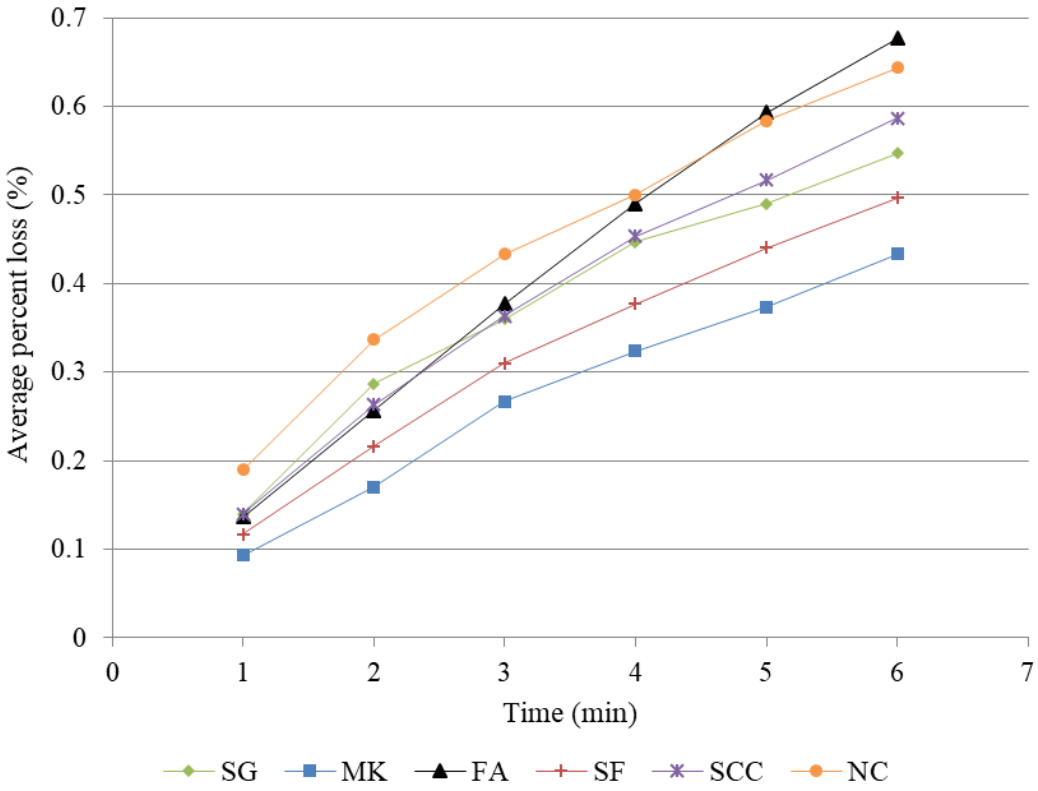

Figure 2-2 Average Percent Loss (%) vs. Time (s)

Table 2-3 Percent Loss Due to Abrasion During Testing

Mixture name	Sample number	Percent loss (%)						Average percent loss (%)
		1 min	2 min	3 min	4 min	5 min	6 min	
NC	S1	0.21	0.35	0.46	0.53	0.64	0.70	0.64
	S2	0.18	0.35	0.43	0.50	0.58	0.63	
	S3	0.18	0.31	0.41	0.47	0.53	0.60	
SCC	S1	0.17	0.33	0.46	0.59	0.66	0.76	0.59
	S2	0.09	0.14	0.22	0.27	0.35	0.40	
	S3	0.16	0.32	0.41	0.50	0.54	0.60	
FA	S1	0.11	0.19	0.27	0.36	0.45	0.53	0.68
	S2	0.17	0.32	0.48	0.61	0.72	0.80	
	S3	0.13	0.26	0.38	0.50	0.61	0.70	
MK	S1	0.08	0.15	0.21	0.27	0.31	0.38	0.43
	S2	0.09	0.18	0.26	0.34	0.42	0.46	
	S3	0.11	0.18	0.33	0.36	0.39	0.46	
SF	S1	0.11	0.22	0.31	0.38	0.44	0.50	0.50
	S2	0.11	0.19	0.28	0.35	0.41	0.47	
	S3	0.13	0.24	0.34	0.40	0.47	0.52	
SG	S1	0.12	0.24	0.32	0.40	0.44	0.48	0.55
	S2	0.13	0.31	0.36	0.46	0.51	0.56	
	S3	0.17	0.31	0.40	0.48	0.52	0.60	

Table 2-4 Wear Depth and Compressive Strength

Mixture name	Sample number	Wear depth (mm)	Average wear depth (mm)	Compressive strength (MPa)	Average compressive strength (MPa)
NC	S1	1.08	0.99	52.1	52.5
	S2	0.97		51.5	
	S3	0.92		53.8	
SCC	S1	0.80	0.93	54.7	54.4
	S2	0.84		53.8	
	S3	1.15		54.6	
FA	S1	0.77	1.18	50.7	51.5
	S2	1.44		52.3	
	S3	1.34		51.4	
MK	S1	0.61	0.60	73.2	72.6
	S2	0.70		72.5	
	S3	0.50		72.6	
SF	S1	0.31	0.66	69.8	68.7
	S2	0.78		67.9	
	S3	0.88		68.4	
SG	S1	0.94	0.86	60.9	58.6
	S2	0.83		57.3	
	S3	0.81		57.8	

2.4.1. Effect of Abrasion Damage on Acoustic Emission Parameters

The graphs in **Figure 2-3** represent the results of one of the tested samples from this study, as an example. The solid curves in **Figure 2-3(a)** through **Figure 2-3(e)** show the variations in *H (t)*, Sr, CSS, cumulative number of hits, and b-value, respectively, throughout the abrasion test. The dotted curve in each figure shows the percentage of loss due to abrasion of the same sample over the course of the testing period. The selected sample illustrated was the FA sample number one (FA S1). This sample is used as a representation of results from this test as the rest of the mixtures and each of their samples all followed similar

trends. The results of these AE parameters from the rest of the tested samples obtained at one and six minutes can be seen in **Table 2-5**. The results of *H (t)* shown in **Table 2-5** represent the maximum values obtained through the one- and six-minute intervals for each sample.

a)

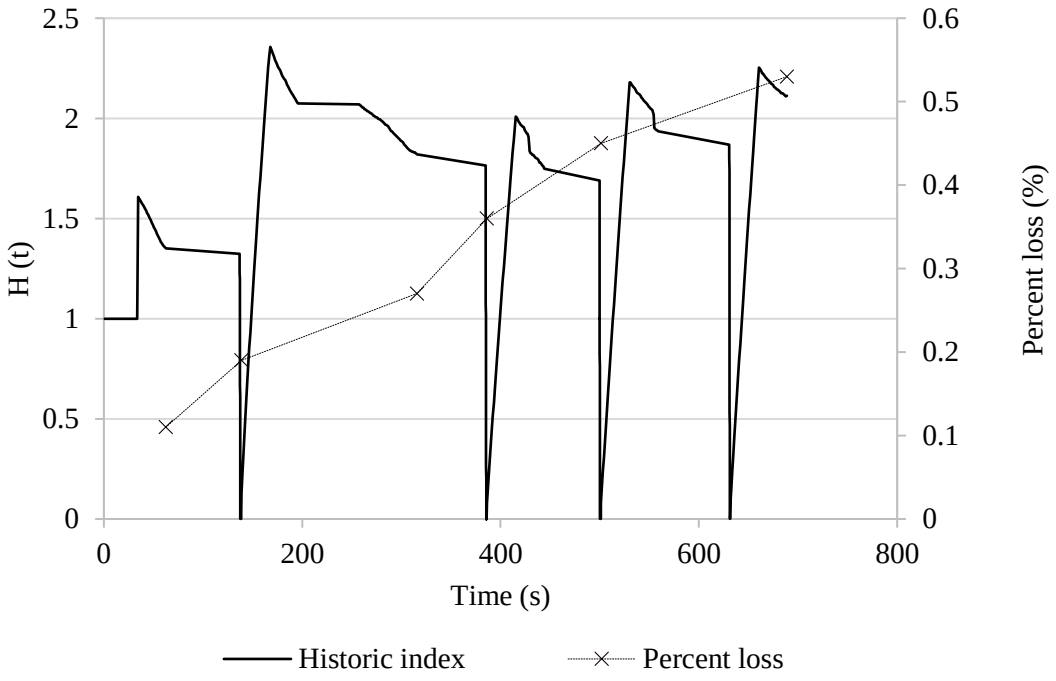

b)

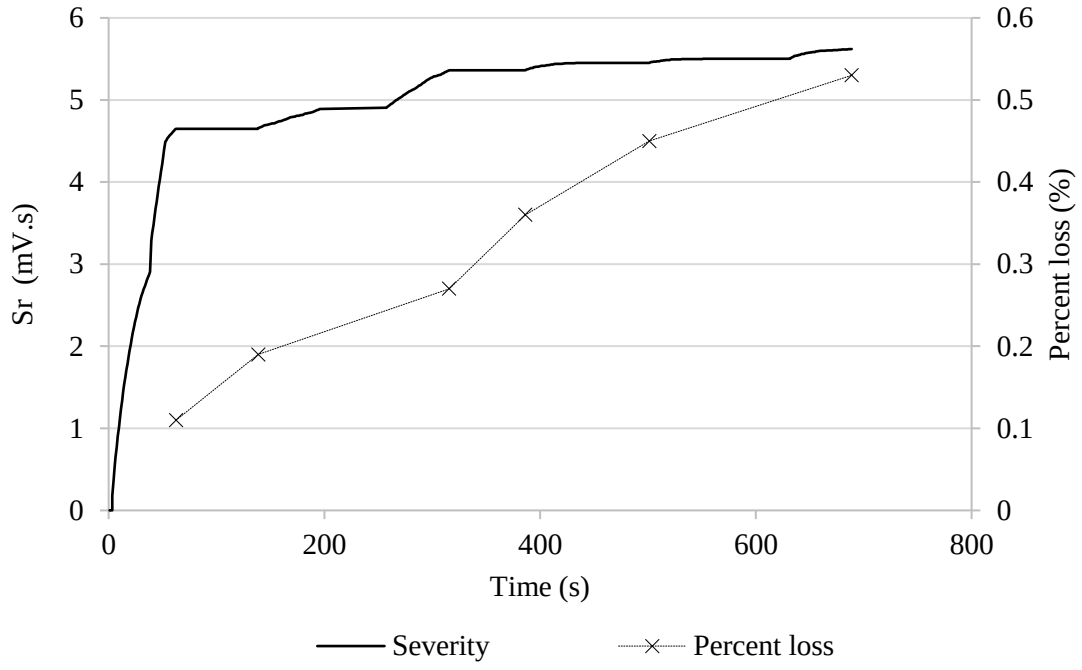
Sr (mV.s)
Percent loss (%)
Time (s)
Severity
Percent loss

c)

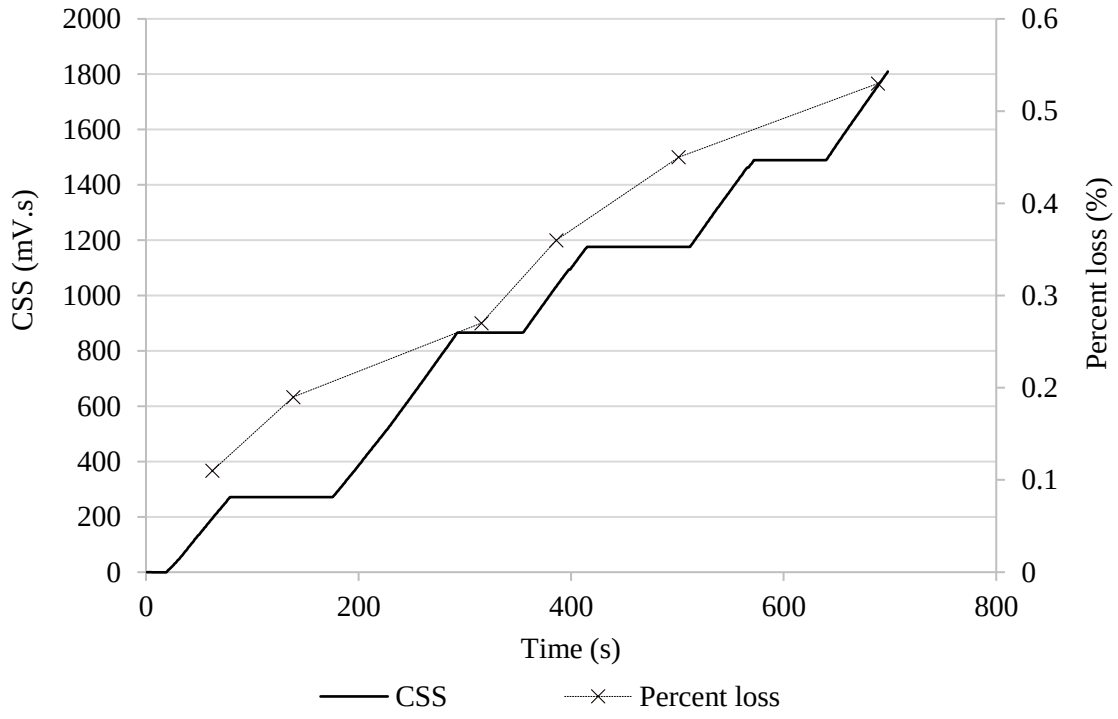
CSS (mV.s)
Percent loss (%)
Time (s)
CSS
Percent loss

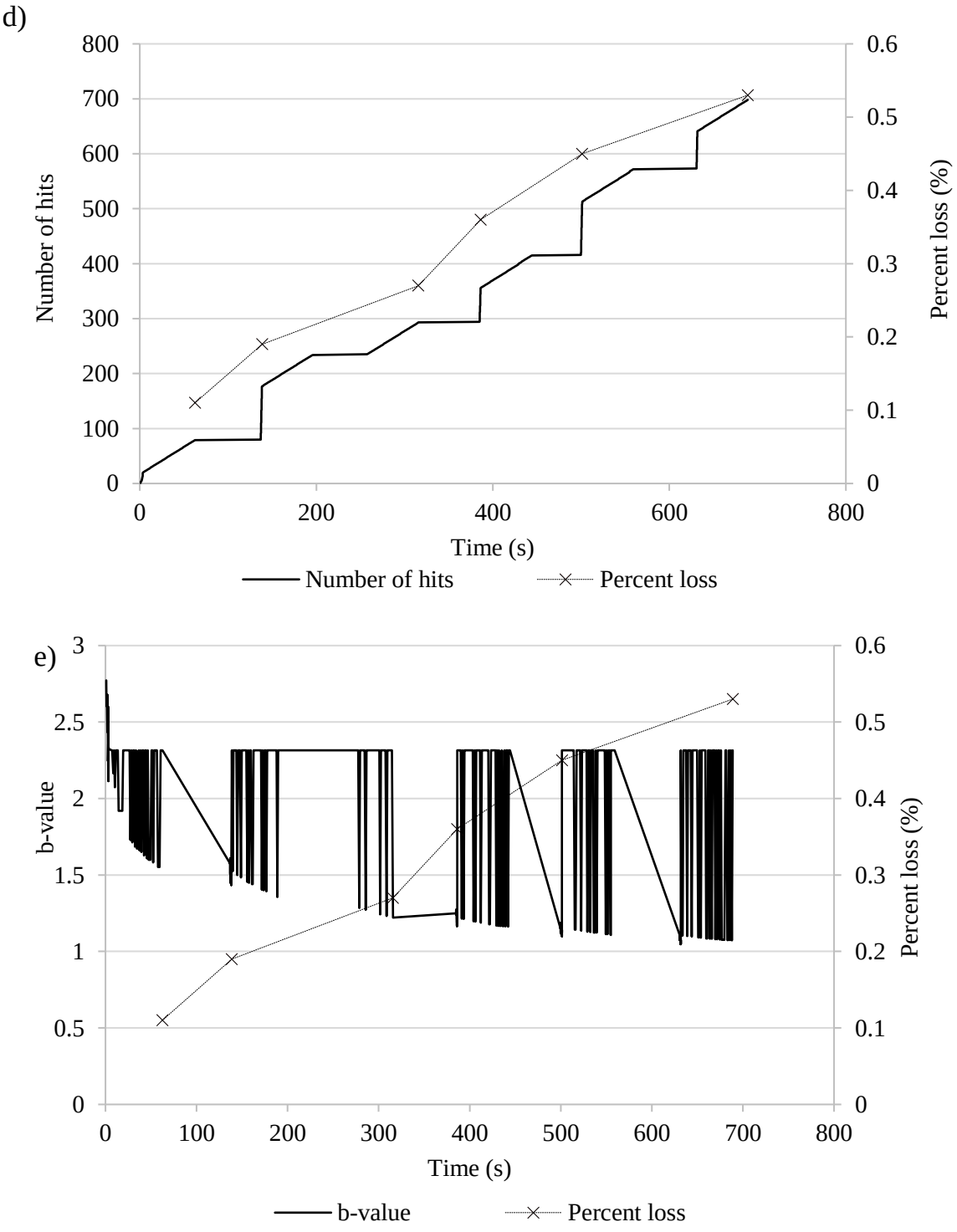

Figure 2-3 AE Parameters Versus Time For FA S1 a) *H (t)*, b) *Sr*, c) CSS, d) Cumulative Number of Hits, and e) b-Value

H (t) indicates the changes in the slope of the CSS versus time curve. *H (t)* is a weighted parameter that varies according to the values of the constant K. From **Figure 2-3(a)**, it can be seen that *H (t)* rises and falls as the abrasion is consistently increasing. The values of *H (t)* kept fluctuating throughout the test at a specific value (2.0), indicating that an almost constant increase in abrasion damage was occurring in the sample over the time. If *H(t)* were to have less fluctuation it would indicate decreased acoustic emission occuring. On the other hand, the CSS versus time curve (**Figure 2-3(c)**) showed a continual increase during the test period (reaching a maximum value of 1810 mV.s), matching that of the changes in weight loss due to abrasion. Cumulative number of hits versus time (**Figure 2-3(d)**) follows the same patterns as the CSS graph: gradual increase over time. *Sr* variations in **Figure 2-3(b)** also showed a continual increase as well; it had an immediate peak following the test initiation and then had a more gradual increase over time (maximum value of 5.62 mV.s). This trend may be attributed to the method of calculating *Sr* which is based on the average of the 50 signals having the maximum signal strength throughout the test.

As seen in **Figure 2-3(e)**, the magnitudes of the b-value followed considerable fluctuations throughout the test. It can also be noticed from the figure that as the abrasion damage progressed, higher fluctuations in the b-value were obtained (and also matched the increasing trend of the Sr, CSS, and cumulative number of hits). In addition, the b-values indicated an overall reduction trend as the abrasion damage increased until reaching its minimum value (1.07) at the end of the test. It has been reported in the literature that the decline in the b-value can be related to damage progression in concrete (increased AE

activity) (Colombo et al., 2003; Ohtsu and Tomoda, 2008; ElBatanouny et al., 2014). Across the many samples tested, a direct correlation was observed between the abrasion damage and the studied AE parameters (**Table 2-5**). More specifically, the values of *Sr*, CSS, and cumulative number of hits will increase and the b-value will decrease as the amount of weight loss increases due to abrasion over time. Besides, *H (t)* values will keep changing around a specific value in the course of the test, representing the amount of abrasion damage occurring in each sample. The acoustic emission data collected for analysis in each of the samples is generated at the point of interface between the cutter and the surface of the sample and just below.

Table 2-5 AE Parameters For Each Mixture at One and Six Minutes of Abrasion

Mix name	Sample #	Signal amplitude (dB)		Number of hits		CSS x 10^3 (mV.s)		*H (t)*		S_r (mV.s)		b-value	
		1 min	6 min	1 min	6 min	1 min	6 min	1 min	6 min	1 min	6 min	1 min	6 min
NC	S1	82	82	137	758	0.44	2.32	2.64	1.74	4.09	6.01	1.49	1.05
	S2	82	80	130	765	0.33	2.23	2.25	2.77	4.09	5.99	1.49	1.01
	S3	87	84	110	670	0.48	2.42	2.15	1.47	5.59	6.01	1.39	1.14
SCC	S1	85	82	115	461	0.36	2.23	1.98	1.35	4.14	5.51	1.45	1.14
	S2	87	86	112	391	0.40	2.34	2.04	1.58	4.55	5.52	1.58	1.25
	S3	87	74	103	1143	0.37	2.41	2.04	2.7	4.55	5.55	1.51	0.95
FA	S1	79	71	79	698	0.27	1.81	1.61	2.36	4.65	5.62	1.55	1.07
	S2	84	75	97	1138	0.27	2.75	2.20	5.33	3.82	6.55	1.52	0.92
	S3	82	80	103	1026	0.32	2.67	1.54	3.54	4.49	6.07	1.49	0.96
MK	S1	88	83	60	407	0.19	2.00	1.44	1.44	3.45	4.78	1.78	1.41
	S2	85	84	66	395	0.28	2.14	1.22	1.33	3.75	4.73	1.76	1.44
	S3	85	70	65	560	0.29	1.77	1.23	1.69	4.44	4.79	1.66	1.32
SF	S1	81	84	77	395	0.26	2.12	1.50	1.50	3.62	5.02	1.69	1.28
	S2	83	73	68	604	0.29	2.14	1.35	2.24	3.94	5.09	1.57	1.24
	S3	84	81	69	447	0.34	2.24	1.36	1.62	4.66	5.04	1.58	1.25
SG	S1	86	84	122	493	0.29	2.15	2.19	1.85	4.24	5.25	1.48	1.13
	S2	87	84	120	493	0.31	2.20	2.13	1.71	4.33	5.21	1.46	1.18
	S3	87	80	118	559	0.32	2.20	2.11	1.92	4.56	5.27	1.5	1.26

2.4.2. Effect of Concrete Type on Abrasion Resistance and Acoustic Emission Data

Two types of concrete were evaluated in this study: SCC and NC (with a higher C/F ratio). The NC mixture showed an average wear depth of 0.99 mm and average percent loss of 0.64%. Also, the average compressive strength of the NC mixture at 28 days was 52.4 MPa. In comparison, the SCC mixture (without SCMs) had improved results with an average wear depth and percent loss of 0.93 mm and 0.59%, respectively, and an average compressive strength of 54.3 MPa. As seen in **Figure 2-2**, above the trend in the SCC mixture line is much lower than the NC mixture line. It should be noted that the percentage of C/F ratio in the mixture plays an important role in concrete abrasion. In this investigation, both SCC and NC mixtures had relatively high cement content (500 kg/m3) and relatively low W/B ratio (0.4), creating a stronger paste to resist abrasion. And because SCC had higher mortar content (less coarse aggregate), it showed higher resistance to abrasion compared to NC mixtures. This reasoning would only be valid in the case that the strength of the mortar is higher than that of the coarse aggregates. In addition, studies show that optimum compaction is valuable for good abrasion resistance (Papenfus, 2003). SCC is inherently more compactable than NC, giving it that added advantage (improved abrasion resistance). It is worth noting that, the increase in the compressive strength of SCC compared to NC mixture could also be another reason of the higher abrasion resistance of SCC over the NC counterpart.

With regards to the AE data, the amplitude did not vary drastically with the change in concrete type. **Figure 2-4** shows the amplitudes for each sample in all mixtures after one minute of abrasion testing. It can be observed from the figure that changing concrete type (NC to SCC) did not significantly affect AE signal amplitudes. On the other hand, the other AE parameters such as number of hits, CSS, b-value, *H (t)*, and *Sr* did display some variations with the change in concrete type. The SCC control mixture had an average number of hits of 655 (9% lower than that of NC), average CSS of 2320 mV.s (1% lower than that of NC), average b-value of 1.11 (4% higher than that of NC), average *H (t)* of 2.70 (6% lower than that of NC), and average *Sr* of 5.53 mV.s (8% lower than that of NC) (**Table 2-5**). And because SCC samples outperformed NC in terms of abrasion resistance, it can be concluded that if a concrete material has improved abrasion resistance, the number of hits, CSS, *H (t)*, and *Sr* parameters will decrease whereas the b-value will increase. These results indicate that varying the concrete type yields changes in the abrasion resistance as well as the studied AE parameters (number of hits, CSS, b-value, *H (t)*, and *Sr*) with no evident impact on the resulting AE signal characteristics (signal amplitude).

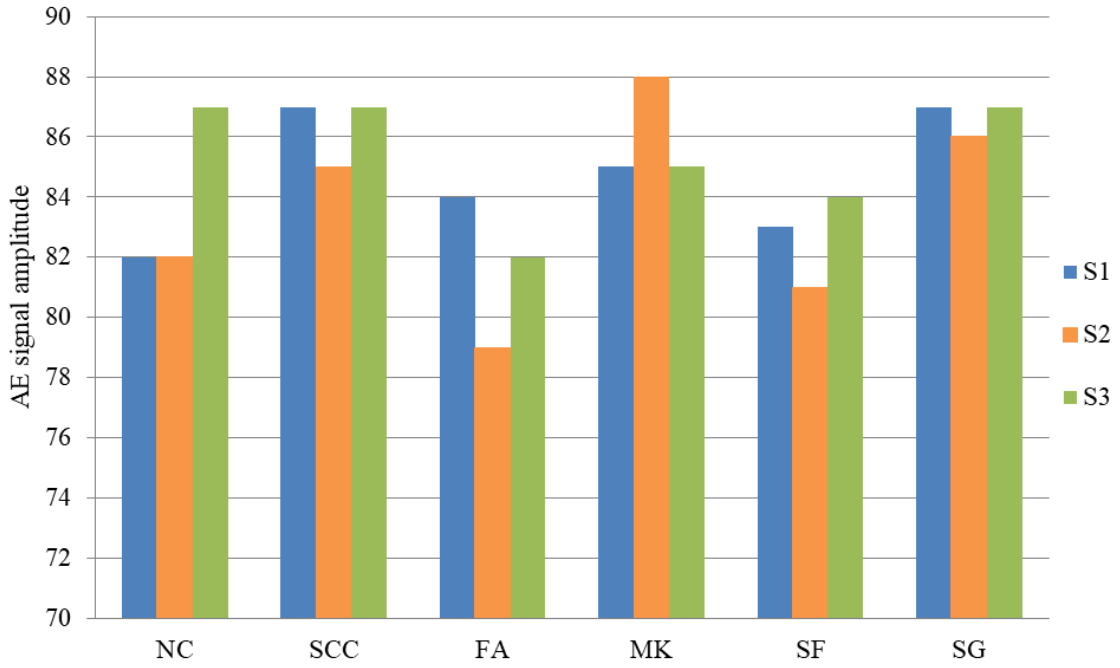

Figure 2-4 Amplitude at One Minute Versus Mixture Type

2.4.3. Effect of SCMs on Abrasion Resistance and Acoustic Emission Data

Figure 2-2 shows the average weight loss over time due to abrasion in all tested mixtures. Significant variations in the abrasion damage were observed from this figure among the tested SCC mixtures with different SCMs. The MK mixture proved to have the highest abrasion resistance of all tested mixtures, with a total average percent loss of 0.43% (**Table 2-3**). This result was anticipated as the compressive strength is correlated to the abrasion resistance (Scott and Safiuddin, 2015); this mixture also had the highest average compressive strength at 28 days (seen in **Table 2-4**). Moreover, MK has a very high pozzolanic reactivity, which makes the paste of this mixture much stronger and leads to a higher abrasion resistance. NC and FA mixtures had the least abrasion resistance as they also had the lowest values for average compressive strength. The results of surface wear

depth also showed a similar trend of variation as the variation in wear loss. MK samples had the least amount of wear depth (0.60 mm) and FA samples had the most (1.18 mm). The SCC mixtures with SCMs are ranked from the lowest to highest abrasion resistance as follows: FA, SG, SF, and MK. The average percent loss and wear depth due to abrasion of these SCMs mixtures, in that order, were 0.68%, 0.55%, 0.50% and 0.43%, and 1.18, 0.86, 0.66, and 0.6 mm, respectively. In general, the results of SCC with SCMs were significantly better than the NC and SCC control mixtures. These results matched the outcomes of a previous study, which indicated that the addition of silica fume as an SCM to NC and SCC significantly improved its abrasion resistance (Ghafoori and Diawara, 1999; Turk and Karatas, 2011). The only exception to this rule is the FA mixture, which had higher percentage of weight loss and larger wear depth compared to the NC mixture. However, the compressive strength of FA mixture was slightly lower than NC mixture, which can directly affect the abrasion resistance of a mixture.

Regarding the AE data, changing the SCM type did not seem to have a significant impact on the signal amplitudes, as can be noticed from **Figure 2-4**. Nevertheless, other AE parameters including the number of hits, CSS, b-value, *H (t)* and *Sr* showed different values for each mixture according to its abrasion performance. For example, the SCC control mixture had an average number of hits of 665, CSS of 2320 mV.s, b-value of 1.11, *H (t)* of 2.70, and *Sr* of 5.53 mV.s at the end of the test. The average values of these AE parameters for the MK mixture, in the same order, were 563, 1970 mV.s, 1.39, 1.69, and 4.77 mV.s, indicating improved abrasion resistance (**Table 2-5**). This result further confirms the correlation between the increased abrasion resistance and decreased number of hits, CSS,

H (t), and *Sr* and increased b-value magnitudes, indicating a strong correlation between the abrasion resistance and the studied AE parameters in all mixtures.

2.4.4. Abrasion Damage Quantification Using Acoustic Emission Intensity Analysis

As the abrasion damage occurs, the values of intensity analysis parameters (*H (t)* and *Sr*) increase over time, which was seen across all the mixtures tested in this study. This subsection covers the damage quantification analysis performed on each of the tested mixtures. The graph seen in **Figure 2-5** relates the corresponding *H (t)* and *Sr* values to certain ranges of depth of wear due to abrasion. The data used was taken at six minutes where the maximum amount of damage occurred in each tested sample (three samples from each mixture). Four ranges of depth wear are detected from this figure. The depth of wear due to abrasion ranges across samples from 0.31 to 1.44 mm. The majority of the data points fall in the 0.77 to 0.88 mm range, with some outliers at the maximum and minimum points. In **Figure 2-5**, for example, at a severity value and a historic index of around 5.0 mV.s and 2.0, respectively, the range for the abrasion wear depth could be predicted to be approximately 0.77 to 0.88 mm. This data quantification chart can ideally be used to identify if abrasion has occurred and evaluate its severity. It should be noted that this data is limited to the rotating cutter test method used in this study. A different test may yield slightly varied data for abrasion intensity parameters. Therefore, it's important to adopt the appropriate abrasion test method that simulates the actual concrete structures.

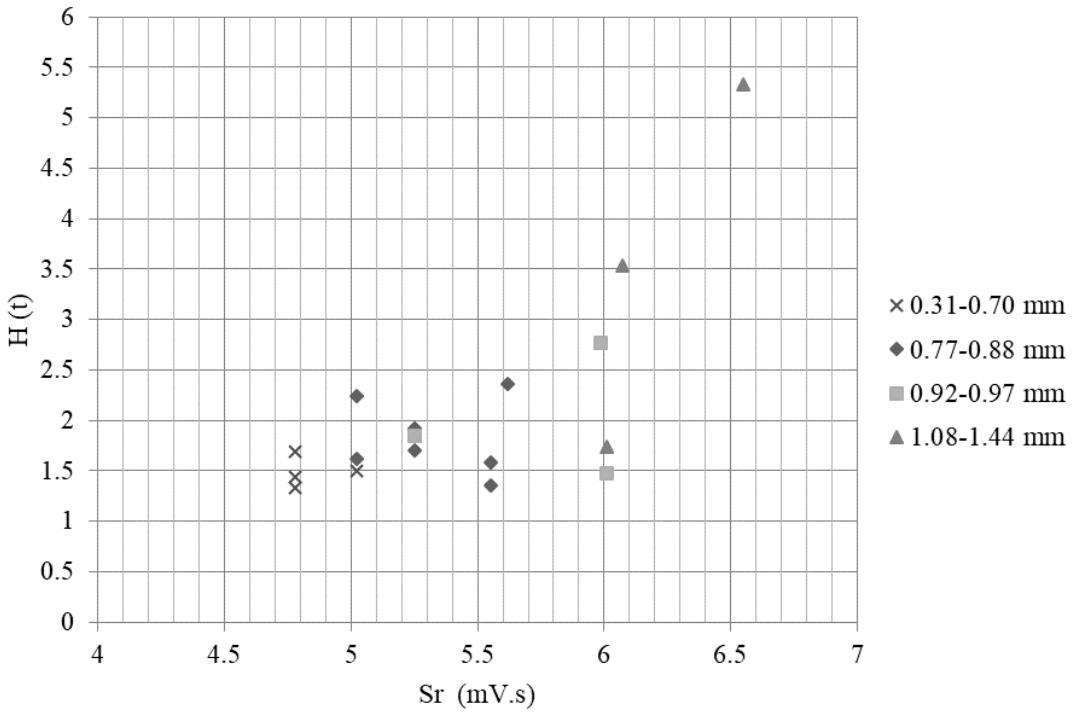

Figure 2-5 Abrasion Damage Quantification Chart With Depth of Wear

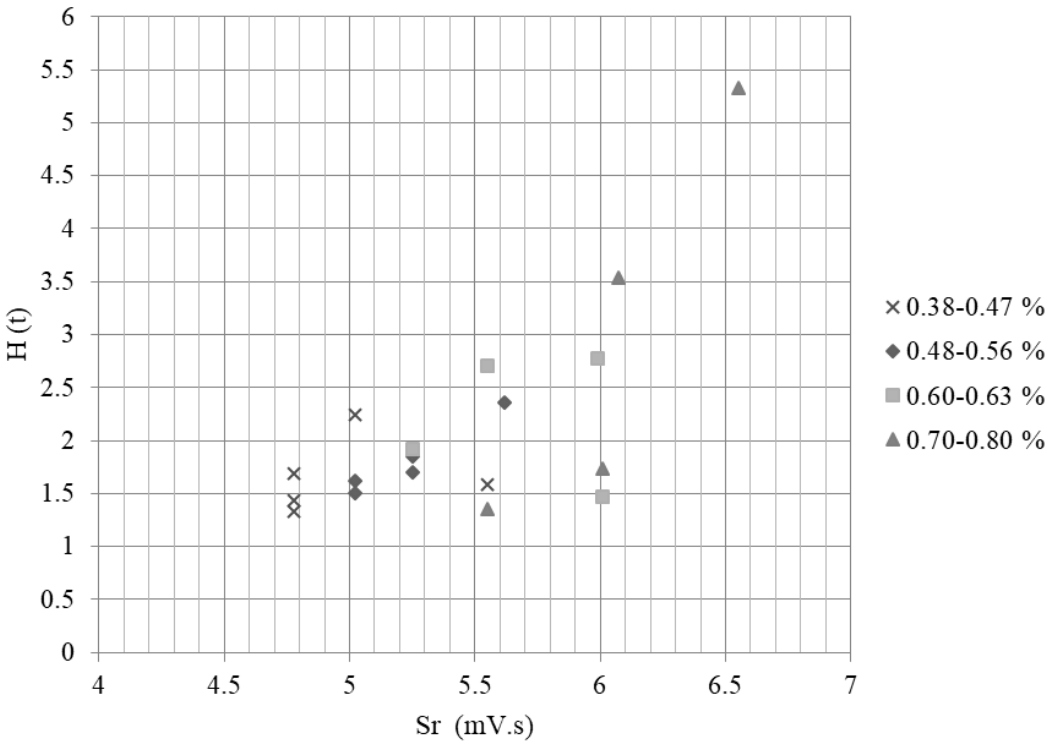

Figure 2-6 Damage Quantification Chart With Percent Mass Loss

The second quantification chart (**Figure 2-6**) compares the percent loss of mass due to abrasion of the samples with *H (t)* and *Sr* intensity analysis parameters. Again, AE data at six minutes was used for the percent loss with its corresponding *H (t)* and *Sr* values. Like the previous chart, there are four ranges of abrasion damage in this quantification chart, as seen in **Figure 2-6**. The overall range of the abrasion percent loss covered in this chart is from 0.38 to 0.8%. The data is more spread out in this situation with the data more evenly distributed in each range. For instance, it can be seen below that at *Sr* and *H (t)* of around 5.5 mV.s and of 2.1, respectively, there can be a percentage of abrasion weight loss of 0.38 to 0.47%. In general, the main goal of the charts in **Figures 2-5** and **2-6** is to determine if abrasion has occurred and to quantify its extent with the help of AE intensity analysis.

These charts would be suitable for predicting the extent and severity of abrasion damage to a concrete surface as AE monitoring has proven successful at detecting abrasion damage in various concrete types in this study.

2.5. Summary

AE monitoring was used while testing the abrasion resistance of various concrete types: NC, SCC, and SCC with various SCMs. The rotating cutter method of abrasion was used to test the abrasion resistance of the samples, and the samples were monitored with attached AE sensors to collect the AE data emitted during testing. An extensive analysis of the collected AE data was completed post-testing, which involved performing the b-value analysis and intensity analysis. The analysis of the abrasion results and AE data gave the following conclusions:

- It was determined that the *Sr*, CSS, and cumulative number of hits generally increased with test time as the abrasion increased gradually throughout the testing period in all tested samples. Meanwhile, *H (t)* values exhibited a continuous fluctuation throughout the test around a certain value that depended on the rate of abrasion in each sample. In contrast, the b-value was found to decrease as a result of abrasion damage progression with high fluctuations throughout the test period (indicating high AE activities). These findings reflect the sensitivity of the AE monitoring technique to the abrasion damage in concrete, regardless of concrete and/or SCM type.
- The control SCC mixture (without SCMs) had lower average percentage of abrasion mass loss/wear depth and increased compressive strength compared to its NC

counterpart. The results of the AE analysis also indicated lower values of the *H (t)*, *Sr*, CSS, cumulative number of hits, and higher b-value in the SCC compared to the NC mixture. However, the AE data shows no significant variations in the AE signal characteristics (signal amplitude) between both NC and SCC mixtures.

- Varying the SCM type in the SCC mixtures yielded no evident changes in the AE signal amplitude obtained from abrasion tests performed herein. On the contrary, the addition of SCMs to those mixtures had a significant impact on both their abrasion resistance and the following AE parameters: *H (t)*, *Sr*, CSS, b-value, and cumulative number of hits.
- The mixture with the highest abrasion resistance overall was the SCC mixture containing 20% MK. This mixture showed the lowest percent loss, wear depth, and highest compressive strength. On the other hand, the SCC mixture with 30% FA exhibited the least performance with respect to the average percent loss and compressive strength. The abrasion resistance of the SCC mixtures containing SCMs can be ranked in order from highest to lowest as MK, SF, SG, and FA. The AE parameters studied (*H (t)*, *Sr*, CSS, b-value, and cumulative number of hits) also indicated this performance order.
- The AE intensity analysis results can successfully be used to quantify abrasion damage regardless of concrete or SCM type. The AE intensity analysis parameters (*H (t)* and *Sr*) were related to the depth of wear and the percent mass loss in developed damage classification charts. These charts can be utilized to predict both the abrasion wear depth and percent loss according to the recorded AE signals.

- This study proved the effectiveness of the AE analysis presented in this paper to detect and characterize abrasion damage in concrete based on laboratory tests. Potential uses for this study include offshore structures and areas where typical visual inspection techniques cannot be carried out on-site or in person for extended periods of time. However, further field testing and verifications on various SCC and NC mixtures are required prior to the application of this technique in actual concrete structures.

2.6. Chapter References

Abdelrahman M, ElBatanouny MK, Ziehl P, Fasl J, Larosche CJ and Fraczek J (2015) Classification of alkali-silica reaction damage using acoustic emission: A proof-of-concept study. Construction and Building Materials 95: 406–413.

Abouhussien AA and Hassan AAA (2015) Optimizing the durability and service life of self-consolidating concrete containing metakaolin using statistical analysis. Construction and Building Materials 76: 297–306.

Aslani F (2013) Effects of specimen size and shape on compressive and tensile strengths of self-compacting concrete with or without fibres. Magazine of Concrete Research 65(15): 914–929.

ASTM (2009) C 1611: Standard test method for slump flow of self-consolidating concrete. ASTM International, West Conshohocken, PA, USA.

ASTM (2011) C 39: Standard test method for compressive strength of cylindrical concrete specimens. ASTM International, West Conshohocken, PA, USA.

ASTM (2012) C 418: Standard test method for abrasion resistance of concrete by sandblasting. ASTM International, West Conshohocken, PA, USA.

ASTM (2012) C 779: Standard test method for abrasion resistance of horizontal concrete surfaces. ASTM International, West Conshohocken, PA, USA.

ASTM (2012) C 944: Standard test method for abrasion resistance of concrete or mortar surfaces by the rotating-cutter method. ASTM International, West Conshohocken, PA, USA.

ASTM (2012) C 1138: Standard test method for abrasion resistance of concrete (Underwater method). ASTM International, West Conshohocken, PA, USA.

ASTM (2013) C 494: Standard specification for chemical admixtures for concrete. ASTM International, West Conshohocken, PA.

ASTM (2014) E1316: Standard terminology for nondestructive examinations. ASTM International, West Conshohocken, PA.

ASTM (2017) C 150: Standard specification for portland cement. ASTM International, West Conshohocken, PA, USA.

Bunnori NM, Lark RJ and Holford KM (2011) The use of acoustic emission for the early detection of cracking in concrete structures. Magazine of Concrete Research 63(9): 683–688.

Colombo IS, Main IG and Forde MC (2003) Assessing damage of reinforced concrete beam using “b-value” analysis of acoustic emission signals. Journal of Materials in Civil Engineering 15(3): 280–286.

Das D and Chatterjee A (2012) A comparison of hardened properties of fly-ash-based self-compacting concrete and normally compacted concrete under different curing conditions. Magazine of Concrete Research 64(2): 129–141.

Dong Q, Wu H, Huang B, Shu X and Wang K (2013) Investigation into laboratory abrasion test methods for pervious concrete. Journal of Materials in Civil Engineering 25(7): 886–892.

ElBatanouny MK, Ziehl PH, Larosche A, Mangual J, Matta F and Nanni A (2014) Acoustic emission monitoring for assessment of prestressed concrete beams. Construction and Building Materials 58: 46–53.

Farhidzadeh A, Salamone S, Luna B and Whittaker A (2012) Acoustic emission monitoring of a reinforced concrete shear wall by b-value-based outlier analysis. Structural Health Monitoring 12(1): 3–13.

Ghafoori N and Diawara H (1999) Abrasion resistance of fine aggregate replaced silica fume concrete. ACI Materials Journal 96(5): 559–569.

Invernizzi S, Lacidogna G and Carpinteri A (2013) Scaling of fracture and acoustic emission in concrete. Magazine of Concrete Research 65(9): 529–534.

Karahan O, Hossain KMA, Ozbay E, Lachemi M and Sancak E (2012) Effect of metakaolin content on the properties self-consolidating lightweight concrete. Construction and Building Materials 31: 320–325.

Lachemi M, Hossain KMA, Patel R, Shehata M and Bouzoubaâ N (2007) Influence of paste/mortar rheology on the flow characteristics of high-volume fly ash self-consolidating concrete. Magazine of Concrete Research 59(7): 517–528.

Liu TC (1981) Abrasion resistance of concrete. ACI Journal 78(5): 341–350.

Mistras Group (2007) PCI-2 based AE system 1 user's manual. Physical Acoustics Corporation, Princeton Junction, NJ, USA.

Ohtsu M and Tomoda Y (2008) Phenomenological model of corrosion process in reinforced concrete identified by acoustic emission. ACI Materials Journal 105(2): 194–199.

Papenfus N (2003) Applying concrete technology to abrasion resistance. Proceedings of the 7th International Conference on Concrete Block Paving (PAVE AFRICA 2003), Sun City, South Africa, ISBN Number: 0-958-46091-4.

Physical Acoustics (2005) R6I-AST sensor. Princeton Junction, NJ, USA.

Rao SV, Rao SMV, Ramaseshu D and Kumar RP (2012) Durability performance of self-compacting concrete. Magazine of Concrete Research 64(11): 1005–1013.

Safiuddin M, Salam MA and Jumaat MZ (2012) Flowing ability of self-consolidating concrete and its binder paste phase including palm oil fuel ash. Magazine of Concrete Research 64(10): 931–944.

Scott BD and Safiuddin M (2015) Abrasion resistance of concrete – Design, construction and case study. Concrete Research Letters 6(3): 136–148.

Turk K and Karatas M (2011) Abrasion resistance and mechanical properties of self-compacting concrete with different dosages of fly ash/ silica fume. Indian Journal of Engineering and Materials Sciences 18: 49–60.

Vélez W, Matta F and Ziehl P (2015) Acoustic emission monitoring of early corrosion in prestressed concrete piles. Structural Control and Health Monitoring 22: 873–887.

Vidya Sagar R and Prasad BKR (2009) AE energy release during the fracture of HSC beams. Magazine of Concrete Research 61(6): 419–435.

3. Evaluation of Abrasion Resistance of Self-Consolidating Rubberized Concrete by Acoustic Emission Analysis

3.1. Abstract

The purpose of this study was to investigate and compare the abrasion resistance of self-consolidating concrete (SCC) with crumb rubber (CR) in conjunction with acoustic emission (AE) monitoring. The variables were concrete type (normal concrete and SCC), coarse aggregate content, use of supplementary cementing materials (SCM), and CR content. AE characteristics like signal amplitude, signal strength, and number of hits were obtained from the AE software used during the abrasion testing. In addition, the signal amplitude and strength data obtained were further analyzed to calculate b-value, severity (S_r), and historic index ($H(t)$). The results showed that the addition of CR negatively affected the abrasion resistance of the tested samples while the addition of SCM greatly enhanced the abrasion. A good correlation was found between the abrasion damage and the AE parameters including the number of hits, signal strength, b-value, $H(t)$, and S_r. The results also presented developed damage classification charts using AE intensity parameters ($H(t)$ and S_r) to determine the ranges that indicate the extent of damage due to abrasion of the tested mixtures.

3.2. Introduction

The disposal of waste rubber is a worldwide issue due to the increasing number of vehicle tires that are scraped yearly (Thomas et al. 2014). If not properly disposed of, those waste

tires represent a significant environmental problem as they are not easily biodegradable (Sadek and El-Attar 2014). For example, burning waste tires leads to the release of toxic fumes causing air, soil, and water pollution (Eldin and Senouci 1994; Turer 2012). To overcome this problem, researchers have been investigating the use of recycled rubber in civil engineering applications including concrete production. In fact, the use of crumb rubber (CR) as a concrete ingredient has many advantages such as the development of eco-friendly buildings and sustainable construction (Su et al. 2015). Besides, replacing part of the aggregates by CR can help produce environmentally friendly semi-lightweight or lightweight concrete.

Self-consolidating concrete (SCC) is a high-performance and extremely workable type of concrete that can be used in areas with congested amounts of reinforcement or when mechanical vibration is not possible (El-Chabib and Syed 2013). In some cases, CR may be added to SCC mixtures in order to suit specific applications (Ismail and Hassan 2016a). The combination of CR and SCC can be referred to as self-consolidating rubberized concrete (SCRC), which merges the benefits of SCC and CR (Ismail and Hassan 2016b). The use of CR usually decreases the mechanical properties of concrete (Najim and Hall 2012; Rahman et al. 2012), but through the incorporation of supplementary cementing materials (SCMs) this can be improved (Ismail and Hassan 2016b). Past studies suggest that the use of metakaolin enhances the mechanical properties and viscosity of SCC, which in turn assists in allowing the CR and aggregates to bind together (Ismail and Hassan 2016b). This improved binding capability improves the mixture stability/particle suspension and prevents segregation within the mixture. The addition of CR as a fine

aggregate replacement can also create concrete with higher energy absorption and acoustic insulation with minimized brittleness (Ismail and Hassan 2016a). On the other hand, studies have suggested that the incorporation of CR in normal concrete can be well utilized in areas where the environment is particularly cold owing to the concrete's sufficient freeze-thaw protection and improved abrasion resistance (Thomas et al. 2014).

Abrasion resistance of concrete refers to how well the material can resist attacks that scrape the surface, resulting in weight loss of the concrete. Abrasion of concrete can occur in many ways, from traffic on floors to high-speed waters (Scott and Safiuddin 2015). To be resistant to abrasion, concrete must have adequate hardness in the paste structure as well as coarse aggregates. SCC normally uses less coarse aggregate compared to normal concrete, which can have a direct impact on its abrasion resistance (Ghafoori et al. 2014). The concrete system on a micro-level must have good bondage and few voids to have a strong paste-aggregate structure. The production of SCC usually involves the use of SCM in the mixtures, which can have a positive effect on improving the abrasion resistance as they typically have a higher surface area. The abrasion resistance of concrete can be evaluated in a multitude of ways including rotating cutter, horizontal concrete surfaces, sandblasting, and underwater methods as outlined in different ASTM standard tests (ASTM 2012a; 2012b; 2012c; 2012d).

Some researchers reported that replacing fine aggregate with CR in normal concrete may increase the abrasion resistance but has a negative effect on the compressive strength (Thomas et al. 2014; Thomas et al. 2016). On the contrary, Ozbay et al. (2011) found that the addition of CR reduced both the compressive strength and abrasion resistance of normal

concrete with and without slag. However, they indicated that the use of slag in the mixture slightly reduced the negative effect of adding CR on its abrasion resistance (Ozbay et al. 2011). Research on the abrasion resistance of rubberized concretes has focused mainly on studying normal concretes with or without SCMs, and there is a noticeable lack of research on the abrasion resistance of SCRC. Furthermore, there is an even clearer research gap on evaluating the resistance of SCRC to abrasion using acoustic emission (AE) technique to better quantify and assess the mass loss in concrete structures due to abrasion.

AE methodology can be used to monitor the structural health of concrete structures, and it is a well-established means of non-destructive testing. AE occurs in a material when it becomes damaged, causing waves to be generated from where the damage has occurred. These emitted waves are then recorded by AE sensors to determine the type and severity of the damage (Pollock 1986; Ziehl et al. 2008; Nair and Cai 2010). AE has been used in many structural applications in civil engineering structures currently in practice. For instance, fatigue damage and acoustic absorption capacity of rubberized and normal concretes have been analyzed via AE monitoring (Wang et al. 2013; Ismail and Hassan 2016a). Unrelated to rubberized concrete, AE has also been employed for evaluating concrete-steel bond deterioration (Abouhussien and Hassan 2017), monitoring crack propagation in reinforced concrete shear walls (Farhidzadeh et al. 2013), and determining damage due to alkali silica reaction (Abdelrahman et al. 2015). As previously stated, there is currently a lack of research regarding the application of AE monitoring for the assessment of SCRC abrasion.

The results from a previous study on the acoustic absorption capacity of SCRC indicated that increasing the rubber content significantly contributes to the AE wave attenuation (Ismail and Hassan 2016a). The core objective of this study is to examine the feasibility of using AE monitoring technique to detect and quantify damage caused by abrasion of SCRC compared to both NC and SCC. The investigation will also focus on studying the impact of increasing the CR percentage, the coarse aggregate content, and the use of SCM on the abrasion resistance of SCRC as well as the attenuation of the resulting AE signals.

3.3. Experimental Procedure

3.3.1. Materials Properties and SCRC Mixtures Design

Seven mixtures including four rubberized concrete mixtures, one normal concrete (NC) mixture, and two plain SCC mixtures were investigated in this study. The rubberized concrete mixtures were previously developed and optimized in a different study (Ismail and Hassan 2017) and have been used for this investigation to evaluate their abrasion resistance. Three of the rubberized concrete mixtures were SCRC containing three variable percentages of CR – 10%, 20%, and 30% designated as SCRC10, SCRC20, and SCRC30, respectively. The fourth rubberized concrete mixture was normal rubberized concrete (NRC) with 40% CR. This NRC mixture was added to study the effect of using a higher percentage of CR since it was not possible to use higher than 30% CR in the development of SCRC. This finding was based on previous studies which indicated that using CR content higher than 30% yielded SCRC mixtures with insufficient fresh properties (Ismail and Hassan 2016a; 2016b; Ismail and Hassan 2017). The tested NC mixture had a high coarse-

to-fine aggregate (C/F) ratio of 2.0 while all SCC mixtures had a C/F ratio of 0.7. This difference in the C/F ratio was chosen to study the effect of the higher coarse aggregate content on the abrasion resistance, if any. The two tested plain SCC mixtures in this study included one without metakaolin (MK) and fly ash (FA) (SCC1) and one with MK and FA (SCC2). These mixtures were chosen to investigate the effect of using SCM on the abrasion resistance.

All mixtures contained Type GU Canadian Portland cement, which had a specific gravity of 3.15 and is in accordance with ASTM Type I (ASTM 2012e). Also, two types of aggregate were used in each mixture: coarse aggregate (C.A.) and fine aggregate (F.A.). The F.A. used was natural sand and the C.A. had a maximum size of 10 mm; both had a specific gravity of 2.6 and water absorption of 1%. Two SCMs (MK and FA) were used in the SCRC10, SCRC20, SCRC30, and NRC mixtures. The MK and FA used in these mixtures had a specific gravity of 2.27 and 2.5, respectively. The CR used in the study had a maximum size of 4.5 mm, no water absorption, and a specific gravity of 0.95. In order to maintain flowability and to reach a target slump flow of 700 ± 50 mm, as per ASTM C1611 (ASTM 2009), a high-range water-reducing admixture (HRWRA) was employed. This HRWRA had a specific gravity of 1.2 and pH of 9.5, similar to what is specified in ASTM Type F (ASTM 2013). For all mixtures, the water-to-binder (W/B) ratio was a constant value of 0.4. **Table 3-1** shows the details of mixture proportions for all mixtures tested in this study.

Table 3-1 SCRC Mixture Proportions

Mixture Name	Cement	MK (kg/m^3)	FA (kg/m^3)	C/F Ratio	W/B	C.A. (kg/m^3)	F.A. (kg/m^3)	Water (kg/m^3)	CR (kg/m^3)	HRWRA (l/m^3)
NC	500	0	0	2.0	0.4	1111.5	555.7	200	0	0
SCC1	500	0	0	0.7	0.4	686.5	980.8	200	0	2.37
SCC2	275	110	165	0.7	0.4	620.3	886.1	220	0	3.43
SCRC10	275	110	165	0.7	0.4	620.3	797.5	220	32.4	3.75
SCRC20	275	110	165	0.7	0.4	620.3	708.9	220	64.8	3.75
SCRC30	275	110	165	0.7	0.4	620.3	620.3	220	97.1	4.38
NRC40	275	110	165	0.7	0.4	620.3	531.7	220	129.5	3.18

3.3.2. Test Sample Details, Abrasion Test Setup, and AE Monitoring Setup

For each mixture, three cylinders and two prisms were cast. All of the cylinders/prisms were cured at 25°C in a moist-curing room for 28 days prior to testing. On day 28, A compressive strength test was performed on the cylinders following ASTM C39 standard (ASTM 2012f). The prism samples were cut into three 100 mm cubes, which were used for the abrasion testing (also at 28 days' maturity). The 100mm cube size was selected due to the size of the cutter to maximize the area of abrasion on the sample and three samples were tested as this is common practice in concrete testing. The ASTM C944 standard (ASTM 2012a) using the rotating-cutter procedure for abrasion testing of concrete was adopted herein. This procedure uses a drill press with a chuck capable of holding and rotating the cutter while applying a force of approximately 10 kg, as illustrated in **Figure 3-1**. The test was run for one-minute intervals with a total abrasion time of six minutes. After each minute, the weight loss of the specimens was measured to the nearest 0.1 g to estimate the percent of weight loss. Also, the depth of wear due to abrasion was measured by electronic calipers at the end of the tests for all samples. These parameters were used to determine the

extent of the damage due to abrasion as they were recommended by the ASTM C944 standard. All tested mixtures had three samples undergo the abrasion and compression testing to determine an average value for each concrete type.

Figure 3-1 Abrasion Test Set up with AE monitor

To monitor the AE signals being emitted during the abrasion testing, AE sensors were attached to the test specimens (one sensor for each specimen) with a two-part epoxy adhesive (as can be seen in **Figure 3-1**). These sensors were piezoelectric AE sensors with an integral preamplifier and were model number R6I-AST (Physical Acoustics 2005). The sensors were connected to a data acquisition system by Mistras Group (2007). AE software (AEwin) was used to record the signals being emitted during the abrasion tests. The system has a set amplitude threshold of 40 dB and a full list of parameters set up in the hardware

(listed in **Table 3-2**). The system records a wide variety of AE parameters such as amplitude, signal strength, duration, energy and absolute energy, counts, rise time, average frequency, and peak frequency. Full descriptions of these parameters are laid out in ASTM E1316 (ASTM 2014).

Table 3-2 AE System Setup

AE Hardware Setup	
Threshold	40 dB_{AE}
Sample Rate	1 MSPS
Pre-Trigger	256 μs
Length	1k points
Preamp Gain	40 dB
Preamp Voltage	28
Analog Filter	1-50 kHz
Digital Filter	100-400 kHz
Peak Definition Time	200 μs
Hit Definition Time	800 μs
Hit Lockout Time	1000 μs
Maximum Duration	1000 μs

3.4. Analysis of AE Data

3.4.1. b-Value Analysis

The traditional AE parameters such as signal amplitude, number of hits, and cumulative signal strength (CSS) were first analyzed and related to abrasion damage for all specimens. Additional analysis, namely b-value analysis, was also performed on the AE amplitude data for the aim of assessing the abrasion damage in all mixtures. This analysis uses the values of amplitude and number of hits collected throughout the tests to create a further parameter

(b-value). This parameter is based on seismic equations and has successfully been utilized to represent the variations of the frequency-magnitude of the AE activities to evaluate various damage types in concrete materials/structures (Colombo et al. 2003; Ohtsu and Tomoda 2008; Sagar and Prasad 2013; ElBatanouny et al. 2014; Li et al. 2015). The magnitudes of the b-value were calculated during the abrasion tests for all specimens by means of **Eq. 1.**

1. $\log(N) = a - b\log(A)$

Where N = the number of hits having amplitudes larger than A; A = the signal amplitude (dB); a = an empirically derived constant; and b = the b-value (Colombo et al. 2003; Ohtsu and Tomoda 2008; Sagar and Prasad 2013; ElBatanouny et al. 2014; Li et al. 2015).

3.4.2. Intensity Analysis

Intensity analysis inspects the strength of AE signals acquired through the testing period to calculate additional AE parameters. The signal strength and amplitude are set up within the system and collected automatically during the testing. In this study, the intensity analysis was performed post testing in order to determine if abrasion damage had occurred and assess the extent of this damage. The AE signal strength data collected during testing was used to attain historic index (*H (t)*) and severity (*Sr*). Historic index detects and quantifies sudden variations in the CSS versus time curve. This parameter was calculated using **Eq. 2.**

2. $H(t) = \frac{N}{N-K} \frac{\sum_{i=K}^{N} S_{oi}}{\sum_{i=1}^{N} S_{oi}}$

In **Eq. 2**, the cumulative number of hits is denoted as N until time (t) and Soi represents the signal strength of the ith event.

Severity, calculated by using **Eq. 3**, was based on the average signal strength of the J number of hits.

3. $S_r = \sum_{i=1}^{J} \frac{S_{oi}}{J}$

The values of the constants K and J in **Eq. 2** and **3** are dependent on the damage mechanism and type of structure (Vélez et al. 2015). The values of K and J for this test have been adopted from previous tests (Abdelrahman et al. 2014, 2015; Abouhussien and Hassan 2017), which incorporated AE analysis and indicated their suitability for use with concrete. The value of K had been calculated based on the cumulative number of hits (N):

a) K = 0: if N ≤ 50, b) K = N – 30: if 51 ≤ N ≤ 200, c) K = 0.85N: if 201 ≤ N ≤ 500, and d) K = N – 75: if N ≥ 501. In the meantime, J was set to a constant value of 50 (Abdelrahman et al. 2014, 2015; Abouhussien and Hassan 2017)

3.5. Results and Discussions

As previously mentioned, the intent of this study was to investigate the influence of the percentage of CR, the use of higher coarse aggregate content (in NC mixture), and the use of SCM on the abrasion resistance. **Table 3-3** shows the results of the percentage of weight loss in each sample due to abrasion after each minute during the test. In addition, **Figure 3-2** was constructed to show the average abrasion percent loss at each minute across three samples in each mixture. The wear depth, which was measured post abrasion testing, and the 28-day compressive strength of all samples are presented in **Table 3-4.**

Table 3-3 Abrasion Percent Loss during Testing

Mixture Name	Sample Number	Percent Loss (%)					
		1 min	2 min	3 min	4 min	5 min	6 min
NC	S1	0.21	0.35	0.46	0.53	0.64	0.70
	S2	0.18	0.35	0.43	0.50	0.58	0.63
	S3	0.18	0.31	0.41	0.47	0.53	0.60
SCC1	S1	0.17	0.33	0.46	0.59	0.66	0.76
	S2	0.09	0.14	0.22	0.27	0.35	0.40
	S3	0.16	0.32	0.41	0.50	0.54	0.60
SCC2	S1	0.10	0.14	0.19	0.26	0.28	0.34
	S2	0.09	0.14	0.17	0.21	0.26	0.31
	S3	0.06	0.08	0.11	0.16	0.25	0.30
SCRC10	S1	0.19	0.31	0.40	0.46	0.51	0.56
	S2	0.25	0.37	0.44	0.49	0.54	0.59
	S3	0.20	0.30	0.36	0.40	0.44	0.54
SCRC20	S1	0.16	0.28	0.37	0.43	0.49	0.55
	S2	0.25	0.35	0.40	0.46	0.52	0.59
	S3	0.20	0.34	0.44	0.48	0.55	0.68
SCRC30	S1	0.31	0.47	0.63	0.76	0.79	0.84
	S2	0.18	0.31	0.41	0.50	0.57	0.62
	S3	0.13	0.23	0.31	0.39	0.44	0.50
NRC40	S1	0.36	0.57	0.71	0.85	0.99	1.09
	S2	0.27	0.42	0.48	0.52	0.57	0.64
	S3	0.23	0.40	0.57	0.69	0.80	0.89

Table 3-4 Abrasion Wear Depth and Compressive Strength Results

Mixture Name	Sample Number	Wear Depth (mm)	Average Wear Depth (mm)	Compressive Strength (MPa)	Average Compressive Strength (MPa)
NC	S1	1.08	0.99	52.08	52.48
	S2	0.97		51.52	
	S3	0.92		53.83	
SCC1	S1	0.80	0.93	54.7	54.40
	S2	0.84		53.8	
	S3	1.15		54.6	
SCC2	S1	0.55	0.71	75.31	75.65
	S2	0.74		76.65	
	S3	0.83		74.98	
SCRC10	S1	0.88	0.93	56.08	53.48
	S2	0.99		51.32	
	S3	0.92		53.03	
SCRC20	S1	1.06	1.24	38.67	38.40
	S2	1.26		41.04	
	S3	1.40		35.49	
SCRC30	S1	0.92	1.51	33.83	31.86
	S2	2.12		31.13	
	S3	1.50		30.61	
NRC40	S1	1.76	1.85	23.68	24.71
	S2	1.56		25.40	
	S3	2.23		25.06	

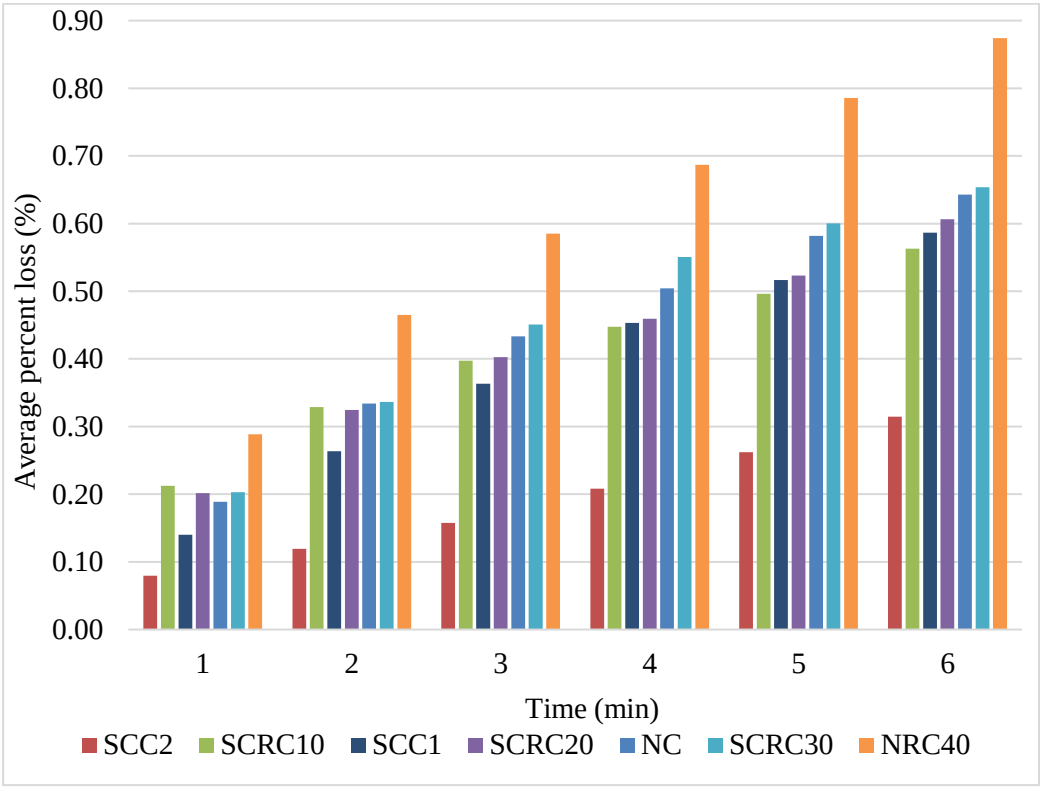

Figure 3-2 Average Percent Loss vs. Time

3.5.1. Impact of Abrasion Damage Progression on AE Data

The results of the abrasion damage and the corresponding AE data over time were correlated. More specifically, AE parameters including number of hits, CSS, b-value, *H (t)*, and S_r were compared with the abrasion damage progression. **Figure 3-3** shows the curves for sample one of the SCRC10 mixture (SCRC10 S1) as an example of the rest of the samples of the seven mixtures examined in this study. The horizontal trend in **Figures 3-3a and 3-3b** represents when the test was the stopped after each minute as no signals were being generated or collected. The complete data of these AE parameters for all other tested samples at one and six minutes can be found in **Table 3-5**. **Figure 3-3a** displays the number of hits and total percent of weight loss versus test time. As the amount of abrasion increases,

the number of hits increases with time, indicating that higher AE events can be anticipated as more abrasion damage occurs. For instance, the number of hits for this sample (SCRC10 S1) at one and six minutes was 109 and 494, respectively, corresponding to an increase in the percent loss from 0.19% to 0.56% at the end of the testing period. This correlation is also seen in **Figure 3-3b** where the changes in the CSS values are almost identical to those of the number of hits. The CSS values increased from 370 to 2270 mV.s due to the increase in the abrasion damage observed from one to six minutes.

In contrast, the variations in the b-values decreased as abrasion damage progressed (**Figure 3-3c).** For example, the magnitudes of the b-value exhibited locations with high fluctuations with a reduction from 1.24 to 0.73 at one to six minutes, respectively. These fluctuations in the b-value indicate higher AE activity, which was also associated with linear increases in the number of hits and CSS graphs (**Figures 3-3a and 3-3b**). As can be seen in **Figure 3-3d**, the historic index shows an overall fluctuation throughout the test period as the abrasion damage increases. *H (t)* has a range of maximum values of 1.6 to 2.1, with locations of sudden increase matching those zones of high variations in the b-values (high AE activities) if these fluctuations were decreased this would indicated lower AE activities. S_r versus time in **Figure 3-3e** has a steady increase during the abrasion test, with an immediate initial peak at the start of the test followed by a less drastic increase towards the end. At minute one, the value of the severity was 4.3 mV.s and then its maximum value at the end of the test was 4.55 mV.s.

The data discussed above illustrates an existing correlation between the abrasion damage and AE parameters (number of hits, CSS, b-value, *H (t)*, and S_r). The percent of weight loss

due to abrasion over the course of the six minutes increased in a linear fashion. It was observed during testing that some particles of CR and concrete were released from the surface being abraded. These pieces leaving the surface represented a visual indication of damage occurring, thus creating AE signals within the concrete specimen. Another source of the AE events over the test period was the presence of friction between the test specimens and the rotating cutter. The friction and pressure placed on the specimen created damage and wear, which led to weight loss and produced AE signals. For each of the mixtures (NC, SCC, SCRC, and NRC), the AE analysis was effective in detecting and evaluating abrasion damage despite variance in concrete type or rubber level (from 10% to 40%).

a)

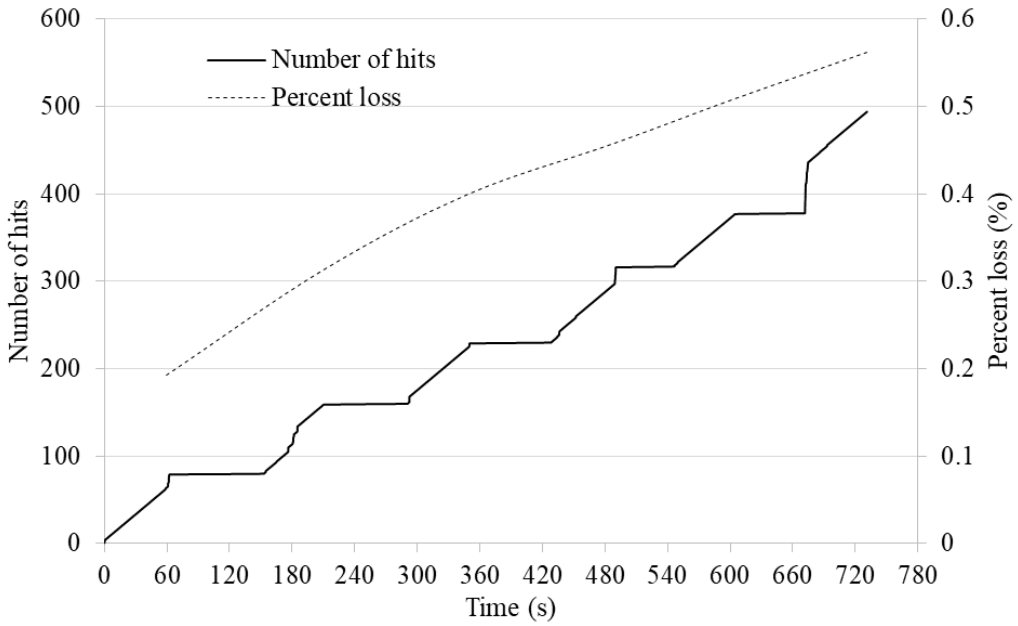

b)

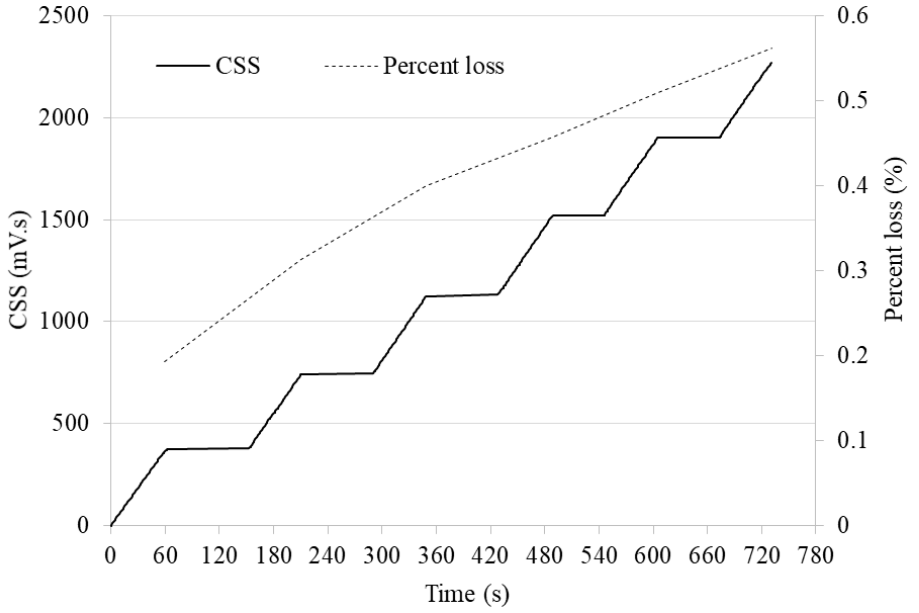
CSS
Percent loss
CSS (mV.s)
Percent loss (%)
Time (s)
2500
2000
1500
1000
500
0
0.6
0.5
0.4
0.3
0.2
0.1
0
0 60 120 180 240 300 360 420 480 540 600 660 720 780

c)

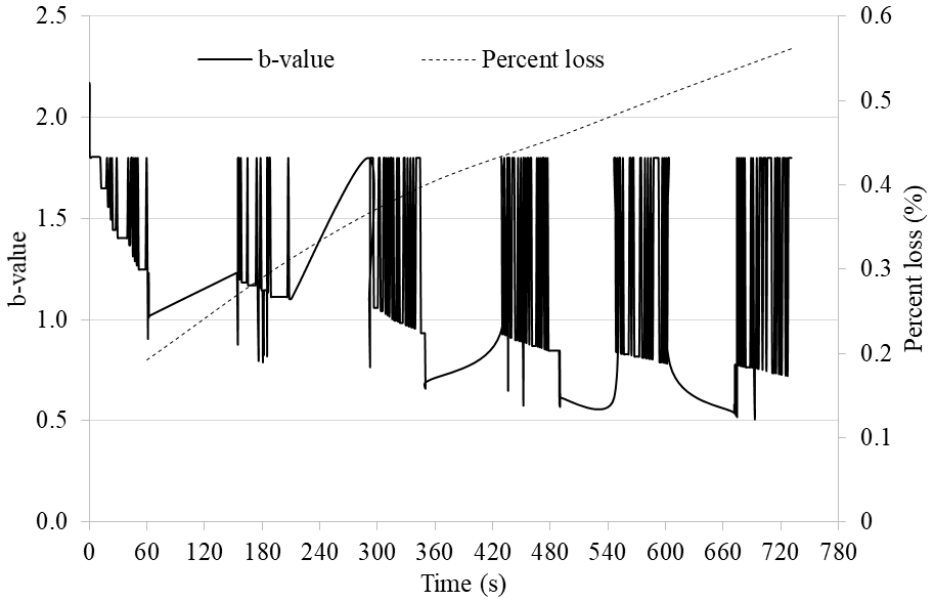
b-value
Percent loss
b-value
Percent loss (%)
Time (s)
2.5
2.0
1.5
1.0
0.5
0.0
0.6
0.5
0.4
0.3
0.2
0.1
0
0 60 120 180 240 300 360 420 480 540 600 660 720 780

d)

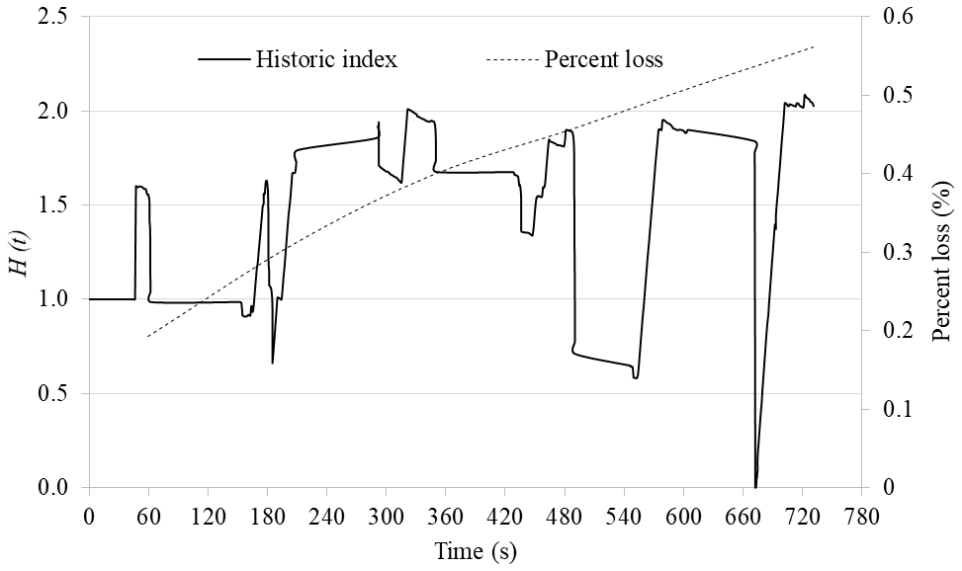

e)

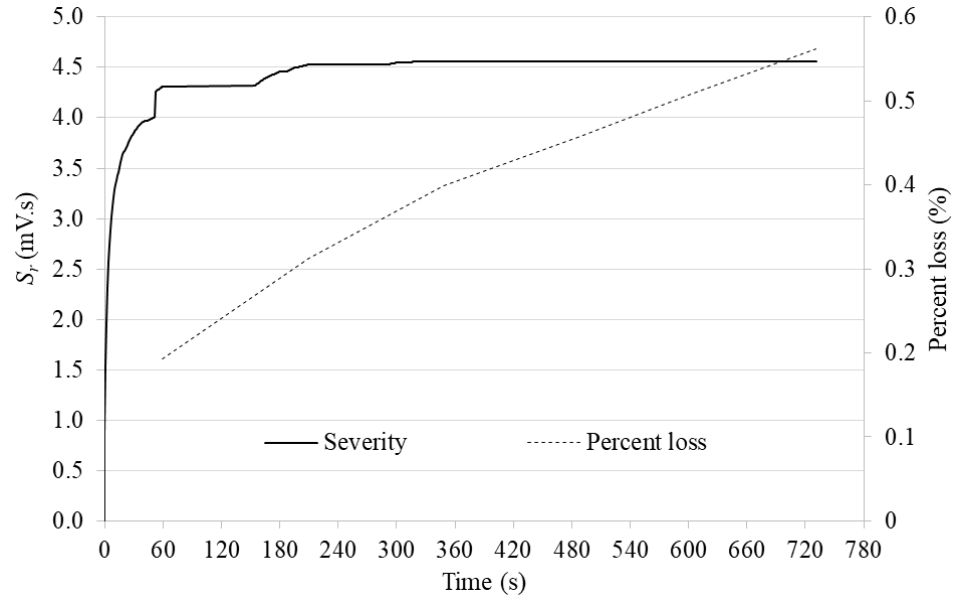

Figure 3-3 AE Parameters Versus Time for SCRC10 S1 a) N – Number of Hits, b) CSS, c) b-Value, d) *H (t)*and e) *Sr*

3.5.2. Influence of CR Content on Abrasion Performance and on AE Signals and Parameters

By evaluating the SCRC mixtures in the study, it was determined that an increase in CR content increased the abrasion damage in terms of percent loss and wear depth. For example, by comparing SCRC10 to SCRC30, there was a 16% increase of average percent loss, 65% increase in average wear depth, and 68% decrease in the average compressive strength. The significant reduction in compressive strength as a result of adding high percentage of CR is expected to be the main reason for the reduction in abrasion resistance, especially with the rotating-cutter abrasion test used in this investigation. It should be mentioned that other studies (Thomas et al. 2014; Thomas et al. 2016) suggested that the use of up to 20% CR can improve the abrasion resistance of normal concrete (in terms of the abrasion depth). However, the abrasion damage was induced in these studies using abrasive powder and a rotation disc compared to the rotating-cutter method performed in this study. Further research is recommended in order to assess the effect of variable test techniques on the abrasion performance of SCRC.

To evaluate the effect of CR content on the AE signal characteristics, the average signal amplitudes at one and six minutes in each sample of the seven mixtures are compared in **Figures 3-4a and 3-4b**, respectively. It can be seen from the figures that the signal amplitudes show a general decreasing trend as the CR content increased both at one and six minutes, which implies that wave attenuation was occurring. Attenuation can be described as the decrease in intensity of a sound as it travels from the source of emitted signal due to the sound absorption properties of the rubber and/or the increased amount of

voids in the mixtures (Ismail and Hassan 2016a). The average signal amplitude across the three samples at six minutes in the SCC2 mixture was 82 dB compared with an average of 68 dB in the NRC40 (**Table 3-5**). This indicated that there is a 17% decrease in signal amplitude from 0% to 40% CR replacement. This reduction in the signal amplitude was the maximum across all tested mixtures at one and six minutes. Similarly, increasing the rubber content from 0% to 10% (SCC2 to SCRC10), from 0% to 20% (SCC2 to SCRC20), and from 0% to 30% (SCC2 to SCRC30) resulted in 7%, 12%, and 15% decrease in the average signal amplitude at six minutes, respectively.

a)

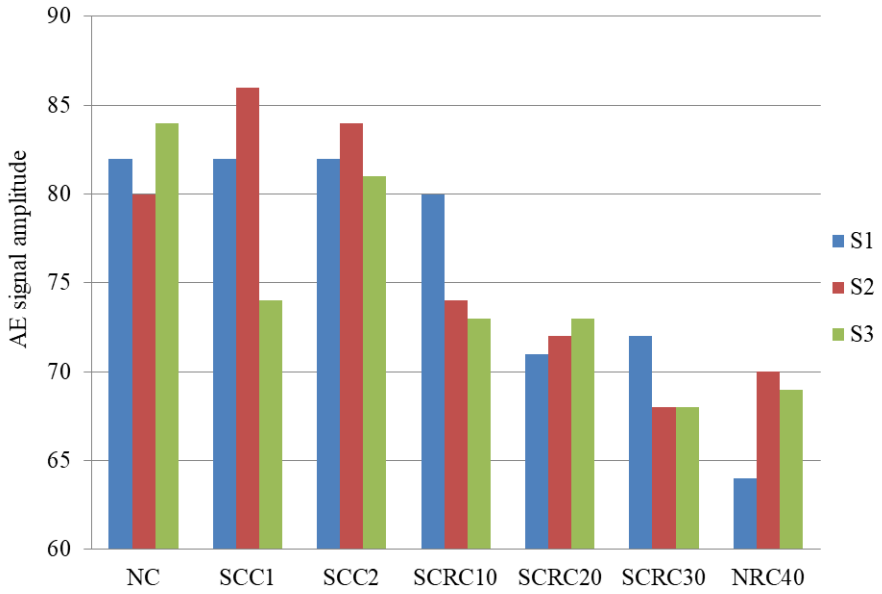

b)

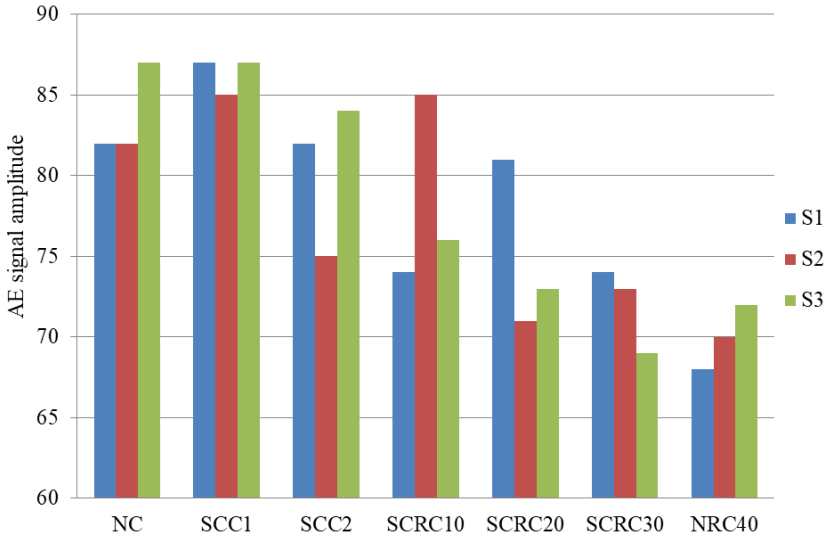

Figure 3-4 Signal Amplitude a) at One Minute, b) at Six Minutes

Table 3-5 AE Parameters at One and Six Minutes

Mixture Name	Sample Number	Average Signal Amplitude (dB)		Number of Hits		CSS x 10^3 (mV.s)		*H (t)*		S_r (mV.s)		b-value	
		1 min	6 min	1 min	6 min	1 min	6 min	1 min	6 min	1 min	6 min	1 min	6 min
NC	S1	82	82	137	758	0.44	2.32	2.64	1.74	4.09	6.01	1.49	1.05
	S2	82	80	130	765	0.33	2.23	2.25	2.77	4.09	5.99	1.49	1.01
	S3	87	84	110	670	0.48	2.42	2.15	1.47	5.59	6.01	1.39	1.14
SCC1	S1	85	82	115	461	0.36	2.23	1.98	1.35	4.14	5.51	1.45	1.14
	S2	87	86	112	391	0.40	2.34	2.04	1.58	4.55	5.52	1.58	1.25
	S3	87	74	103	1143	0.37	2.41	2.04	2.7	4.55	5.55	1.51	0.95
SCC2	S1	75	82	97	552	0.26	1.82	1.83	1.53	2.33	3.78	1.81	1.21
	S2	82	84	77	301	0.24	1.83	1.46	1.24	2.08	3.87	1.86	1.28
	S3	84	81	68	291	0.21	1.75	1.18	1.57	2.01	3.93	1.96	1.47
SCRC10	S1	85	80	109	494	0.37	2.27	1.6	2.1	4.3	4.55	1.24	0.73
	S2	74	74	134	985	0.41	2.18	2.66	2.46	4.35	6.39	1.23	0.72
	S3	76	73	143	986	0.42	2.18	2.73	2.71	4.43	6.43	1.64	1.16
SCRC20	S1	71	71	200	977	0.32	2.12	1.7	2.94	5.32	6.52	0.92	0.52
	S2	81	72	80	636	0.37	2.09	1.84	2.3	3.36	6.16	1.12	0.65
	S3	73	73	76	1091	3.81	2.03	1.93	2.9	3.57	6.01	1.44	0.95
SCRC30	S1	73	72	83	977	0.32	2.21	1.55	2.94	3.49	6.41	0.99	0.49
	S2	74	68	100	1271	0.35	2.33	1.78	3.8	2.81	6.55	1.29	0.62
	S3	69	68	122	636	0.36	2.33	1.88	1.86	4.03	6.17	1.16	0.55
NRC40	S1	70	64	187	1022	0.48	2.6	2.94	3.07	4.75	6.19	0.88	0.44
	S2	68	70	159	1121	0.44	2.89	2.8	3.14	5.61	6.75	0.96	0.58
	S3	72	69	149	1209	0.42	3.16	2.49	3.25	5.72	6.81	0.91	0.52

These findings also indicated that rubber is excellent at increasing the sound absorption. It is worth noting that, even though there was a decrease in signal amplitude with higher CR content, the AE analysis was sufficient at detecting damage due to abrasion in the seven mixtures as the signal amplitudes remained above the 40 dB limit (the threshold set) during all tests (as seen in **Table 3-5**). This capability of AE technique is valid for the contents of rubber studied in this paper (maximum 40% replacement of sand by CR). The results shown in **Table 3-5** also indicate that the increase in the CR percentage had a significant impact on the AE parameters studied (number of hits, CSS, b-value, *H (t)*, and S_r) at both one and six minutes. For instance, changing the CR percentage from 0% to 40% (SCC to NRC40) was associated with 66% higher average number of hits, 38% higher average CSS, 53% higher average *H (t)*, 41% higher average S_r, and 61% lower average b-value at six minutes. Similar effects were also observed at one minute for all tests and other CR replacements. This overall increasing trend can be related to the increase in the abrasion damage as a result of higher CR ratios, which was confirmed in all tested specimens. These results highlight the sensitivity of the AE parameters (number of hits, CSS, b-value, *H (t)*, and S_r) to the abrasion damage extent in all tested mixtures.

3.5.3. Effect of Concrete Type and SCM on Abrasion Performance and AE Parameters

The results show that using NC with higher C/F ratios yielded a direct effect on the abrasion resistance (**Tables 3-3 and 3-4**). For example, the NC mixture showed 8% higher average percentage of weight loss, 6% higher average wear depth, and 4% lower compressive strength than those for the SCC counterpart mixture (SCC1). SCC typically has increased

abrasion resistance due to its inherently superior compaction, less coarse aggregate volume, and increased compressive strength (Papenfus 2003; Ghafoori et al. 2014). These two mixtures had the same proportions but with variable C/F ratio (0.7 for SCC1 and 2.0 for NC). Therefore, this enhanced abrasion resistance can be attributed to the influence of using lower coarse aggregate content in the SCC mixture compared to NC. It should be noted that the better flowability and optimum compaction of SCC may also have some contribution on improving the abrasion resistance (Papenfus 2003). However, this factor might not be significant in this study as only small prism samples were used.

Similarly, the addition of SCMs (MK and FA) was found to improve the abrasion performance of SCC mixtures. The SCC1 mixture exhibited 46% higher average percentage of weight loss, 24% higher average wear depth, and 28% lower compressive strength compared to SCC2 (**Tables 3-3 and 3-4**). These results indicate that the incorporation of SCMs has a significant impact on the abrasion resistance of SCC. Particularly, the use of MK in the mixture has a significant effect on enhancing the paste microstructure and improving the compressive strength of the mixture (Ismail and Hassan 2016a; 2016b; Ismail and Hassan 2017).

In general, the SCC mixture with SCMs (SCC2) exhibited the highest abrasion resistance overall among the tested NC, SCC, SCRC, and NRC mixtures. As can be noticed from **Figure 3-2**, the SCC2 mixture was followed by SCRC10, SCC1, SCRC20, NC, SCRC30, and NRC40 in the order of increasing abrasion percent loss at six minutes. In terms of the average wear depth, the order of performance changes slightly to SCC2 followed by SCC1, SCRC10, NC, SCRC20, SCRC30, and NRC40 having the maximum value of average wear

depth. The average compressive strengths follow the same order as that of average wear depth seen in **Table 3-4**. Compressive strength has been correlated to an increase in abrasion resistance in past studies (Scott and Safiuddin 2015), which matched the findings of this investigation.

NC with higher coarse aggregate content also showed a noticeable influence on the AE parameters (number of hits, CSS, b-value, *H (t)*, and S_r), as seen in **Table 3-5**. For instance, the average number of hits, CSS, b-value, *H (t)*, and S_r for the NC mixture at six minutes were 731, 2320 mV.s, 1.07, 1.99, and 6.0 mV.s, respectively, while these parameters were 381, 1800 mV.s, 1.32, 1.45, and 3.86 mV.s, respectively, for the SCC2 mixture. Overall, it can be seen that the NC parameters were larger than those of SCC2 mixture (except the b-value), indicating higher AE activities in the NC mixture. These results can be attributed to the lower abrasion resistance capacity for the NC mixture than the SCC2 counterpart. Same trends as the comparison of NC to SCC2 were also obtained by comparing the NC to the SCC1 and NRC40 mixtures. This further confirmed the correlation between the AE parameters studied and the severity of abrasion damage in concrete. In contrast, no significant changes between NC, SCC1, and SCC2 were observed in the signal amplitudes throughout the tests (**Figure 3-4**). It is worth noting that, all the studied AE parameters (number of hits, CSS, b-value, *H (t)*, and S_r) were found equally significant for the assessment of abrasion resistance of all tested mixtures, regardless of concrete type and/or CR content. Yet, the AE signal amplitude is a critical parameter and requires special consideration in evaluating rubberized concrete abrasion due to the impact of increased CR content on signal attenuation, as described in the previous section.

3.5.4. Abrasion Damage Quantification of SCRC by AE Intensity Analysis

In this investigation, abrasion damage was evaluated in terms of depth of wear (mm) and percentage of weight lost (%). The results of intensity analysis parameters (*H (t)* and S_r) were related to those forms of abrasion damage to develop damage classification charts. The data at six minutes was used for all mixtures to create the quantification charts shown in **Figures 3-5 and 3-6**. These charts are both composed of three ranges of abrasion damage in all tested mixtures, which were determined based on the distribution of the data points in three regions after drawing the *H (t)* versus S_r in each chart. The chart in **Figure 3-5** may be used to quantify the abrasion damage using depth of wear based on the calculated values of *H (t)* and S_r. This chart has three ranges for damage (depth of wear): 0.55 to 0.88 mm, 0.92 to 1.50 mm, and 1.56 to 2.23 mm. The corresponding ranges for *H (t)* and S_r are as follows: 1.24 to 3.8 and 3.78 to 6.81 mV.s, respectively. The chart can be used to predict the depth of wear by using a pair of values for *H (t)* and S_r. For instance, if *H (t)* was equal to 2.2 and S_r to 6.0 mV.s, there would be a predicted amount of abrasion damage from 0.92 to 1.50 mm.

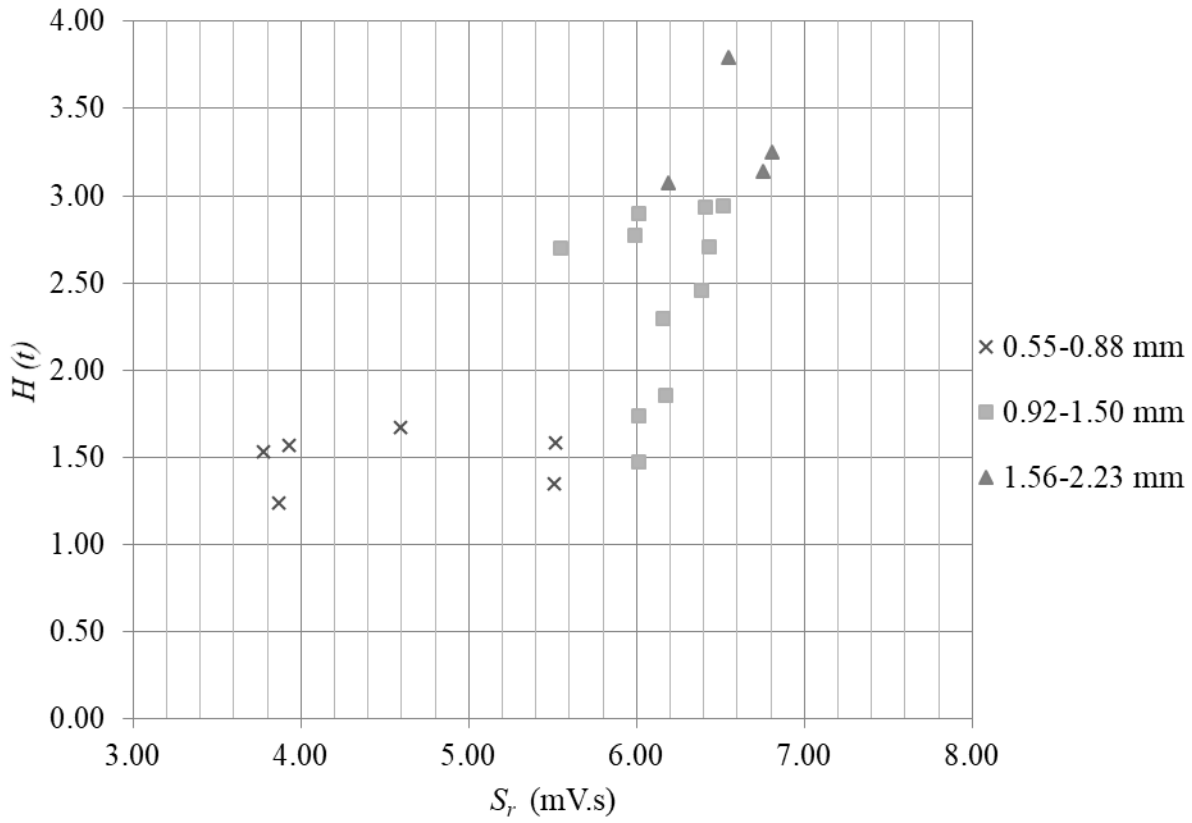

Figure 3-5 Damage Quantification Chart for Depth of Wear

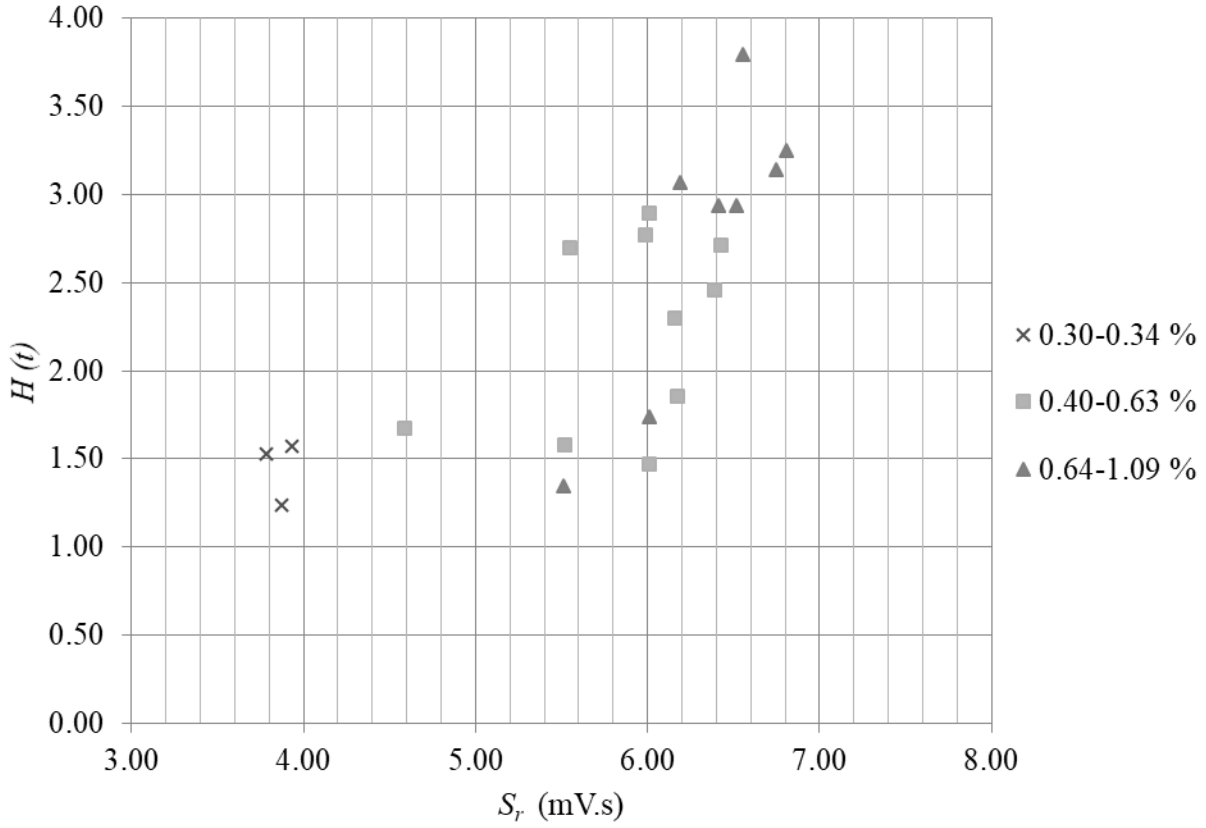

Figure 3-6 Damage Quantification Based on Percent of Mass Lost

Similarly, the chart in **Figure 3-6** may be utilized to determine the percent of weight lost due to abrasion using these two AE intensity analysis parameters. This chart works in the same way as the previous one, but instead it expresses the abrasion damage in terms of percent loss. This chart also has three ranges of abrasion damage – 0.30% to 0.34%, 0.40% to 0.63%, and 0.64% to 1.09%. Whilst, the *H (t)* and S_r had the same ranges of magnitudes as those used in the first chart. In this instance, using the same values as the previous example, the amount of abrasion damage could be placed at approximately 0.40% to 0.63%. It should be mentioned that some limitations exist for these quantification charts, such as the range of the mixture proportions used in this study. The mixtures classified in these

quantification charts contained CR replacements up to 40%. Therefore, additional tests are needed in order to adequately predict abrasion damage for mixtures with CR levels greater than 40%.

3.6. Summary

Abrasion resistances of NC and SCC with varying levels of CR replacements were tested in conjunction with AE monitoring. A rotating cutter abraded the concrete, while AE sensors attached to the specimens gathered the AE data being emitted. Through analyzing various AE parameters and abrasion test results, the following conclusions were made:

- A good correlation was found between the abrasion damage and the evaluated AE parameters including the number of hits, CSS, b-value, *H (t)*, and S_r. The amount of AE number of hits, CSS, and S_r increase as a result of abrasion damage progression (percent of weight loss and wear depth over time). Also, the b-value had a declining trend and the *H (t)* showed continuous fluctuations throughout the tests, regardless of the concrete type or CR percentage, indicating a good correlation with the abrasion damage.
- The increase in the CR content resulted in higher abrasion damage in terms of average percent loss and wear depth in all mixtures. This higher abrasion damage was reflected in an increase in the number of hits, CSS, *H (t)*, and S_r and a decrease in the b-value. In addition, the signal amplitudes had noticeably decreased values in the mixtures with higher CR percentages, which manifested the occurrence of some attenuation in the AE signals. Yet, all recorded signals exhibited higher

amplitudes than the 40 dB threshold and enabled the characterization of abrasion damage in all tests.

- The inclusion of SCMs (MK and FA) in the SCC mixtures resulted in a noticeable improvement in their abrasion resistance (in terms of both weight loss and wear depth). In addition, the use of lower coarse aggregate content in the SCC mixtures slightly enhanced their abrasion resistance compared to the NC counterpart mixture.
- The highest abrasion resisting mixture was the SCC2 mixture, with 0% CR and containing SCMs, followed by SCRC10, SCC1, SCRC20, NC, SCRC30, and NRC40 in terms of percent of weight loss at the end of the tests. The extent of abrasion percent loss and wear depth were well correlated to the studied AE parameters (number of hits, CSS, b-value, *H (t)*, and S_r) in all mixtures. On the contrary, changing the concrete type (NC versus SCC) and/or adding SCMs led to non-significant variations in the AE signal characteristics (signal amplitude) during the tests.
- AE intensity analysis parameters *H (t)* and S_r were related separately to the depth of wear and percent of weight loss of the tested samples to develop damage quantification charts. These charts can be adequately used to assess abrasion damage using the ranges of *H (t)* and S_r of 1.24 to 3.8 and 3.78 to 6.81 mV.s, respectively. Continued testing in the laboratory and in the field on NC, SCC, and SCRC mixtures is recommended to refine the classification charts presented in this paper.

3.7. Chapter References

Abdelrahman, M., ElBatanouny, M. K., and Ziehl, P. H. (2014). "Acoustic emission based damage assessment method for prestressed concrete structures: Modified index of damage." Engineering Structures, 60, 258–264.

Abdelrahman, M., ElBatanouny, M. K., Ziehl, P., Fasl, J., Larosche, C. J. and Fraczek, J. (2015). "Classification of alkali–silica reaction damage using acoustic emission: A proof-of-concept study." Construction and Building Materials, 95, 406–413.

Abouhussien, A. A., and Hassan, A. A. A. (2017). "Acoustic emission monitoring for bond integrity evaluation of reinforced concrete under pull-out tests." Advanced Structural Engineering, 20(9), 1390–1405.

ASTM C1611-09, "Standard Test Method for Slump Flow of Self-Consolidating Concrete," ASTM International, West Conshohocken (2009).

ASTM C944/C944M-12, "Standard Test Method for Abrasion Resistance of Concrete or Mortar Surfaces by the Rotating-Cutter Method," ASTM International, West Conshohocken (2012a).

ASTM C779/C779M-12, "Standard Test Method for Abrasion Resistance of Horizontal Concrete Surfaces," ASTM International, West Conshohocken (2012b).

ASTM C418-12, "Standard Test Method for Abrasion Resistance of Concrete by Sandblasting," ASTM International, West Conshohocken (2012c).

ASTM C1138-M-12, "Standard Test Method for Abrasion Resistance of Concrete (Underwater Method)," ASTM International, West Conshohocken (2012d).

ASTM C150-12, “Standard Specification for Portland Cement,” ASTM International, West Conshohocken (2012e).

ASTM C39-12, “Standard Test Method for Compressive Strength of Cylindrical Concrete Specimens,” ASTM International, West Conshohocken (2012f).

ASTM C493-13, “Standard Specification for Chemical Admixtures for Concrete,” ASTM International, West Conshohocken (2013).

ASTM E1315-14, “Standard Terminology for Nondestructive Examinations,” ASTM International, West Conshohocken (2014).

Colombo, I. S., Main, I. G., and Forde, M. C. (2003). “Assessing damage of reinforced concrete beam using ‘‘b-value’’ analysis of acoustic emission signals.” Journal of Materials in Civil Engineering, 15(3), 280–286.

ElBatanouny, M. K., Mangual, J., Ziehl, P. H., and Matta, F. (2014). “Early corrosion detection in prestressed concrete girders using acoustic emission.” Journal of Materials in Civil Engineering, 26, 504–511.

El-Chabib, H., and Syed, A. (2013). “Properties of self-consolidating concrete made with high volumes of supplementary cementitious materials.” Journal of Materials in Civil Engineering, 25(11), 1579–1586.

Eldin, N. N., and Senouci, A. B. (1994). “Measurement and prediction of the strength of rubberized concrete.” Cement and Concrete Composites, 16 (4), 287–298.

Farhidzadeh, A., Dehghan-Niri, E., Salamone, S., Luna, B., and Whittaker, A. (2013). “Monitoring crack propagation in reinforced concrete shear walls by acoustic emission.” Journal of Structural Engineering, 139(12), 04013010.

Ghafoori, N., Najimi, M., and Aqel, M. A. (2014). “Abrasion resistance of self-consolidating concrete.” Journal of Materials in Civil Engineering, 26(2), 296–303.

Ismail, M. K., and Hassan, A. A. A. (2016a). “Impact resistance and acoustic absorption capacity of self-consolidating rubberized concrete.” ACI Materials Journal, 113(6), 725–736.

Ismail, M. K., and Hassan, A. A. A. (2016b). “Use of metakaolin on enhancing the mechanical properties of SCC containing high percentages of crumb rubber.” Journal of Cleaner Production, 125, 282–295.

Ismail, M. K., and Hassan, A. A. A. (2017). “Impact resistance and mechanical properties of self-consolidating rubberized concrete reinforced with steel fibers.” Journal of Materials in Civil Engineering, 29(1), 04016193.

Li, D., Chen, Z., Feng, Q., and Wang, Y. (2015). “Damage analysis of CFRP-confined circular concrete-filled steel tubular columns by acoustic emission techniques.” Smart Materials and Structures, 24, 085017 (11pp).

Mistras Group. (2007). “PCI-2 based AE system 1 user’s manual.” Physical Acoustics Corporation, Princeton Junction, NJ, USA.

Najim, K. B., and Hall, M. (2012). “Mechanical and dynamic properties of self-compacting crumb rubber modified concrete.” Construction and Building Materials, 27(1), 521–530.

Nair, A., and Cai, C. S. (2010). “Acoustic emission monitoring of bridges: Review and case studies.” Engineering Structures, 32(6), 1704–1714.

Ohtsu, M., and Tomoda, Y. (2008). “Phenomenological model of corrosion process in reinforced concrete identified by acoustic emission.” ACI Materials Journal, 105(2), 194–199.

Ozbay, E., Lachemi, M., and Sevim, U. K. (2011). “Compressive Strength, abrasion resistance and energy absorption capacity of rubberized concrete with and without slag.” Materials and Structures, 44(7), 1297–1307.

Papenfus, N. (2003). “Applying concrete technology to abrasion resistance.” In: Proceedings of the 7th International Conference on Concrete Block Paving (PAVE AFRICA 2003), Sun City, South Africa, ISBN Number: 0-958-46091-4.

Physical Acoustics. (2005). “R6I-AST sensor.” Physical Acoustics Corporation, Princeton Junction, NJ, USA.

Pollock, A. A. (1986). “Classical wave theory in practical AE testing.” In: Proceedings, International Acoustic Emission Symposium, Japanese Society for Nondestructive Testing, 708–721.

Rahman, M. M., Usman, M., and Al-Ghalib, A. A. (2012). “Fundamental properties of rubber modified self-compacting concrete (RMSCC).” Construction and Building Materials, 36, 630–637.

Sadek, D. M., and El-Attar, M. M., (2014). “Structural behavior of rubberized masonry walls.” Journal of Cleaner Production, 89, 174–186.

Sagar, R. V., and Prasad, B. K. R. (2013). “Laboratory investigations on cracking in reinforced concrete beams using on-line acoustic emission monitoring technique.” Journal of Civil Structural Health Monitoring, 3, 169–186.

Scott, B. D., and Safiuddin, M. (2015). “Abrasion resistance of concrete – Design, construction and case study.” Concrete Research Letters, 6(3), 136–148.

Su, H., Yang, J., Ling, T., Ghataora, G. S., and Dirar, S. (2015). “Properties of concrete prepared with waste tyre rubber particles of uniform and varying sizes.” Journal of Cleaner Production, 91, 288–296.

Thomas, B. S., Gupta, R. C., Kalla, P., and Cseteneyi, L. (2014). “Strength, abrasion and permeation characteristics of cement concrete containing discarded rubber fine aggregates.” Construction and Building Materials, 59, 204–212.

Thomas, B. S., Kumar, S., Mehra, P., Gupta, R. C., Joseph, M., and Csetenyi L. J. (2016). “Abrasion resistance of sustainable green concrete containing waste tire rubber particles.” Construction and Building Materials, 124, 906–909.

Turer, A. (2012). Recycling of Scrap Tires, Material Recycling – Trends and Perspectives, Dr. Dimitris Achilias (Ed.), 195–212. ISBN: 978-953-51-0327-1, InTech, Available from: http://www.intechopen.com/books/materialrecycling-trends-and-perspectives/use-of-scrap-tires-in-industry.

Wang, C., Zhang, Y., and Ma, A. (2013). “Investigation into the fatigue damage process of rubberized concrete and plain concrete by AE analysis.” Journal of Materials in Civil Engineering, 23(7), 886–892.

Ziehl, P. H., Galati, N., Nanni, A., and Tumialan, J. G. (2008). “In-situ evaluation of two concrete slab systems. II: evaluation criteria and outcomes.” Journal of Performance of Constructed Facilities, 22, 217–227.

Vélez, W., Matta, F., and Ziehl, P. (2015). “Acoustic emission monitoring of early corrosion in prestressed concrete piles.” Structural Control and Health Monitoring, 22, 873–887.

4. Assessing Abrasion Performance of Self-Consolidating Concrete Containing Synthetic Fibers Using Acoustic Emission Analysis

4.1. Abstract

The key objective of this investigation was to evaluate the abrasion resistance of self-consolidating concrete (SCC) with and without synthetic fibers (SFs). The abrasion resistance of normal concrete (NC) was also investigated in this study for comparison. The abrasion test was performed on concrete specimens according to the rotating-cutter method along with simultaneously monitoring the acoustic emission (AE) using attached AE sensors. The effects of changing concrete type and incorporating various types (flexible and semi-rigid) and lengths of SFs on the abrasion behaviour were investigated with the aid of AE analysis. AE signal characteristics such as amplitude, signal strength, number of hits, and test duration were gathered during testing. Furthermore, the collected AE data was used to complete b-value analysis as well as intensity analysis resulting in three additional parameters: b-value, severity (S_r), and historic index ($H(t)$). The results showed that the AE parameters were directly correlated with the abrasion damage in all tested mixtures. Adding SFs to all SCC mixtures enhanced their abrasion resistance. The flexible-fibers variety exhibited better abrasion performance on average than the semi-rigid fibers. Meanwhile, longer fibers showed lower abrasion resistance than the shorter ones with the same type. The results also indicated that AE intensity analysis was able to determine the ranges for $H(t)$ and S_r that identify the extent of damage due to abrasion of SF-reinforced SCC.

4.2. Introduction

Self-consolidating concrete (SCC) was invented to make the process of pouring concrete easier. SCC is an ideal concrete for heavily reinforced areas and for use where the formworks are hard to reach. SCC can be developed by increasing the amount of fine materials (such as adding supplementary cementing materials – SCMs), reducing the coarse aggregate content, and/or using high-range water-reducing admixtures (HRWRA) or viscosity-modifying admixtures (Lachemi, Hossain, et al., 2003). In some cases, rubberized materials, steel fibers, and synthetic fibers (SFs) are used for the purpose of enhancing some properties of SCC (Ismail and Hassan, 2017).

The addition of fibers in concrete mixtures can generally increase the flexural strength, tensile strength, and toughness (Ismail and Hassan, 2017). Optimizing concrete mixtures with higher dosages of fibers also proved to increase the modulus of rupture and impact resistance (Bolat, Şimşek, et al., 2014). In addition, crack control is made possible by incorporating fibers in concrete as they provide omnidirectional reinforcement within the structure (Yap, Alengaram, et al., 2014), (Grabois, Cordeiro, et al., 2016). Among the different types of fibers, SFs have become widely used and have received a lot of attention. SFs come in a variety of materials such as man-made polypropylene, nylon, polyester, and polyethylene. Similar to any fiber, using SFs in SCC decreases the fresh properties of the mixture, which makes it more difficult to optimize successful SCC fresh properties. The physical properties of SFs showed to have some effect on the fresh properties and the demand of HRWRA in SCC mixtures. For example, flexible SFs have shown to require less demand of HRWRA compared to semi-rigid SFs. On the other hand, the length of SFs

has proven to have little to no effect on the fresh properties or the demand of HRWRA (AbdelAleem, Ismail and Hassan, 2017).

Durability, impact resistance, and other forms of natural attack have been studied primarily on normal concrete with SFs. Nevertheless, there is a noticeable lack of information regarding the properties of SCC containing SFs in the mixture, including its abrasion resistance. Abrasion resistance is defined as the ability of a material to resist being scraped. Abrasion can occur in high-traffic areas like concrete floors in plants and factories or in hydraulic structures with high-speed waters, which cause cavitation's (Scott and Safiuddin, 2015). Abrasion of concrete can be evaluated in a variety of ways designated by ASTM standards from rotating-disc to sandblasting methods (ASTM, 2012), but the most simplified procedure is the rotating-cutter method (ASTM, 2012). Few studies have focused on the abrasion resistance of normal concrete reinforced with fibers. One in particular studied the abrasion resistance of normal concrete reinforced with SFs (Bolat, Şimşek, et al., 2014). This study indicated that adding SFs greatly improved the abrasion resistance of normal concrete. SCC itself usually has better abrasion resistance than normal concrete (Ghafoori, Naijimi, and Aqel, 2014) and adding SFs is expected to further increase the abrasion resistance of SCC. Therefore, research that examines the abrasion resistance of SCC with SFs is needed.

Acoustic emission (AE) monitoring is a form of non-destructive testing of concrete materials/structures. This method is ideal in areas where traditional forms of structural health monitoring (SHM) cannot be carried out. AE is a process that happens in a solid material when it has been damaged. This damage emits waves that can then be recorded by

the AE sensors attached to the material. The emitted signals are recorded and analyzed to evaluate and determine the type of damage that has occurred (Ziehl, Galati, et al., 2008), (Zaki, Chai, et al., 2015). AE is a very well established form of SHM and has been employed in various studies to evaluate concrete slab systems (Ziehl, Galati, et al., 2008); to characterize the fracture process of steel-fiber-reinforced concrete (Zhou, Yang, et al., 2016); to determine the extent of expansion due to alkali-aggregate reaction (Abdelrahman, ElBatanouny, et al., 2015); to assess the condition of prestressed concrete bridges (Anay, Cortez, et al., 2016); and to detect yielding of pre-stressed concrete beams (Salamone, Veletzos, et al., 2012). However, there is a clear gap in research dealing with the application of AE to monitor abrasion of concrete in general, and specifically for SF-reinforced SCC.

The main objective of this study was to evaluate the abrasion resistance of SF-reinforced SCC by the aid of AE analysis. This study will help determine the feasibility of using SF-reinforced SCC as a way to control abrasion compared to normal concretes. The study examined the effects of using different concrete types, different types of SFs (flexible versus semi-rigid), and different lengths of fibers on the abrasion resistance and the resulting AE parameters. Moreover, an extensive analysis of the attained AE data was also performed to detect, characterize, and quantify the damages resulting from abrasion of various SF-reinforced SCC mixtures.

4.3. Research Significance

Investigating SCC's abrasion resistance is a particular aspect of the long-term performance of this concrete in structures. More specifically, very limited research has been done on the abrasion resistance of SCC with SFs incorporated into the mixture. This study will

potentially fill that research gap and allow for some discovery concerning the abrasion resistance of SCC with different types and lengths of SFs. In addition, this study will be beneficial to detecting and quantifying the extent of damage due to abrasion through the use of AE monitoring. The outcomes of this experimental investigation will also contribute to the knowledge of AE application as an SHM tool for monitoring concrete abrasion.

4.4. Experimental Procedure

4.4.1. Materials and Mixture Design

This experiment tested a total of seven mixtures including one plain normal concrete (NC), one SCC without SCMs, one SCC with SCMs, and four SCC mixtures containing two lengths and types of SFs. Semi-rigid and flexible fibers composed of polypropylene with two variable lengths each were employed for each mixture type. The semi-rigid fibers were 27 mm and 54 mm, and the flexible fibers were 19 mm and 38 mm. The geometrical and mechanical characteristics of these fibers are described in **Table 4-1**. The SCC mixtures were previously developed in a past study (AbdelAleem, Ismail and Hassan, 2017) and the fibers were selected based on their commercial availability. The volume of fibers (V_f) was chosen as 0.2% in all SCC mixtures with SFs. This percentage was also taken from a previous study conducted to optimize SCC with maximized percentage of SFs (AbdelAleem, Ismail and Hassan, 2017).

Table 4-1 Properties of Synthetic Fibers

Fiber type	Description	Length (mm)	Diameter (mm)	Specific gravity	Tensile strength (MPa)
SF19	Flexible synthetic fiber	19	0.66	0.91	300
SF38	Flexible synthetic fiber	38	0.64	0.91	515
SF27	Semi-rigid synthetic fiber	27	0.80	0.91	585
SF54	Semi-rigid synthetic fiber	54	0.80	0.91	585

All tested mixtures contained Type GU cement, which was in compliance with ASTM Type I (ASTM, 2012) and had a specific gravity of 3.15. To allow for the fibers to properly bind in the mixture, two SCMs were used in the SCC mixtures – fly ash (FA) and metakaolin (MK), except for a control SCC mixture (SCC1). These SCMs had a specific gravity of 2.5 and 2.27, respectively. Coarse aggregate (C.A.) and fine aggregate (F.A.) were used in all mixtures, and both had a specific gravity of 2.6 and water absorption of 1%. The coarse-to-fine aggregate ratio (C/F) was 0.7 for all SCC mixtures and 2.0 for the NC mixture. The main objective of using a higher percentage of coarse aggregate in the NC mixture was to magnify the influence of lower C/F ratio in SCC (which is commonly used in SCC mixtures) on the abrasion resistance, if any. The water-to binder-ratio (W/B) was kept constant at 0.4 in all mixtures. To achieve successful SCC mixtures (in terms of fresh properties), a high-range water-reducing admixture (HRWRA) was added to the SCC mixtures to help obtain a desired slump-flow of 700 ± 50 mm, as per ASTM C C1611 (ASTM, 2009). The HRWRA used had a specific gravity of 1.2 and a pH level of 9.5; it is similar to that described in ASTM Type F (ASTM, 2013). The full details of all mixture proportions involved in this study are shown in **Table 4-2**.

Table 4-2 Mixture Proportions

Mixture type	Cement (kg/m^3)	MK (kg/m^3)	FA (kg/m^3)	C/F ratio	W/B	C.A. (kg/m^3)	F.A. (kg/m^3)	Water (L/m^3)	V_f (%)	HRWRA (L/m^3)
NC	500	0	0	2.0	0.4	1111.5	555.7	200	0	0
SCC1	500	0	0	0.7	0.4	686.5	980.8	200	0	2.37
SCC2	275	110	165	0.7	0.4	620.3	886.1	220	0	3.43
SF19	275	110	165	0.7	0.4	620.3	886.1	220	0.2	4.35
SF38	275	110	165	0.7	0.4	620.3	886.1	220	0.2	4.69
SF27	275	110	165	0.7	0.4	620.3	886.1	220	0.2	3.91
SF54	275	110	165	0.7	0.4	620.3	886.1	220	0.2	5.25

4.5. Test Setup

Three cylinders and three prisms were cast for each mixture for compression and abrasion testing, respectively. The prism samples were cut into three 100 mm cubes (one cube was selected from each prism) for abrasion testing. The 100mm size was chosen based on the width of the cutter to maximize the abrasive area. And three samples were tested to provide averaged results as is common in concrete testing. All specimens were cured in a moist-curing room at approximately 25°C until they matured at 28 days. At 28 days, the compressive and abrasion tests were carried out for each mixture. The compression test was conducted in accordance with ASTM C39 (ASTM, 2012) and the abrasion test was done according to the rotating-cutter standard ASTM C944 method (ASTM, 2012). This ASTM standard abrasion test calls for the use of a drill press with a rotating chuck, which can inflict a constant pressure of 10 kg on the specimens (ASTM, 2012). The full abrasion test setup can be seen in **Figure 4-1**. In this study, six intervals (one minute each) were adopted and the weight loss was weighed at the end of each minute. Meanwhile, the depth of wear as a result of abrasion was measured by electronic calipers in each sample at the end of the tests.

Wear depth and percent mass lost were used as a determination of the extent of damage to the concrete by abrasive processes because the C944 standard gives these as the two methods of quantifying the damage.

Figure 4-1 AE and Abrasion Test Setup

AE sensors were attached to the exterior of the specimens with a two-part epoxy to detect and monitor the signals being emitted while the abrasion testing was performed (**Figure 4-1**). In this study, piezoelectric AE sensors (model number R6I-AST) with an integral preamplifier were used (Mistras Group, 2005). The sensors attached to the specimens were connected to a cable and then to the data acquisition system by Mistras Group (Mistras Group, 2007). AE software called AEwin was utilized to collect the AE data and control the data acquisition system. The system had an amplitude threshold of 40 dB set and was

used to record different AE signal parameters emitted during the abrasion testing period. A full list of the AE parameters determined in the system can be seen in **Table 4-3**. These AE parameters included amplitude, signal strength, duration, energy and absolute energy, counts, rise time, average frequency, and peak frequency. Full descriptions of these parameters are discussed in ASTM E1316 (ASTM, 2014).

Table 4-3 AE System Details

AE hardware setup	
Threshold	40 dB_{AE}
Sample rate	1 MSPS
Pre-trigger	256 μs
Length	1k points
Preamp gain	40 dB
Preamp voltage	28
Analog filter	1-50 kHz
Digital filter	100-400 kHz
Peak definition time	200 μs
Hit definition time	800 μs
Hit lockout time	1000 μs
Maximum duration	1000 μs

4.6. AE Data Analysis

The results of AE signal amplitudes and number of hits underwent a b-value analysis to assess the abrasion damage in all tested specimens. The b-value is originally based on seismic equations and has effectively been employed to indicate the changes in the frequency-magnitude of the AE events to evaluate several damage mechanisms in concrete (Colombo, Main, and Forde, 2003). The b-value was calculated throughout the abrasion tests for all tested specimens using **Eq. 1**.

1. $log\ N = a - b\ log\ A$

Where N = the number of hits having amplitudes larger than A; A = the signal amplitude (dB); a = an empirically derived constant; and b = the b-value (Li, Chen, et al., 2015).

In addition, an AE intensity analysis was completed on the strength of the signals emitted in order to calculate more intricate AE parameters. These calculated parameters were then used to determine the correlations between the extent of abrasion damage and AE parameters as well as to study the effects of concrete type, fiber type, and fiber length on the AE data. The intensity analysis involved calculating two parameters: historic index ($H(t)$) and severity (S_r). The historic index distinguishes and measures any sudden peaks or lows in the cumulative signal strength (CSS) versus time curve. $H(t)$ was calculated using **Eq. 2** below.

2. $$H(t) = \frac{N}{N-K}\frac{\sum_{i=K+1}^{N} S_{oi}}{\sum_{i=1}^{N} S_{oi}}$$

In this equation, the cumulative number of hits is stated as N until time (t) and S_{oi} represents the signal strength of the i^{th} event. Next, the severity was calculated by using **Eq. 3** and was based on the average signal strength of the J number of hits.

3. $$S_r = \sum_{i=1}^{J} \frac{S_{oi}}{J}$$

The constants used in **Eqs. 2 and 3**, K and J, may have varying values depending on the damage mechanism and type of material being tested (Vélez, Matta, and Ziehl, 2015). The values of K and J used in this study have been determined in previous studies involving AE analysis in concrete [28, 31-32].

K was calculated based on the value for N;

a) $K = 0$: if $N \leq 50$, b) $K = N - 30$: if $51 \leq N \leq 200$, c) $K = 0.85N$: if $201 \leq N \leq 500$, and d) $K = N - 75$: if $N \geq 501$. Instead of being calculated, J was set to a constant value of 50

(Abdelrahman, ElBatanouny, et al., 2015), (Nair and Cai, 2010), (Abdelrahman, ElBatanouny, et al., 2014).

4.7. Results and Discussion

Tables 4-4 and 4-5 display the data collected and some of the calculated results during the abrasion tests. The average values of the percentages of weight loss throughout the abrasion tests of all mixtures are graphed in **Figure 4-2**.

Table 4-4 Percentage of Weight Loss of All Samples

Mixture name	Sample number	Percentage of weight loss (%)					
		1 min	2 min	3 min	4 min	5 min	6 min
NC	S1	0.21	0.35	0.46	0.53	0.64	0.70
	S2	0.18	0.35	0.43	0.50	0.58	0.63
	S3	0.18	0.31	0.41	0.47	0.53	0.60
SCC1	S1	0.17	0.33	0.46	0.59	0.66	0.76
	S2	0.09	0.14	0.22	0.27	0.35	0.40
	S3	0.16	0.32	0.41	0.50	0.54	0.60
SCC2	S1	0.10	0.14	0.19	0.26	0.28	0.34
	S2	0.09	0.14	0.17	0.21	0.26	0.31
	S3	0.06	0.08	0.11	0.16	0.25	0.33
SF19	S1	0.06	0.13	0.18	0.21	0.24	0.27
	S2	0.05	0.09	0.13	0.16	0.19	0.21
	S3	0.06	0.10	0.15	0.17	0.21	0.24
SF38	S1	0.05	0.10	0.13	0.17	0.22	0.25
	S2	0.08	0.13	0.17	0.22	0.25	0.27
	S3	0.05	0.13	0.18	0.25	0.29	0.32
SF27	S1	0.07	0.13	0.16	0.19	0.21	0.23
	S2	0.06	0.10	0.16	0.25	0.26	0.28
	S3	0.05	0.09	0.13	0.17	0.22	0.26
SF54	S1	0.10	0.18	0.24	0.28	0.32	0.37
	S2	0.09	0.13	0.18	0.23	0.26	0.30
	S3	0.08	0.14	0.18	0.21	0.24	0.26

Table 4-5 Abrasion Wear Depth and Compressive Strength Data

Mixture name	Sample number	Wear depth (mm)	Average wear depth (mm)	Compressive strength (MPa)	Average compressive strength (MPa)
NC	S1	1.08	0.99	52.08	52.48
	S2	0.97		51.52	
	S3	0.92		53.83	
SCC1	S1	0.80	0.93	54.7	54.40
	S2	0.84		53.8	
	S3	1.15		54.6	
SCC2	S1	0.55	0.71	75.31	75.65
	S2	0.74		76.65	
	S3	0.83		74.98	
SF19	S1	0.56	0.53	80.74	78.85
	S2	0.48		81.15	
	S3	0.55		74.64	
SF38	S1	0.58	0.62	80.13	76.26
	S2	0.62		82.11	
	S3	0.65		66.56	
SF27	S1	0.58	0.58	85.36	77.32
	S2	0.62		58.23	
	S3	0.53		88.36	
SF54	S1	0.71	0.64	74.46	75.82
	S2	0.65		78.10	
	S3	0.56		74.89	

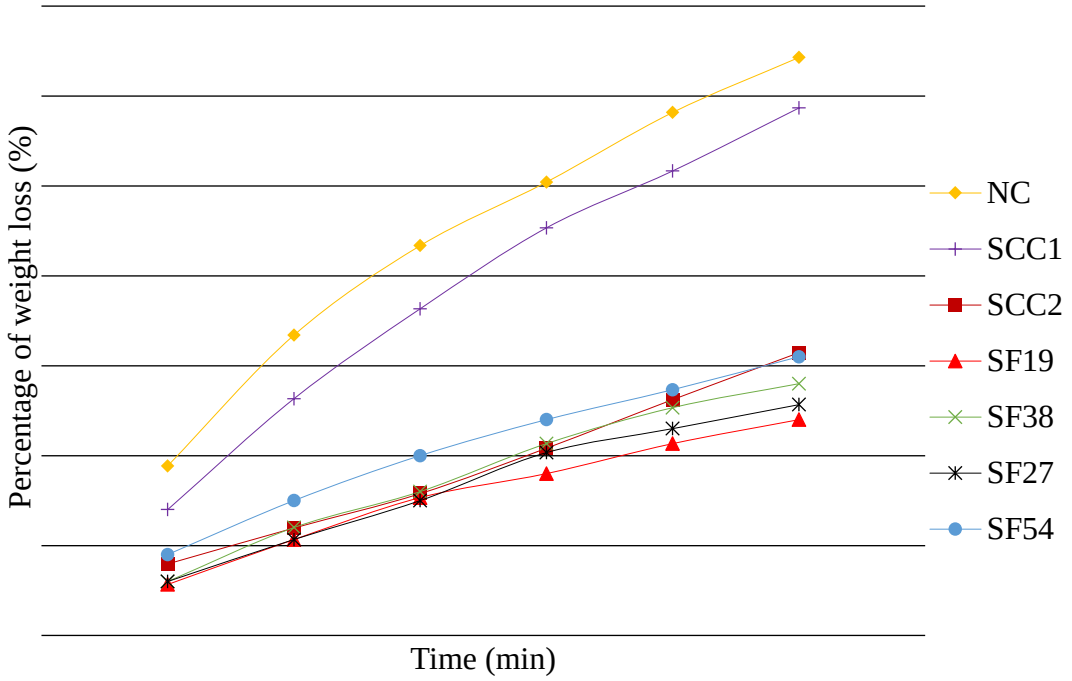

Figure 4-2 Average Percentage of Weight Loss of All Mixtures

4.7.1. Identification of Abrasion Damage Using AE Analysis

The variations in the AE parameters throughout the tests were analyzed in order to develop a correlation between the abrasion damage and the corresponding AE signals obtained during testing. For example, **Figure 4-3** shows changes in the number of hits, CSS, b-value, *H (t)*, and S_r versus time of sample two of SF38 mixture (SF38 – S2). Each graph in **Figure 4-3** also displays the percentage of weight loss versus time resulting from abrasion. The portions with smaller slopes or that are horizontal in these graphs (**Figures 4-3a and 5-3b**) indicate the time between tests when the abrasion had been halted and reinitiated each minute to measure the weight loss. The figure indicates that the abrasion damage followed a linear increase in the percentage of weight loss with time. **Figure 4-3a** shows that the

number of hits over time increased throughout the test period. The number of hits for this sample at one minute was 61 and at six minutes was 335 (**Figure 4-3a**). This increased AE activity matched the increase in the percentage of weight loss from 0.08% to 0.27% during the same period. CSS followed a similar trend like the number of hits versus time curve, as seen in **Figure 4-3b**, and CSS increased linearly from 200 to 1350 mV.s as the abrasion damage increased from 0.08% to 0.27%.

The b-value curve (**Figure 4-3c**) followed an overall declining trend as the abrasion weight loss progressed. Meanwhile, the locations of the higher fluctuations in the b-value chart were associated with the times that have higher AE activates (linear increase in the number of hits and CSS) and higher abrasion damage. For instance, the b-value decreased from 2.56 to 1.79 due to increased weight loss in the same sample from 0.08% to 0.27% (**Figure 4-3c**). Similarly, the *H (t)* magnitudes showed peaks and decreases throughout the test, but they rise and fall constantly around 1.1, with a maximum value of 1.15 (**Figure 4-3d**). This result can be related to the linear rising trend in the abrasion damage after each minute. In contrast, S_r spiked in the first minute of testing to a value of 2.53 mV.s and followed a more gradual increase for the remaining time in the test period, reaching its ultimate maximum value of 3.03 mV.s at the end of the six minutes (**Figure 4-3e**). Other samples tested herein showed similar trends of variations in the previously noted AE parameters, as the example sample described in **Figure 4-3** shows. Therefore, it can be stated that the analysis of these AE parameters can be used as a tool to identify the abrasion damage propagation in the tested mixtures. The values of these studied AE parameters (number of hits, CSS, b-value, *H (t)*, and S_r) from all other tested specimens are summarized in **Table 4-6.**

a)

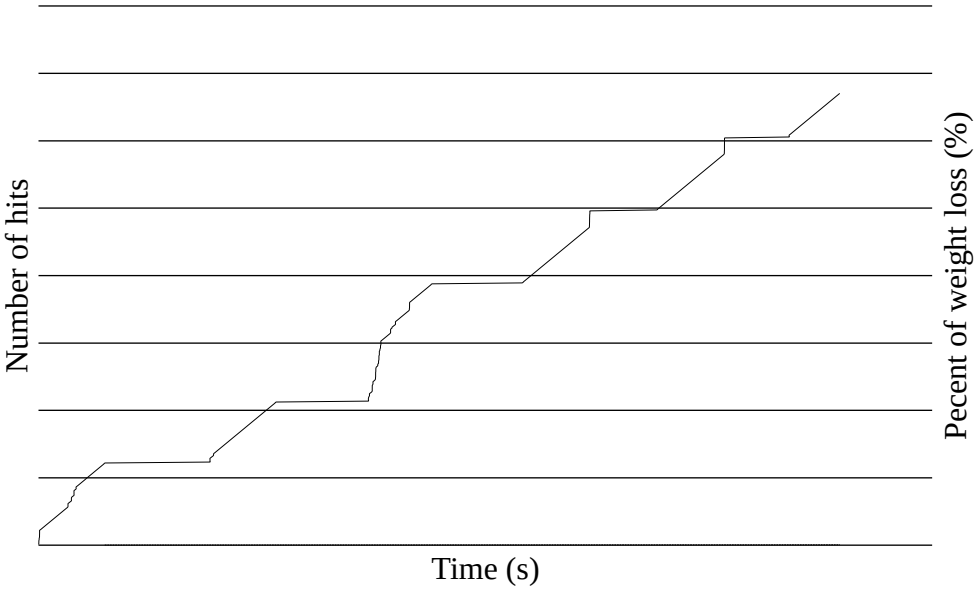
Number of hits
Pecent of weight loss (%)
Time (s)

b)

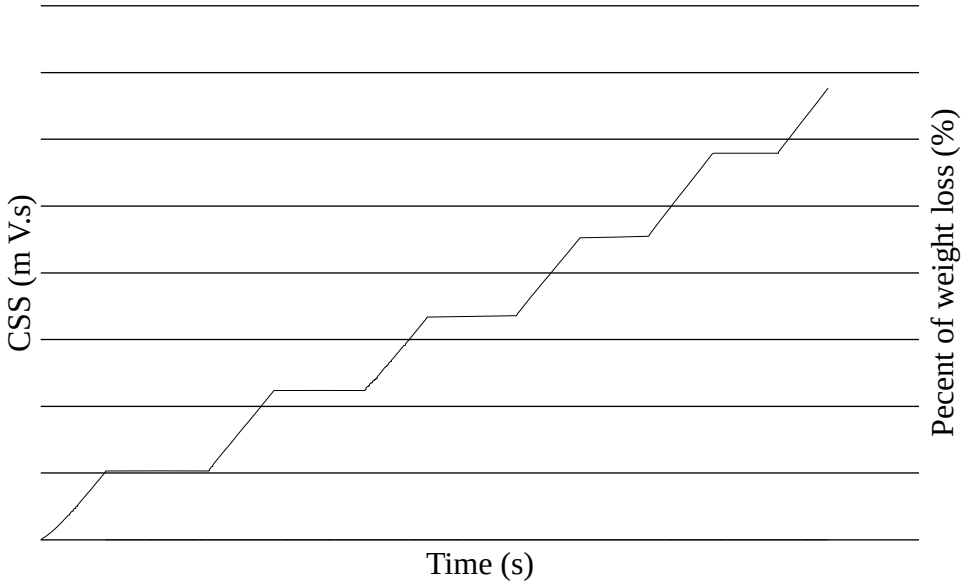
CSS (m V.s)
Pecent of weight loss (%)
Time (s)

c)

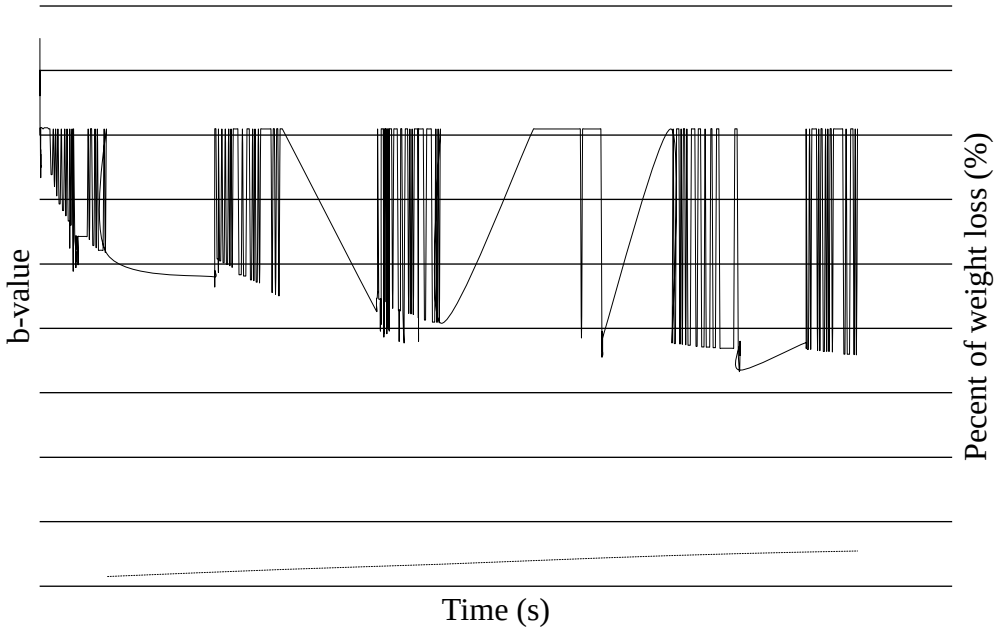
b-value
Pecent of weight loss (%)
Time (s)

d)

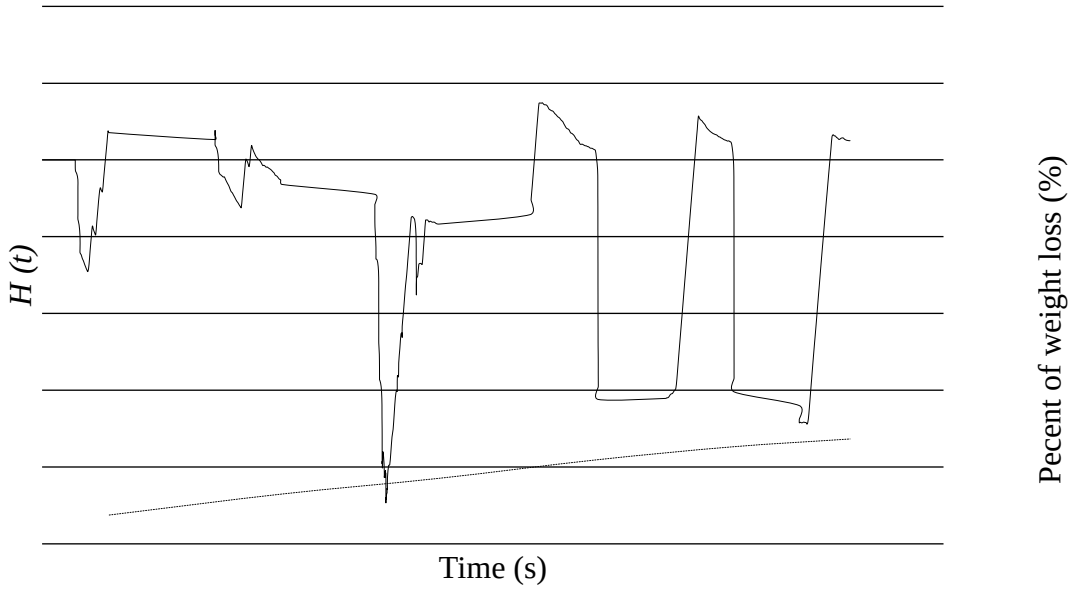
H (t)
Pecent of weight loss (%)
Time (s)

e)

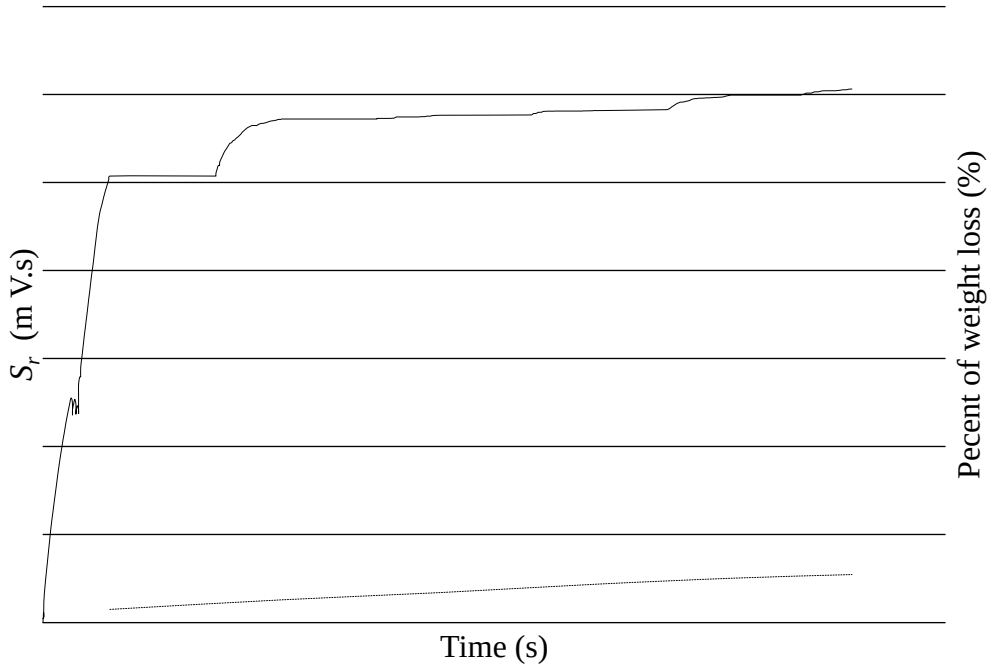

Figure 4-3 Variations in AE Parameters for SF38 S2: a) Number of hits, b) CSS, c) b-Value, d) *H (t)*, and e) *Sr*

Table 4-6 Summary of AE Parameters

Mixture name	Sample number	Average signal amplitude (dB)		Number of hits		CSS x 10^3 (mV.s)		*H (t)*		S_r (mV.s)		b-value	
		1 min	6 min	1 min	6 min	1 min	6 min	1 min	6 min	1 min	6 min	1 min	6 min
NC	S1	82	82	137	758	0.44	2.32	2.64	1.74	4.09	6.01	1.49	1.05
	S2	82	80	130	765	0.33	2.23	2.25	2.77	4.09	5.99	1.49	1.01
	S3	87	84	110	670	0.48	2.42	2.15	1.47	5.59	6.01	1.39	1.14
SCC1	S1	85	82	115	461	0.36	2.23	1.98	1.35	4.14	5.51	1.45	1.14
	S2	87	86	112	391	0.4	2.34	2.04	1.58	4.55	5.52	1.58	1.25
	S3	87	74	103	1143	0.37	2.41	2.04	2.7	4.55	5.55	1.51	0.95
SCC2	S1	75	82	97	552	0.26	1.82	1.83	1.53	2.33	3.78	1.81	1.21
	S2	82	84	77	301	0.24	1.83	1.46	1.24	2.08	3.87	1.86	1.28
	S3	84	81	68	291	0.21	1.75	1.18	1.57	2.01	3.93	1.96	1.47
SF19	S1	77	77	52	209	0.17	1.13	0.95	0.87	1.42	2.56	2.69	1.95
	S2	79	80	47	371	0.16	1.26	0.89	1.17	1.72	2.94	3.26	1.96
	S3	84	77	56	303	0.18	1.24	1.02	1.12	1.47	2.86	2.55	1.81
SF38	S1	85	77	74	359	0.21	1.40	1.32	1.25	1.65	3.19	2.11	1.67
	S2	80	77	61	335	0.20	1.35	1.07	1.15	2.53	3.03	2.56	1.79
	S3	87	83	48	342	0.18	1.37	0.87	1.20	1.38	3.08	2.59	1.67
SF27	S1	85	77	58	319	0.18	1.19	0.96	1.09	1.84	2.65	2.91	1.78
	S2	80	77	67	327	0.19	1.28	1.14	1.17	1.74	3.04	2.40	1.80
	S3	87	83	57	338	0.18	1.38	0.94	1.21	1.82	3.26	2.43	1.77
SF54	S1	87	82	78	452	0.24	1.47	1.34	1.35	2.43	3.88	2.08	1.56
	S2	88	89	77	372	0.20	1.42	1.39	1.21	2.01	3.74	2.41	1.77
	S3	88	73	77	348	0.20	1.35	1.40	1.19	2.01	3.70	2.26	1.71

4.7.2. Effect of Concrete Type on Abrasion and AE Data

Regarding the abrasion resistance, the NC mixture had an average weight loss of 0.64% and average wear depth of 0.99 mm. In comparison, the counterpart NC mixture, SCC1 had an average weight loss of 0.59% and an average wear depth of 0.93. The improvement in the abrasion performance in the SCC mixtures compared with NC may be attributed to the reduced content of coarse aggregates in SCC mixtures (C/F ratios of 0.7 for SCC mixtures and 2.0 for NC). It should be noted that the tested mixtures in this investigation had a relatively strong paste (500 kg/m^3 cement and low W/B ratio of 0.4). Therefore, the increased paste/coarse aggregate volume in SCC mixtures may have contributed to increasing the abrasion resistance. Furthermore, the use of SCMs (metakaolin and fly ash) in SCC2 can be the reason for the additional enhancement in the abrasion resistance as SCC2 exhibited significantly better abrasion resistance than both NC and SCC1 mixtures. By comparing the SCC2 mixture to the overall average of the four SF-reinforced SCC mixtures, it was found that the addition of SFs reduced the average weight loss from 0.31% to 0.27% and the average wear depth from 0.71 mm to 0.59 mm (**Tables 4-4 and 4-5**). This improvement in the abrasion resistance of the SF-reinforced SCC can be attributed to the SF contribution to crack binding and reducing the concrete destruction, which was also confirmed in previous studies on normal concrete (Bolat, Şimşek, et al., 2014), (Horszczaruk, 2009).

The effect of adding fibers or using different concrete types on the AE signal characteristics (amplitude values) was examined. **Figures 4-4 and 5-5** demonstrate the values of signal

amplitudes among all mixtures at one and six minutes, respectively. It can be concluded from the figures that adding fibers or using different concrete types had no real effect on the amplitudes across the various mixtures. For instance, the average overall signal amplitudes of SCC mixtures with SFs were 81 at six minutes and 83 for other NC and SCC mixtures (without SFs) throughout the tests (**Table 4-6**). These results indicate no presence of significant attenuation, and therefore the addition of SFs had no effect on the AE characteristics. Further investigations on mixtures with higher volumes of fibers (above 0.2%) are recommended to study their influence on signal attenuation, if any. In the meantime, the increase in the abrasion performance yielded a decline in the number of hits, CSS, *H (t)*, and S_r and an increase in the b-value in all mixtures. This trend was observed across the mixture types examined in this study. For instance, the average AE parameters in the NC mixture at six minutes were as follows: number of hits of 731, CSS of 2323 mV.s, b-value of 1.07, *H (t)* of 1.99, and S_r of 6.00 mV.s. These average results, in the same order, for SCC2 at six minutes were 381, 1800 mV.s, 1.32, 1.45, and 3.86 mV.s. Also, at six minutes, the average values of these parameters, in the same order, for all SF-reinforced mixtures were 339, 1320 mV.s, 1.77, 1.16, and 3.16 mV.s. These results confirmed the clear correlation between the abrasion damage and the AE parameters.

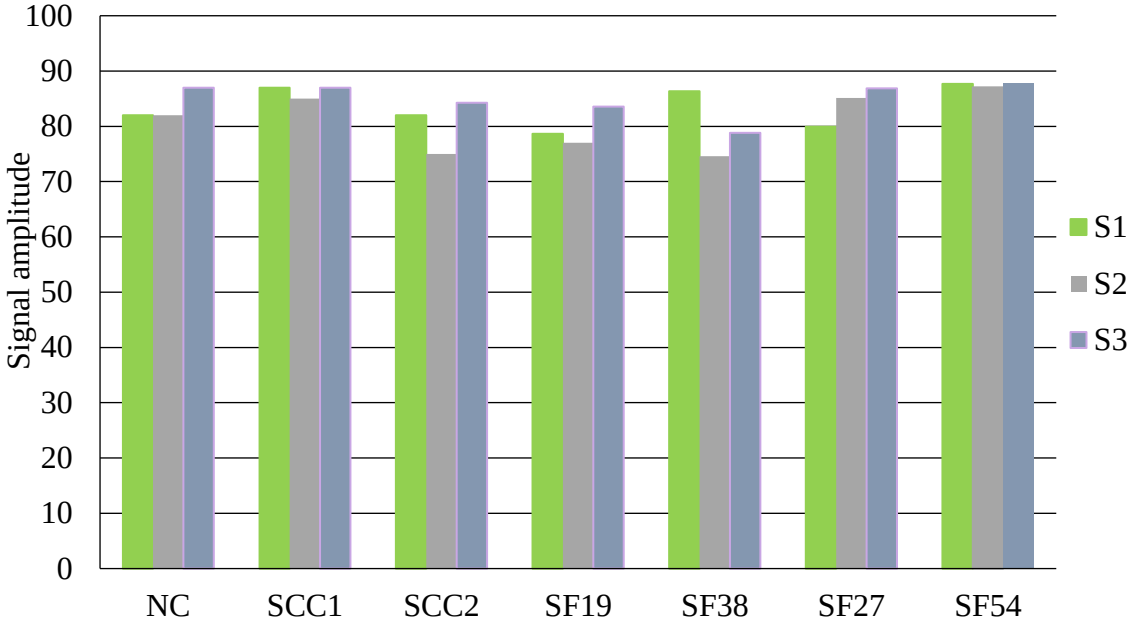

Figure 4-4 Average Signal Amplitudes of All Samples at One Minute

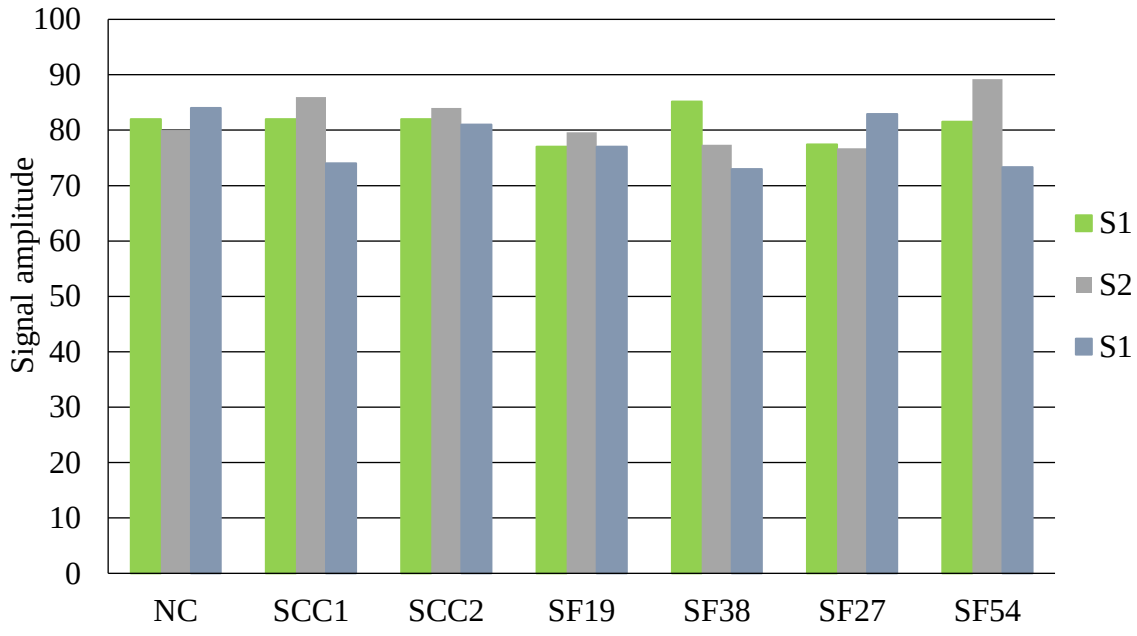

Figure 4-5 Average Signal Amplitudes of All Samples at Six Minutes

4.7.3. Effect of Fiber Types on Abrasion and AE Data

Two types of SFs were used in the SCC mixtures (semi-rigid and flexible). For the two mixtures utilizing the semi-rigid fibers, the average percentage of mass loss due to abrasion of the two fiber lengths was 0.29% and the average wear depth was 0.61 mm at six minutes. The flexible fibers averaged a 0.26% weight loss and a 0.57 mm of wear depth at six minutes. These results indicated that the flexible fibers had higher abrasion performance than the semi-rigid fibers. The AE data results also indicated that the flexible fibers, on average, performed better at resisting abrasion than the semi-rigid fibers. The average number of hits, CSS, *H (t),* and S_r were lower and the average b-value was higher in the flexible fibers compared to the semi-rigid fibers. The average magnitudes of these parameters, in that order, were 320, 1290 mV.s, 1.13, 2.94 mV.s, and 1.81 in the flexible fibers and 359, 1350 mV.s, 1.20, 3.38 mV.s, and 1.73 in the semi-rigid fibers at six minutes, as seen in **Table 4-6**. On the other hand, the AE signal amplitudes did not seem to be influenced by changing the fiber type, both at one and six minutes, as can be observed from **Figures 4-4 and 5-5**. Further testing on SCC mixtures containing higher volumes of fibers (above 0.2%) is needed in order to substantiate these outcomes.

4.7.4. Effect of Fiber Length on Abrasion and AE Data

It has been determined that concrete and fiber type both affect abrasion resistance. Four fiber lengths were used in this study: two were flexible (19 mm and 38 mm) and two were semi-rigid (27 mm and 54 mm). For the flexible fibers, the 19-mm type showed an average mass loss of 0.24% and an average wear depth of 0.53 mm at the end of the test. The 38-

mm flexible fiber saw an average mass loss of 0.28% and an average wear depth of 0.62 mm at six minutes. As for the semi-rigid fibers, the SF27 mixture saw an average mass loss of 0.26% with an average wear depth of 0.58 mm, and the SF54 mixture saw an average mass loss of 0.31% during testing and an average wear depth of 0.64 mm. These results suggest that increasing the length of fibers resulted in lower abrasion resistance in both the flexible and semi-rigid fibers. This effect may be attributed to reduced values of the average compressive strength as a result of increasing the fiber length, which can be seen in **Table 4-5**. Also, at the same percentage of fiber in the mixture (0.2%), reducing the fiber length resulted in a higher number of fibers distributed in the mixture, which can have a greater effect on binding the cracks and reducing the concrete destruction. The AE parameters including the number of hits, CSS, b-value, *H (t)*, and S_r followed the same trends, as expected (**Table 4-6**). For example, changing the flexible fiber length from 19 mm to 38 mm yielded 14% higher average number of hits, 11% higher average CSS, 10% lower average b-value, 12% higher average *H (t)*, and 10% higher average S_r at six minutes, which matched the decrease in the abrasion resistance between the SF19 and SF38 mixtures. Again, the AE signal amplitudes witnessed no clear variations as a result of increasing the fiber length in all tested samples (both flexible and semi-rigid) as can be seen in **Figures 4-4 and 5-5**.

4.7.5. Damage Quantification Using AE Intensity Analysis

The goal of this study was to correlate the extent of the abrasion damage to the AE intensity analysis data that was previously obtained and calculated. To achieve this goal, two charts were created (**Figures 4-6 and 4-7**) using the *H (t)* and S_r values at six minutes attained

from all mixtures. **Figure 4-6** can ideally be employed to determine if abrasion damage has occurred and to quantify this damage in terms of the percentage of weight loss using the magnitudes of *H (t)* and S_r. The data in this chart falls into three brackets: 0.21% to 0.32%, 0.33% to 0.40%, and 0.60% to 0.76%. The range for *H (t)* was 0.87 to 2.77 and for S_r was 2.56 to 6.01 mV.s, which were the same ranges in both quantification charts. The chart can be used to predict the abrasion damage by using a pair of values for *H (t)* and S_r. As an example, if *H (t)* was equal to 1.5 and S_r was approximately 4.5 mV.s, the predicted amount of damage would fall in the range of 0.33% to 0.40%. Alternatively, **Figure 4-7** can quantify and determine abrasion damage with respect to the wear depth as a function of *H (t)* and S_r. This chart works in the same way as the previous one with the data falling in three brackets as well: 0.48 mm to 0.65 mm, 0.71 mm to 0.84 mm, and 0.92 mm to 1.15 mm. Using the previous example, the amount of damage can be placed at approximately 0.71 mm to 0.84 mm of wear depth (**Figure 4-7**). These charts are only valid for the mixtures used in this investigation. Further testing following the same technique presented in this study would be necessary for other SCC mixtures reinforced with different types and volumes of SFs in order to adequately predict and evaluate the abrasion damage.

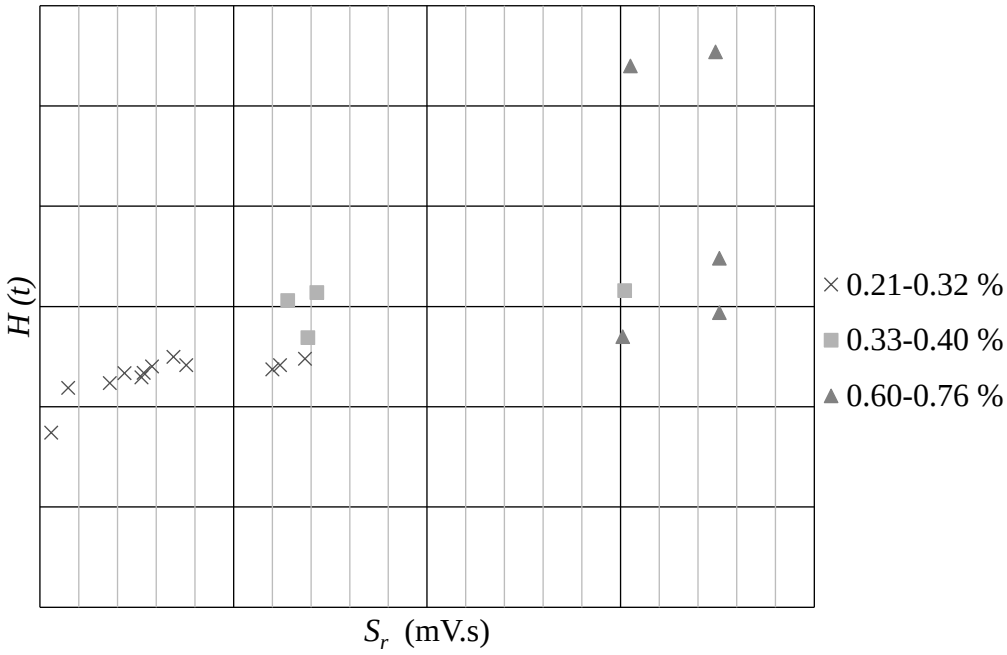

Figure 4-6 Percent of Weight Loss Quantification Chart

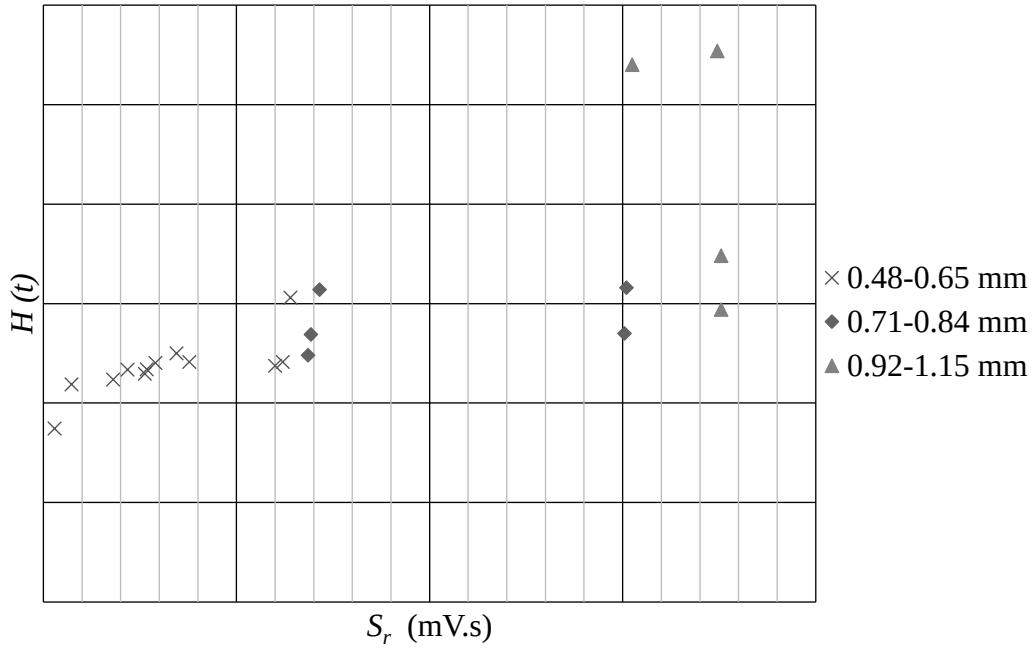

Figure 4-7 Wear Depth Quantification Chart

4.8. Conclusions

This study focused on evaluating the abrasion resistances of normal concrete, SCC, and SCC incorporating SFs of varying types and lengths. The rotating-cutter test was used in conjunction with attached AE sensors to obtain the signals created within the specimens during testing. Upon analyzing the AE and abrasion data sets, the following conclusions were attained:

- A direct correlation between the studied AE parameters (number of hits, CSS, b-value, *H (t)*, and S_r) and the abrasion damage was established. The results showed that the increase in the percentage of weight loss due to abrasion in all tested mixtures was related to an overall increase in the number of hits, CSS, and S_r and

to an overall decrease in the b-values throughout the test period. The magnitudes of the *H (t)* kept fluctuating over the test period at a specific value representing the severity of the abrasion damage in each sample.

- The control SCC mixture exhibited higher abrasion resistance (in terms of weight loss and wear depth) than its NC counterpart due to the lower coarse aggregate content used in SCC mixtures. In addition, incorporating metakaolin and fly ash into the SCC mixtures significantly enhanced the abrasion resistance compared to both NC and SCC control mixtures. The addition of SFs to SCC mixtures (up to 0.2% by volume) further increased their abrasion resistance when compared with the SCC counterpart mixtures (without fibers).
- Changing the concrete type (NC to SCC) and adding SCMs as well as SFs to the SCC mixtures did not significantly affect the AE signal characteristics (signal amplitude) attained from all abrasion tests. It was found that no noticeable attenuation occurred owing to the addition of SFs in SCC mixtures. However, other studied AE parameters (number of hits, CSS, b-value, *H (t)*, and S_r) were varied corresponding to the changes in the abrasion damage regardless of concrete type.
- The flexible fibers showed higher abrasion resistance than the semi-rigid fibers with respect to the average percentage of both weight loss and wear depth. This improvement was also associated with lower average number of hits, CSS, *H (t)*, and S_r and higher average b-value in the flexible fibers compared to the semi-rigid ones. Yet, varying the type of fiber did not show any evident effect on the AE signal amplitudes collected throughout the test periods.

- Increasing the length of fibers (both flexible and semi-rigid) led to higher average values of abrasion weight loss and wear depth, which was also related to higher average number of hits, CSS, *H (t)*, and S_r and lower average b-value, indicating increased damage due to abrasion. On the other hand, the use of longer fibers (both flexible and semi-rigid) also did not significantly affect the amplitudes of the AE signals recorded during all abrasion tests.
- Classification charts were developed based on the results from AE intensity analysis to adequately quantify the abrasion damage. The *H (t)* and S_r parameters were related in pairs to the depth of wear and the percentage of weight loss due to abrasion for all tested samples. The ranges for *H (t)* and S_r were found to be 0.87 to 2.77 and 2.56 to 6.01 mV.s, respectively. Using these charts, abrasion damage can be identified and its value can be predicted according to the magnitudes of *H (t)* and S_r obtained from AE monitoring. Additional testing on SCC, SCC with SFs, and NC mixtures with different proportions would need to be performed in order to refine the results used in these charts.

4.9. Chapter References

AbdelAleem BH, Ismail MK, Hassan AAA. Properties of self-consolidating rubberised concrete reinforced with synthetic fibres. Magazine of Concrete Research 2017; 69(10): 525-540.

Abdelrahman M, ElBatanouny MK, Ziehl PH. Acoustic emission based damage assessment method for prestressed concrete structures: Modified index of damage. Engineering Structures 2014; 60: 258-264.

Abdelrahman M, ElBatanouny MK, Ziehl P, Fasl J, Larosche CJ, Fraczek J. Classification of alkali–silica reaction damage using acoustic emission: A proof-of-concept study. Construction and Building Materials 2015; 95: 405-413.

Anay R, Cortez TM, Jáuregui DV, ElBatanouny MK, Ziehl P. On-site acoustic-emission monitoring for assessment of a prestressed concrete double-tee-beam bridge without plans. Journal of Performance of Constructed Facilities 2016; 30(4): 04015062.

ASTM. Standard test method for abrasion resistance of horizontal concrete surfaces. ASTM C779. ASTM International: West Conshohocken, PA, USA, 2012.

ASTM. Standard test method for abrasion resistance of concrete by sandblasting. ASTM C418. ASTM International: West Conshohocken, PA, USA, 2012.

ASTM. Standard test method for abrasion resistance of concrete or mortar surfaces by the rotating-cutter method. ASTM C944. ASTM International: West Conshohocken, PA, USA, 2012.

ASTM. Standard specification for Portland cement. ASTM C150. ASTM International: West Conshohocken, PA, USA, 2012.

ASTM. Standard test method for slump flow of self-consolidating concrete. ASTM C1611. ASTM International: West Conshohocken, PA, USA, 2009.

ASTM. Standard specification for chemical admixtures for concrete. ASTM C494. ASTM International: West Conshohocken, PA, USA, 2013.

ASTM. Standard test method for compressive strength of cylindrical concrete specimens. ASTM C39. ASTM International: West Conshohocken, PA, USA, 2012.

ASTM. Standard terminology for nondestructive examinations. ASTM E1316. ASTM International: West Conshohocken, PA, USA, 2014.

Bolat H, Şimşek O, Çullua M, Durmuş G, Can Ö. The effects of macro synthetic fiber reinforcement use on physical and mechanical properties of concrete. Composites Part B: Engineering 2014; 61: 191-198.

Colombo IS, Main IG, Forde MC. Assessing damage of reinforced concrete beam using ‘‘b-value’’ analysis of acoustic emission signals. Journal of Materials in Civil Engineering 2003; 15(3): 280-286.

ElBatanouny MK, Mangual J, Ziehl PH, Matta F. Early corrosion detection in prestressed concrete girders using acoustic emission. Journal of Materials in Civil Engineering 2014; 26: 503-511.

Ghafoori N, Najimi M, Aqel MA. Abrasion resistance of self-consolidating concrete. Journal of Materials in Civil Engineering 2014; 26(2): 295-303.

Grabois TM, Cordeiro GC, Toledo Filho RD. Fresh and hardened-state properties of self-compacting lightweight concrete reinforced with steel fibers. Construction and Building Materials 2016; 104: 283-292.

Horszczaruk EK. Hydro-abrasive erosion of high performance fiber-reinforced concrete. Wear 2009; 267: 110-115.

Ismail MK, Hassan AAA. Impact resistance and mechanical properties of self-consolidating rubberized concrete reinforced with steel fibers. Journal of Materials in Civil Engineering 2017; 29(1): 04016193.

Lachemi M, Hossain KMA, Lambros V, Bouzoubaâ N. Development of cost-effective self-compacting concrete incorporating fly ash, slag cement, or viscosity-modifying admixtures. ACI Materials Journal 2003; 100(5): 419-425.

Li D, Chen Z, Feng Q, Wang Y. Damage analysis of CFRP-confined circular concrete-filled steel tubular columns by acoustic emission techniques. Smart Materials and Structures 2015; 24: 085017.

Mistras Group. R6I-AST sensor. Physical Acoustics Corporation, Princeton Junction, NJ, USA, 2005.

Mistras Group. PCI-2 based AE system user's manual. Physical Acoustics Corporation, Princeton Junction, NJ, USA, 2007.

Nair A, Cai CS. Acoustic emission monitoring of bridges: Review and case studies." Engineering Structures 2010; 32(6): 1703-1714.

Ohtsu M, Tomoda Y. Phenomenological model of corrosion process in reinforced concrete identified by acoustic emission. ACI Materials Journal 2008; 105(2): 193-199.

Sagar RV, Prasad BKR. Laboratory investigations on cracking in reinforced concrete beams using on-line acoustic emission monitoring technique. Journal of Civil Structural Health Monitoring 2013; 3: 169-186.

Salamone S, Veletzos MJ, Lanza di Scale F, Restrepo JI. Detection of initial yield and onset of failure in bonded posttensioned concrete beams. Journal of Bridge Engineering 2012; 17: 965-974.

Scott BD, Safiuddin M. Abrasion resistance of concrete – Design, construction and case study. Concrete Research Letters 2015; 6(3): 135-148.

Vélez W, Matta F, Ziehl P. Acoustic emission monitoring of early corrosion in prestressed concrete piles. Structural Control and Health Monitoring 2015; 22: 873-887.

Yap SP, Bu CH, Alengaram UJ, Mo KH, Jumaat MZ. Flexural toughness characteristics of steel–polypropylene hybrid fibre-reinforced oil palm shell concrete. Materials and Design 2014; 57: 652-659.

Zaki A, Chai HK, Aggelis DG, Alver N. Non-destructive evaluation for corrosion monitoring in concrete: A review and capability of acoustic emission technique. Sensors 2015; 15: 19069-19101.

Zhou X, Yang Y, Li X, Zhao G. Acoustic emission characterization of the fracture process in steel fiber reinforced concrete. Computers and Concrete 2016; 18(4): 923-936.

Ziehl PH, Galati N, Nanni A, Tumialan JG. In-situ evaluation of two concrete slab systems. II: evaluation criteria and outcomes. Journal of Performance of Constructed Facilities 2008; 22: 217-227.

5. Summary and Recommendations

5.1. Summary

The previous chapters describe in detail the individual studies carried out for this research project. The project was divided into three parts to display the results in a straightforward manner. The studies performed in Chapters 2, 3 and 4, evaluated the abrasion resistance of SCC with SCM's, SCRC and SCC reinforced with SFs, respectively. The same procedure was followed both in the laboratory and analysis stages. An experimental program involving the development of various mixtures and abrasion testing using the rotating cutter method was completed. AE monitoring was performed simultaneously with the abrasion tests to collect the AE data emitted during all experiments. An extensive analysis of said AE data was then completed after concluding all tests. This post-testing analysis involved performing the b-value analysis and intensity analysis. The analysis of the abrasion results and AE data for all of the mixtures tested in this study gave the following conclusions:

- A general correlation was established between the abrasion damage data (in terms of depth of wear and percent of mass loss) and the AE parameters (number of hits, CSS, b-value, *H(t)* and *Sr).* Number of hits, CSS and S_r generally increased with test time as the abrasion damage gradually increased across all tested samples. *H(t)* showed level fluctuations around a certain value and the b-value analysis indicated a decrease with abrasion damage progression. These observations indicate the sensitivity of the AE monitoring system and its ability to detect abrasion damage regardless of concrete type, the inclusion of SCM's, CR and/or SFs.

- Broadly speaking, plain SCC had improved abrasion resistance when compared to its NC counterpart. On average, the percent of mass loss as well as the depth of wear were lower for the SCC samples compared with NC ones. Higher compressive strength in SCC was also observed in comparison to NC which typically correlates to enhanced abrasion resistance in concrete.
- When the four various SCM's were incorporated into the SCC mixtures, a positive impact on the abrasion resistance became evident. The results indicated that the SCC mixture containing 20% of MK had the highest abrasion resistance and outperformed the remaining SCC mixtures with SCM's. The SCM's ranked by performance from highest to lowest resistance were as follows – MK, SF, SG, and FA.
- AE signal characteristics such as amplitude were evaluated in each test to ensure signal attenuation was insignificant and potentially disturbing the results. Overall, signal amplitude remained unaffected regardless of concrete type, having SCM's incorporated or with the addition of SF's. On the other hand, it was noticed that some attenuation occurred with the increased in the percentage of CR in the mixtures. However, the decreased amplitudes remained above the threshold of 40dB and therefore all signals were still detectable.
- Increasing the percent of CR in a mixture regardless of concrete type (NC or SCC) increased the amount of damage done during abrasion tests. In general, the plain SCC mixture outperformed the SCRC mixtures. Meanwhile, the SCRC with the maximum abrasion resistance was SCRC10 followed by SCRC20, SCRC30 and

NRC40. In fact, the plain NC mixture performed better than the SCC mixture with 30% of CR.

- The SCC mixtures containing flexible SFs provided better resistance than the semi-rigid SFs. counterparts. In addition, increasing the length of the SFs was found to increase the abrasion damage. These results were supported by the analysis of the AE data in conjunction with the abrasion test data.
- The three studies also included the generation of the damage quantification charts based on intensity analysis parameters (*H(t)* and S_r) and abrasion damage. *H(t)* and S_r were related to the wear depth and the percent of mass loss due to abrasion during testing of the samples. These charts were created to determine the extent of the damage to a specimen being monitored based on the data attained from AE monitoring.
- Largely, this research proved the usefulness of AE monitoring at detecting abrasion damage in a laboratory setting. The research also provided a strong insight into the abrasion resistance of a wide variety of both NC and SCC mixtures. The potential application of the AE monitoring utilized in this research is in the areas where SCC may be employed in concrete structures subjected to abrasion. The AE sensors could be attached to such structures to continuously gather data which could then be analyzed quickly to detect any possible abrasion damage.

5.2. Potential Applications and Recommendations for Future Research

Potential applications for this study include non-destructive testing for offshore structures and on projects where typical visual inspection techniques are not possible to be carried out on site or in person for extended periods of time. This project was focused on small-scale testing. The abrasion tests were performed in categorically "ideal" conditions, in a controlled lab setting on 100mm cubic specimens.

There are many possible applications for furthering this research in the laboratory and in the field. It is recommended that more research be conducted on larger-scale samples with higher surface area of abrasion to generate and redefine more thorough quantification charts that were presented in this thesis. The study of larger samples would allow for better understanding of variation in acoustic emission signatures. Increasing the size of a tested specimen and altering the material would directly alter the AE results as acousitc signature is defined by the variety and size of a material. Larger specimens would also introduce the concept of wave reflection and how that would effect the AE data.

Along with increasing the size of the samples, the number of samples tested could also be increased, this would assist in enhancing the reliability of the results. Lastly, investigating the effects of ice abrasion on concrete samples would also be greatly recommended to better understand the interactions between concrete off-shore structure and sea ice.

Bibliography

AbdelAleem BH, Ismail MK, Hassan AAA (2017). "Properties of self-consolidating rubberised concrete reinforced with synthetic fibres." Magazine of Concrete Research, 69(10): 525-540.

Abdelrahman M, ElBatanouny MK, Ziehl P, Fasl J, Larosche CJ and Fraczek J (2015) "Classification of alkali-silica reaction damage using acoustic emission: A proof-of-concept study." Construction and Building Materials, 95: 406–413.

Abdelrahman M., ElBatanouny M. K., and Ziehl P. H. (2014). "Acoustic emission based damage assessment method for prestressed concrete structures: Modified index of damage." Engineering Structures, 60, 258–264.

Abouhussien AA and Hassan AAA (2015). "Optimizing the durability and service life of self-consolidating concrete containing metakaolin using statistical analysis." Construction and Building Materials, 76: 297–306.

Abouhussien AA, and Hassan, AAA (2017). "Acoustic emission monitoring for bond integrity evaluation of reinforced concrete under pull-out tests." Advanced Structural Engineering, 20(9), 1390–1405.

Anay R, Cortez TM, Jáuregui DV, ElBatanouny MK, Ziehl P (2016). "On-site acoustic-emission monitoring for assessment of a prestressed concrete double-tee-beam bridge without plans." Journal of Performance of Constructed Facilities, 30(4): 04015062.

Aslani F (2013). "Effects of specimen size and shape on compressive and tensile strengths of self-compacting concrete with or without fibres." Magazine of Concrete Research, 65(15): 914–929.

ASTM (2009) C 1611: “Standard test method for slump flow of self-consolidating concrete.” ASTM International, West Conshohocken, PA, USA.

ASTM (2011) C 39: “Standard test method for compressive strength of cylindrical concrete specimens.” ASTM International, West Conshohocken, PA, USA.

ASTM (2012) C 418: “Standard test method for abrasion resistance of concrete by sandblasting.” ASTM International, West Conshohocken, PA, USA.

ASTM (2012) C 779: “Standard test method for abrasion resistance of horizontal concrete surfaces.” ASTM International, West Conshohocken, PA, USA.

ASTM (2012) C 944: “Standard test method for abrasion resistance of concrete or mortar surfaces by the rotating-cutter method.” ASTM International, West Conshohocken, PA, USA.

ASTM (2012) C 1138: “Standard test method for abrasion resistance of concrete (Underwater method)”. ASTM International, West Conshohocken, PA, USA.

ASTM (2013) C 494: “Standard specification for chemical admixtures for concrete.” ASTM International, West Conshohocken, PA.

ASTM (2014) E1316: “Standard terminology for nondestructive examinations.” ASTM International, West Conshohocken, PA.

ASTM (2017) C 150: “Standard specification for portland cement.” ASTM International, West Conshohocken, PA, USA.

Bolat H, Şimşek O, Çullua M, Durmuş G, Can Ö (2014). “The effects of macro synthetic fiber reinforcement use on physical and mechanical properties of concrete.” Composites Part B: Engineering, 61: 191-198.

Bunnori NM, Lark RJ and Holford KM (2011). “The use of acoustic emission for the early detection of cracking in concrete structures.” Magazine of Concrete Research, 63(9): 683–688.

Colombo IS, Main IG, and Forde MC (2003). “Assessing damage of reinforced concrete beam using ‘‘b-value’’ analysis of acoustic emission signals.” Journal of Materials in Civil Engineering, 15(3), 280–286.

Das D and Chatterjee A (2012). “A comparison of hardened properties of fly-ash-based self-compacting concrete and normally compacted concrete under different curing conditions.” Magazine of Concrete Research, 64(2): 129–141.

Dong Q, Wu H, Huang B, Shu X and Wang K (2013). “Investigation into laboratory abrasion test methods for pervious concrete.” Journal of Materials in Civil Engineering, 25(7): 886–892.

ElBatanouny MK, Ziehl PH, Larosche A, Mangual J, Matta F and Nanni A (2014). “Acoustic emission monitoring for assessment of prestressed concrete beams.” Construction and Building Materials, 58: 46–53.

ElBatanouny, M. K., Mangual, J., Ziehl, P. H., and Matta, F. (2014). “Early corrosion detection in prestressed concrete girders using acoustic emission.” Journal of Materials in Civil Engineering, 26, 504–511.

El-Chabib, H., and Syed, A. (2013). “Properties of self-consolidating concrete made with high volumes of supplementary cementitious materials.” Journal of Materials in Civil Engineering, 25(11), 1579–1586.

Eldin, N. N., and Senouci, A. B. (1994). “Measurement and prediction of the strength of rubberized concrete.” Cement and Concrete Composites, 16 (4), 287–298.

Farhidzadeh A, Salamone S, Luna B and Whittaker A (2012). “Acoustic emission monitoring of a reinforced concrete shear wall by b-value-based outlier analysis.” Structural Health Monitoring 12(1): 3–13.

Farhidzadeh, A., Dehghan-Niri, E., Salamone, S., Luna, B., and Whittaker, A. (2013). “Monitoring crack propagation in reinforced concrete shear walls by acoustic emission.” Journal of Structural Engineering, 139(12), 04013010.

Ghafoori N and Diawara H (1999). “Abrasion resistance of fine aggregate replaced silica fume concrete.” ACI Materials Journal 96(5): 559–569.

Ghafoori, N., Najimi, M., & Aqel, M. A. (2013). “Abrasion resistance of self-consolidating concrete.” Journal of Materials in Civil Engineering 26(2): 296-303.

Grabois TM, Cordeiro GC, Toledo Filho RD (2016). “Fresh and hardened-state properties of self-compacting lightweight concrete reinforced with steel fibers.” Construction and Building Materials, 104: 283-292.

Horszczaruk EK (2009). “Hydro-abrasive erosion of high performance fiber-reinforced concrete.” Wear, 267: 110-115.

Invernizzi S, Lacidogna G and Carpinteri A (2013). “Scaling of fracture and acoustic emission in concrete.” Magazine of Concrete Research, 65(9): 529–534.

Ismail MK and Hassan AAA (2016a). “Impact resistance and acoustic absorption capacity of self-consolidating rubberized concrete.” ACI Materials Journal, 113(6), 725–736.

Ismail MK and Hassan AAA (2016b). “Use of metakaolin on enhancing the mechanical properties of SCC containing high percentages of crumb rubber.” Journal of Cleaner Production, 125, 282–295.

Ismail MK, Hassan AAA (2017). “Impact resistance and mechanical properties of self-consolidating rubberized concrete reinforced with steel fibers.” Journal of Materials in Civil Engineering, 29(1): 04016193

Karahan O, Hossain KMA, Ozbay E, Lachemi M and Sancak E (2012). “Effect of metakaolin content on the properties self-consolidating lightweight concrete.” Construction and Building Materials, 31: 320–325.

Lachemi M, Hossain KMA, Lambros V, Bouzoubaâ N (2003). “Development of cost-effective self-compacting concrete incorporating fly ash, slag cement, or viscosity-modifying admixtures.” ACI Materials Journal, 100(5): 419-425.

Lachemi M, Hossain KMA, Patel R, Shehata M and Bouzoubaâ N (2007). “Influence of paste/mortar rheology on the flow characteristics of high-volume fly ash self-consolidating concrete.” Magazine of Concrete Research, 59(7): 517–528.

Li, D., Chen, Z., Feng, Q., and Wang, Y. (2015). “Damage analysis of CFRP-confined circular concrete-filled steel tubular columns by acoustic emission techniques.” Smart Materials and Structures, 24, 085017 (11pp).

Liu TC (1981). “Abrasion resistance of concrete.” ACI Journal 78(5): 341–350.

McGraw-Hill (2002). “Dictionary of Scientific and Technical Terms, 6th ed.” McGraw-Hill, New York.

Mehta P, Monteiro P (2014). “Concrete: Microstructure, Properties, and Materials.” 4th Edition, McGraw-Hill Education.

Meyer C (2002). “Concrete Materials and Sustainable Development in the United States.” Columbia University Special Publication ACI 206.

Mistras Group (2005). “R6I-AST sensor.” Physical Acoustics Corporation, Princeton Junction, NJ, USA.

Mistras Group (2007). “PCI-2 based AE system 1 user’s manual.” Physical Acoustics Corporation, Princeton Junction, NJ, USA.

Najim, K. B., and Hall, M. (2012). “Mechanical and dynamic properties of self-compacting crumb rubber modified concrete.” Construction and Building Materials, 27(1), 521–530.

Nair, A., and Cai, C. S. (2010). “Acoustic emission monitoring of bridges: Review and case studies.” Engineering Structures, 32(6), 1704–1714.

Ohtsu, M., and Tomoda, Y. (2008). “Phenomenological model of corrosion process in reinforced concrete identified by acoustic emission.” ACI Materials Journal, 105(2), 194–199.

Ozbay, E., Lachemi, M., and Sevim, U. K. (2011). “Compressive Strength, abrasion resistance and energy absorption capacity of rubberized concrete with and without slag.” Materials and Structures, 44(7), 1297–1307.

Papenfus, N. (2003). “Applying concrete technology to abrasion resistance.” In: Proceedings of the 7th International Conference on Concrete Block Paving (PAVE AFRICA 2003), Sun City, South Africa, ISBN Number: 0-958-46091-4.

Peurifoy R, Schexnayder C, Schmitt R, Shapira A (2018). “Construction Planning, Equipment, and Methods, Ninth Edition.” McGraw Hill Education Publishing.

Physical Acoustics. (2005). “R6I-AST sensor.” Physical Acoustics Corporation, Princeton Junction, NJ, USA.

Pollock, A. A. (1986). “Classical wave theory in practical AE testing.” In: Proceedings, International Acoustic Emission Symposium, Japanese Society for Nondestructive Testing, 708–721.

Rahman, M. M., Usman, M., and Al-Ghalib, A. A. (2012). “Fundamental properties of rubber modified self-compacting concrete (RMSCC).” Construction and Building Materials, 36, 630–637.

Rao SV, Rao SMV, Ramaseshu D and Kumar RP (2012). “Durability performance of self-compacting concrete.” Magazine of Concrete Research, 64(11): 1005–1013.

Sadek, D. M., and El-Attar, M. M., (2014). “Structural behavior of rubberized masonry walls.” Journal of Cleaner Production, 89, 174–186.

Safiuddin M, Salam MA and Jumaat MZ (2012). “Flowing ability of self-consolidating concrete and its binder paste phase including palm oil fuel ash.” Magazine of Concrete Research, 64(10): 931–944.

Sagar RV, Prasad BKR (2013). “Laboratory investigations on cracking in reinforced concrete beams using on-line acoustic emission monitoring technique.” Journal of Civil Structural Health Monitoring, 3: 169-186.

Salamone S, Veletzos MJ, Lanza di Scale F, Restrepo JI (2012). “Detection of initial yield and onset of failure in bonded posttensioned concrete beams.” Journal of Bridge Engineering, 17: 965-974.

Scott BD and Safiuddin M (2015). “Abrasion resistance of concrete – Design, construction and case study.” Concrete Research Letters, 6(3): 136–148.

Su, H., Yang, J., Ling, T., Ghataora, G. S., and Dirar, S. (2015). “Properties of concrete prepared with waste tyre rubber particles of uniform and varying sizes.” Journal of Cleaner Production, 91, 288–296.

Thomas, B. S., Gupta, R. C., Kalla, P., and Cseteneyi, L. (2014). “Strength, abrasion and permeation characteristics of cement concrete containing discarded rubber fine aggregates.” Construction and Building Materials, 59, 204–212.

Thomas, B. S., Kumar, S., Mehra, P., Gupta, R. C., Joseph, M., and Csetenyi L. J. (2016). “Abrasion resistance of sustainable green concrete containing waste tire rubber particles.” Construction and Building Materials, 124, 906–909.

Turer, A. (2012). “Recycling of Scrap Tires, Material Recycling – Trends and Perspectives”, Dr. Dimitris Achilias (Ed.), 195–212. ISBN: 978-953-51-0327-1, InTech, Available from: http://www.intechopen.com/books/materialrecycling-trends-and-perspectives/use-of-scrap-tires-in-industry.

Turk K and Karatas M (2011). “Abrasion resistance and mechanical properties of self-compacting concrete with different dosages of fly ash/ silica fume.” Indian Journal of Engineering and Materials Sciences, 18: 49–60.

Vélez W, Matta F and Ziehl P (2015). “Acoustic emission monitoring of early corrosion in prestressed concrete piles.” Structural Control and Health Monitoring, 22: 873–887.

Vidya Sagar R and Prasad BKR (2009). “AE energy release during the fracture of HSC beams.” Magazine of Concrete Research, 61(6): 419–435.

Wang, C., Zhang, Y., and Ma, A. (2013). “Investigation into the fatigue damage process of rubberized concrete and plain concrete by AE analysis.” Journal of Materials in Civil Engineering, 23(7), 886–892.

Yap SP, Bu CH, Alengaram UJ, Mo KH, Jumaat MZ (2014). “Flexural toughness characteristics of steel–polypropylene hybrid fibre-reinforced oil palm shell concrete.” Materials and Design, 57: 652-659.

Zaki A, Chai HK, Aggelis DG, Alver N (2015). “Non-destructive evaluation for corrosion monitoring in concrete: A review and capability of acoustic emission technique.” Sensors, 15: 19069-19101.

Zhou X, Yang Y, Li X, Zhao G (2016). “Acoustic emission characterization of the fracture process in steel fiber reinforced concrete.” Computers and Concrete, 18(4): 923-936.

Ziehl, P. H., Galati, N., Nanni, A., and Tumialan, J. G. (2008). “In-situ evaluation of two concrete slab systems. II: evaluation criteria and outcomes.” Journal of Performance of Constructed Facilities, 22, 217–227.